

Anti-Neurofascin Autoantibodies:  
Assay Development and Analysis of Inflammatory  
Diseases of the Peripheral and Central Nervous Systems

Submitted by Judy King Man Ng  
Dissertation of the the Graduate School of Systemic Neurosciences  
Ludwig-Maximilians University Munich

Munich, July 2012





First reviewer/supervisor

Prof. Dr. Edgar Meinl

Second reviewer

Prof. Dr. Nikolaus Plesnila

Supervisor

PD Dr. Klaus Dornmair

Day of Oral Defense: November 20, 2012



Antigenicity of proteins is a purely chemical property, their immunogenicity is a biological property that has a meaning only in the context of a particular host.

(van Regenmortel, 2000)



## Abstract

Neurofascin (NF) is a cell-adhesion molecule that is found at the nodes of Ranvier. The 186 kDa isoform of neurofascin (NF186) is expressed on the axon in the exposed node, and the 155 kDa isoform (NF155) is expressed on myelinating glia at the paranode. NF186 is essential for clustering of sodium channels to the nodes while NF155 is needed for close paranodal interactions between myelinating glia and axons. The neurofascins are found in both the peripheral and central nervous system (PNS and CNS).

NF-specific autoantibodies were identified in serum of multiple sclerosis (MS) patients using a proteomics approach with two-dimensional Western blotting of human myelin glycoproteins. A monoclonal antibody (mAb) specific for NF was shown to induce axonal injury in an animal model of MS, experimental autoimmune encephalomyelitis. This indicated that NF is a relevant autoantibody target in patients with inflammatory diseases of the nervous system (central and peripheral), but actual abundance of anti-NF autoantibodies is unknown.

The objectives of the thesis were the following: 1) Develop assays to detect autoantibodies against human NF. 2) Determine the prevalence in patients with MS and with inflammatory diseases of the PNS. 3) Characterize the reactivity by immunoglobulin isotyping, serial dilution, epitope mapping, and staining of nodal structures in tissue sections. 4) Affinity purify anti-NF antibodies from plasma exchange material. 5) Determine possible *in vivo* effects of anti-NF antibodies in the PNS using a neuritis animal model.

First, we expressed the complete human NF155 and NF186 on the surface of stable human cell lines, produced the complete extracellular portion of the NFs in HEK293 cells, and expressed truncated variants of the NFs in *E. coli*. With these reagents, we set up three antibody detection assays: cell-based assay by flow cytometry, ELISA, and Western blot. These assays were validated using NF-specific monoclonal and polyclonal antibodies, and optimized with a test cohort of serum samples.

We screened 687 serum and 48 plasma exchange samples from patients with MS (n = 233), inflammatory diseases in the PNS (n = 294), and controls (n = 208). From serum analysis, we observed low prevalence of anti-NF reactivity (3%) by flow cytometry and/or ELISA despite broad reactivity in almost half of the serum samples analyzed by Western blot. Reactivity observed by flow cytometry and by ELISA were congruent only in the patients with the highest reactivities. The anti-NF antibodies were NF-isoform specific, mainly IgG subclasses, and at high titres in some cases. Using truncated variants of NF fused to super green fluorescence

protein (sGFP), we showed that reactivity of anti-NF Abs was largely directed towards the membrane proximal extracellular domains that are unique to each isoform, while the membrane distal immunoglobulin-like domains and fibronectin domains were not recognized.

A small proportion (3%; 8/254) of patients with GBS and CIDP showed reactivity to human NF by ELISA. A few showed a particularly high reactivity (up to 1:10 000 dilution) to NF. Two CIDP patients showed a particularly high (up to 1:10 000 dilution) anti-NF155 reactivity by FACS and ELISA, recognized paranodes in tissue sections, and exhibited dominant IgG4 subclass usage. Another CIDP patient who benefited from plasma exchange had a persistent anti-NF155 reactivity by ELISA in serum, and after affinity purification, anti-NF186 and -NF155 reactivity by FACS and ELISA were detected in addition. These antibodies were mainly IgG3, with minor contribution of IgM and IgA. To investigate possible functions of anti-NF antibodies in inflammatory PNS diseases, we injected two different monoclonal antibodies (mAbs) into a P2-peptide induced experimental autoimmune neuritis (EAN) animal model at disease onset. We found that while the anti-NF mAbs prolonged and exacerbated clinical disease in these animals, they could not induce disease on their own.

We detected NF-reactivity in a small proportion of MS samples (3%; 7/225) by ELISA and flow cytometry. We obtained follow-up material from two NF-reactive patients and saw a persistent NF reactivity in one of them. To increase detection sensitivity, we affinity purified anti-NF antibodies from plasma exchange material of patients with MS (n = 8). IgG, IgM, and IgA were isolated from most of the samples; they were found to recognize NF155 and to a lower extent NF186 by ELISA and in a few also by flow cytometry. This indicates that low levels of anti-NF antibodies exist in a proportion of MS patients.

In conclusion, 3% of serum samples from patients with PNS inflammatory neuropathies (GBS and CIDP) showed reactivity by ELISA and none of the controls. In an animal model of autoimmune peripheral nerve inflammation, we showed, using two anti-NF mAbs, that antibody targeting of NF can enhance and prolong disease course. This suggests that antibodies to NF may be relevant for a small group of patients with peripheral inflammatory neuropathies. In MS patients, 3% showed anti-NF reactivity by flow cytometry and ELISA. Furthermore, low levels of anti-NF antibodies that could be detected by ELISA and flow cytometry after affinity purification were additionally found in some MS patient samples that were unreactive by serum screening. This raises the possibility that low levels of antibodies to NF are present in some MS patients and may contribute to the pathogenesis of this chronic disease.







# Contents

<b>List of Abbreviations</b>	<b>vii</b>
<b>1 Introduction</b>	<b>1</b>
1.1 Neurons and glia	2
1.2 Impulse conduction	2
1.3 Myelination and saltatory conduction	3
1.4 Molecular view of the myelinated axon	4
1.5 Neurofascin	5
1.6 Effects of myelin disruption	6
1.7 Inflammatory diseases in the nervous system	7
1.7.1 Inflammatory demyelinating diseases in the PNS	8
1.7.2 Inflammatory demyelinating disease in the CNS	9
1.8 Autoantibodies against neurofascin in inflammatory diseases in the PNS and CNS	10
<b>2 Objectives and Strategy</b>	<b>13</b>
2.1 Objectives	14
2.2 Strategy	14
<b>3 Material and Methods</b>	<b>17</b>
3.1 Molecular cloning	18
3.1.1 Molecular biological methods	18
3.1.1.1 Reverse-transcriptase polymerase chain reaction (RT-PCR)	18
3.1.1.2 Polymerase chain reaction (PCR)	18
3.1.1.3 Overlap-extension PCR	19
3.1.1.4 Cloning primers for NF155, NF186, and truncated NF variants	20
3.1.1.5 Agarose gel electrophoresis	21
3.1.1.6 DNA extraction from agarose gel	22
3.1.1.7 DNA quantification	22
3.1.1.8 DNA digestion with restriction endonuclease	22
3.1.1.9 DNA blunt end synthesis	23
3.1.1.10 DNA ligation	23
3.1.1.11 TOPO TA cloning	24
3.1.1.12 Alcohol precipitation of DNA	24
3.1.1.13 DNA sequencing	24
3.1.2 Microbiological methods	25
3.1.2.1 Transformation of bacterial cells	25
3.1.2.2 Bacterial colony screening for plasmid identification	25
3.1.2.3 Plasmid purification from bacterial cells	26
3.2 Recombinant protein expression	27
3.2.1 Generation of NF-expressing stable cell lines	27
3.2.1.1 Cell culture conditions	27
3.2.1.2 DNA plasmid preparation	27

3.2.1.3	Transfection protocols . . . . .	28
3.2.1.4	Selection of transfected cells with antibiotics . . . . .	28
3.2.1.5	Maintenance of stable cell lines . . . . .	29
3.2.1.6	Storage of stable cell lines . . . . .	29
3.2.2	Generation of soluble NF by transient protein expression . . . . .	29
3.2.2.1	Cell culture conditions . . . . .	30
3.2.2.2	DNA plasmid preparation . . . . .	30
3.2.2.3	Transfection using Polyethylenimine (PEI) . . . . .	30
3.2.2.4	Harvesting of supernatant . . . . .	30
3.2.2.5	Purification and preparation of soluble NF . . . . .	31
3.2.3	Protein expression in bacterial cells . . . . .	31
3.2.3.1	Transformation of Rosetta cells . . . . .	32
3.2.3.2	Protein expression by IPTG induction . . . . .	32
3.2.3.3	Protein purification . . . . .	33
3.3	General protein analytics . . . . .	34
3.3.1	Protein purification by fast protein liquid chromatography . . . . .	34
3.3.1.1	Immobilized metal affinity chromatography . . . . .	34
3.3.1.2	Affinity purification of antibodies using Protein G . . . . .	34
3.3.2	Protein separation and analysis . . . . .	35
3.3.2.1	Gel electrophoresis . . . . .	35
3.3.2.2	Protein staining by Coomassie brilliant blue . . . . .	36
3.3.2.3	Protein staining by silver . . . . .	36
3.3.3	Mass spectrometry . . . . .	36
3.3.4	Measurement of protein concentration . . . . .	37
3.3.4.1	Bicinchoninic acid assay . . . . .	37
3.3.4.2	UV spectrophotometry by Nanodrop . . . . .	37
3.3.5	Circular dichroism spectroscopy . . . . .	37
3.4	Patient material . . . . .	39
3.4.1	Ethical standard and patient consent . . . . .	39
3.4.2	Storage and handling of patient material . . . . .	39
3.4.3	Patient material list . . . . .	40
3.5	Antibody detection assays . . . . .	41
3.5.1	List of primary and secondary antibodies used in this project . . . . .	41
3.5.2	Serum screening . . . . .	42
3.5.2.1	Cell-based assay by flow cytometry . . . . .	42
3.5.2.2	ELISA . . . . .	42
3.5.2.3	Western blot . . . . .	43
3.5.3	Epitope mapping by cell-based assay . . . . .	44
3.5.4	Epitope mapping by Western blot . . . . .	44
3.5.5	Isotyping . . . . .	44
3.5.6	Serial dilution . . . . .	45
3.5.7	Immunohistochemistry . . . . .	45
3.5.8	Antibody purification by antibody-antigen affinity chromatography . . . . .	45
3.5.9	Antibody quantification by ELISA . . . . .	46
3.6	Experimental autoimmune neuritis animal experiments . . . . .	47
<b>4</b>	<b>Results</b>	<b>49</b>
4.1	Cloning and recombinant expression of neurofascin . . . . .	50
4.1.1	Construction of expression plasmids . . . . .	50
4.1.1.1	Complete transmembrane form of NF155 and NF186 . . . . .	50
4.1.1.2	Soluble form of NF155 and NF186 . . . . .	53
4.1.1.3	Transmembrane form of truncated NF variants . . . . .	53
4.1.1.4	Soluble form of truncated NF variants . . . . .	55

4.1.1.5	List of plasmids generated for this study . . . . .	56
4.1.2	Recombinant expression of complete NFs and truncated variants . . . . .	57
4.1.2.1	Cell lines expressing complete NF155 and NF186 . . . . .	57
4.1.2.2	Cell lines expressing truncated NF variants . . . . .	57
4.1.2.3	Soluble complete NF155 and NF186 . . . . .	58
4.1.2.4	Soluble truncated NF variants . . . . .	60
4.2	Establishment of anti-NF antibody detection assays . . . . .	61
4.2.1	Cell-based assay by flow cytometry . . . . .	61
4.2.2	ELISA . . . . .	62
4.2.2.1	ratNF155-NS0 is not a specific antigen to detect anti-NF reactivity	63
4.2.3	Western blot . . . . .	64
4.2.4	Reactivity of pan-NF monoclonal antibodies and NF155-specific rabbit serum in the assays . . . . .	65
4.3	Neurofascin-specific autoantibodies in Guillain-Barré syndrome and chronic inflammatory demyelinating polyneuropathy . . . . .	68
4.3.1	Serum screening for anti-NF antibodies . . . . .	68
4.3.2	Detailed analysis of NF-reactive serum samples . . . . .	70
4.3.3	Effects of anti-NF antibodies on experimental autoimmune neuritis . . . . .	74
4.4	Neurofascin-specific autoantibodies in multiple sclerosis . . . . .	76
4.4.1	Serum screening for anti-NF antibodies . . . . .	76
4.4.2	Characterization of serum samples showing anti-NF reactivity . . . . .	78
4.4.3	Affinity purification of anti-NF antibodies from RR-MS plasma exchange material . . . . .	80
4.4.3.1	Purification of anti-NF antibodies from plasma exchange material	80
4.4.3.2	Reactivity of purified antibodies by ELISA and flow cytometry . . . . .	81
<b>5</b>	<b>Discussion</b> . . . . .	<b>85</b>
5.1	Summary of findings . . . . .	86
5.2	Assay comparison and evaluation . . . . .	86
5.3	Anti-NF antibodies in peripheral inflammatory neuropathies . . . . .	89
5.4	Anti-NF antibodies in multiple sclerosis . . . . .	90
5.5	Potential pathogenic relevance of anti-NF autoantibodies . . . . .	92
5.6	Outlook . . . . .	93

# List of Figures

1.1	Impulse conduction in myelinated and unmyelinated axons . . . . .	4
1.2	Domains of a myelinated axon . . . . .	5
1.3	Localization of neurofascins at the node of Ranvier . . . . .	6
3.1	OE-PCR schematic . . . . .	19
3.2	Protein expression by IPTG induction . . . . .	32
4.1	Amplification and digestion for fragments of NF155 and NF186 . . . . .	51
4.2	Schematic of NF155 and NF186 cloning strategy . . . . .	52
4.3	Map of pRSV5neo-NF186TM . . . . .	52
4.4	pRSV5neo-sGFP cassette vector . . . . .	53
4.5	Schematic of sGFP fusion truncated NF variants . . . . .	54
4.6	Schematic of soluble truncated NF variants . . . . .	55
4.7	Expression profile of TE671 cells transfected with NF155 and NF186 . . . . .	57
4.8	Expression profile of sGFP fusion truncated NF variants . . . . .	58
4.9	Soluble NF155 and NF186 by SDS-PAGE and Western blot . . . . .	59
4.10	CD-Spectra of soluble NF155 and NF186 . . . . .	59
4.11	Soluble NF truncation variants by SDS-PAGE and Western blot . . . . .	60
4.12	Optimization of cell-based assay by flow cytometry . . . . .	62
4.13	Optimization of the ELISA protocol . . . . .	63
4.14	ELISA reactivity to ratNF155-NS0 crossreacts with other NS0-derived antigens . . . . .	64
4.15	Reactivity of pan-NF mAbs and NF155-specific rabbit serum . . . . .	66
4.16	Domain specificity of pan-NF mAbs by flow cytometry . . . . .	67
4.17	Serum screening by ELISA and flow cytometry . . . . .	69
4.18	ELISA screening with ratNF155-NS0 . . . . .	70
4.19	A Japanese CIDP patient with high NF155 reactivity . . . . .	71
4.20	A German CIDP patient with high NF155 reactivity . . . . .	72
4.21	NF155 reactivity in a CIDP patient benefiting from plasma exchange . . . . .	74
4.22	Two different mAbs to NF enhance experimental autoimmune neuritis . . . . .	75
4.23	Serum screening by ELISA and flow cytometry . . . . .	77
4.24	Serum screening by Western blot . . . . .	77
4.25	Anti-NF155 reactivity in 2 RR-MS patients . . . . .	78
4.26	Anti-NF186 reactivity in an RR-MS patient . . . . .	79
4.27	Purified antibodies visualized by SDS-PAGE . . . . .	81
4.28	NF-reactivity of purified antibodies . . . . .	82
4.29	Characterization of NF155-specific antibodies reactive by flow cytometry . . . . .	83

# List of Tables

3.1	Cloning primers for NF155, NF186, and truncated NF variants . . . . .	20
3.2	Restriction enzymes used in this project . . . . .	23
3.3	Patient material list . . . . .	40
3.4	List of primary and secondary antibodies used in this project . . . . .	41
4.1	Plasmid list . . . . .	56
4.2	Plasma exchange material from RR-MS patients: unpurified original material, purified anti-NF155 and anti-NF186 antibodies . . . . .	80





# List of Abbreviations

<i>E. coli</i>	<i>Escherichia coli</i>
Ab	antibody
AChR	acetylcholine receptor
AIDP	acute inflammatory demyelinating polyneuropathy
ALS	amyotrophic lateral sclerosis
AMAN	acute motor axonal neuropathy
AMPA	alpha-amino-3-hydroxy-5-methylisoxazole-4-propionic acid
ANA	anti-nuclear antibody
ANCA	anti-neutrophil cytoplasmic antibody
BBB	blood-brain barrier
BCA	bicinchoninic acid
BIS-TRIS	bis(2-hydroxyethyl) aminotris (hydroxymethyl) methane
BNB	blood-nerve barrier
BSA	bovine serum albumin
Caspr	contactin-associated protein
CD spectroscopy	circular dichroism spectroscopy
cDNA	complementary deoxyribonucleic acid
CFA	Complete Freund's Adjuvant
CIDP	chronic inflammatory demyelinating polyneuropathy
CIS	clinically isolated syndrome
CMV	cytomegalovirus
CO <sub>2</sub>	carbon dioxide
DMSO	dimethyl sulfoxide
DNA	deoxyribonucleic acid
Dnase I	deoxyribonuclease I
dNTP	deoxynucleoside triphosphate
EAE	experimental autoimmune encephalomyelitis
EAN	experimental autoimmune neuritis
EBNA	Epstein-Barr virus nuclear antigen
EBV-ori	Epstein-Barr virus origin of replication
ECL	enzymatic chemiluminescence

EDTA	ethylenediaminetetraacetic acid
ELISA	enzyme-linked immunosorbent assay
EMG	electromyography
ENA	extractable nuclear antigen
FBS	fetal bovine serum
Fc	fragment crystallizable
FCS	fetal calf serum
FITC	fluorescein isothiocyanate
FPLC	fast protein liquid chromatography
GABAb	$\gamma$ -Aminobutyric acid-B receptor
GAD65	glutamic acid decarboxylase 65
GalC	galactocerebroside
GBS	Guillain-Barré syndrome
HC	healthy controls
HCl	hydrochloric acid
HEK293	human embryonic kidney cell line
HeLa	cervical cancer cell line Henrietta Lacks
His-tag	polyhistidine tag
HRP	horseradish peroxidase
IPTG	isopropyl $\beta$ -D-1-thiogalactopyranoside
ivIG	intravenous immunoglobulin
KCl	potassium chloride
$\text{KH}_2\text{PO}_4$	potassium dihydrogen phosphate
LB media	Luria-Bertani media
LDS	lithium dodecyl sulfate
Lgi1	leucine-rich, glioma-inactivated 1
LM-Amp	Luria-Bertani media with ampicillin
mAb	monoclonal antibody
MFI	mean fluorescence intensity
$\text{MgCl}_2$	magnesium chloride
MOG	myelin oligodendrocyte glycoprotein
MOPS-SDS	3-(N-morpholino)propanesulfonic acid - sodium dodecyl sulfate
MuSK	muscle specific tyrosine kinase
$\text{Na}_2\text{HPO}_4$	disodium hydrogen phosphate
NaCl	sodium chloride
$\text{NaN}_3$	sodium azide
NaOH	sodium hydroxide
NF	neurofascin
NHS	N-hydroxysuccinimide

Ni-NTA	nickel-nitrilotriacetic acid
NMDA	N-methyl-D-aspartate
NMO	neuromyelitis optica
NS0 cells	NS0 murine myeloma cells
OE-PCR	overlap extension-polymerase chain reaction
Olig-2	oligodendrocyte transcription factor 2
OMgp	oligodendrocyte myelin glycoprotein
ON	other neuropathies
OND	other neurological (non-inflammatory) diseases
PBS	phosphate buffered saline
PBST	phosphate buffered saline with Tween-20
PCR	polymerase chain reaction
PE	phycoerythrin
PE	plasma exchange
PMSF	phenylmethylsulfonyl fluoride
PP-MS	primary progressive multiple sclerosis
PVDF	polyvinylidene fluoride
RNA	ribonucleic acid
RPMI	Roswell Park Memorial Institute medium
RR-MS	relapsing-remitting multiple sclerosis
RT-PCR	reverse-transcript polymerase chain reaction
SDS-PAGE	sodium dodecyl sulfate polyacrylamide gel electrophoresis
sGFP	super green fluorescent protein
SOC	super optimal broth with catabolite repression (glucose)
SP-MS	secondary progressive multiple sclerosis
TAG-1	transiently expressed axonal glycoprotein 1
TBE	tris/borate/EDTA
TE671	human rhabdomyosarcoma cell line
TG	thyroglobulin
TMB	3,3',5,5'-Tetramethylbenzidine
TPO	thyroid peroxidase
UV	ultraviolet
VGCC	voltage-gated calcium channel
VGKC	voltage-gated potassium channel



# **Chapter 1**

## **Introduction**

## 1.1 Neurons and glia

The nervous system contains neurons and glia. Neurons receive sensory input, transduce this information via electrical impulses to communicate with other neurons, and finally evoke bodily responses to the sensations. Glia are supporting cells that insulate and nourish neurons, and they regulate the chemistry of the extracellular space.

A neuron consists of a soma, an axon, and a varying number of dendrites. The soma contains the cytoplasm and nucleus of the neuron; in particular, it is where protein synthesis and cellular respiration takes place. The axon extends from the soma; the initial segment is the axon hillock where action potentials are initiated, and the terminal segment is the axon terminal where the axon passes on information to other cells. Dendrites branch out of the soma and receive synaptic inputs from axon terminals of other neurons.

Glia refer to astrocytes, myelinating cells, ependymal cells, and microglia. Astrocytes regulate the chemical content of extracellular space and fill the spaces between neurons. Myelinating glia, oligodendrocytes in the central nervous system (CNS) and Schwann cells in the peripheral nervous system (PNS), produce large amounts of myelin as part of their cell membranes to ensheath neuronal axons and provide trophic support. Ependymal cells line fluid-filled ventricles in the brain and are involved in cell migration during neural development. Microglia are CNS resident phagocytes that scavenge for damaged cells, plaques and infectious agents.

## 1.2 Impulse conduction

For a neuron to respond to stimuli and conduct impulses, it requires a membrane potential: an unequal distribution of charge across the cell membrane. The membrane potential, negative in the intracellular side and positive in the extracellular side, is established actively by ion pumps and passively by ion channels. At rest, the sodium ( $\text{Na}^+$ ) - potassium ( $\text{K}^+$ ) pump exchanges internal  $\text{Na}^+$  for external  $\text{K}^+$ , and  $\text{Na}^+$  channels are closed while some  $\text{K}^+$  channels are open. Thus,  $\text{K}^+$  ions are more concentrated inside the cell, and  $\text{Na}^+$  ions are more concentrated outside the cell.

Neurons convey information to other cells through action potentials. An action potential is essentially a rapid change in the membrane potential that propagates down the axon when the cell is stimulated. It is generated when a stimulus induces  $\text{Na}^+$  channels to briefly open,

allowing  $\text{Na}^+$  ions to diffuse into the nerve cell, thereby rendering the inside of the membrane positive relative to the outside. Then  $\text{K}^+$  channels open and  $\text{K}^+$  ions diffuse out of the cell; the inside of the membrane becomes more negative again. After a refractory period and without further stimulation, the membrane potential returns to the resting state.

For information to travel from one cell to another in the nervous system, the action potential, localized in only a small area of nerve cell membrane, must travel down the axon. When an action potential occurs on one patch of membrane, the adjacent membrane patch have opposite charges across the membrane in relation. Essentially an electric circuit is created between the two patches of membrane, and the  $\text{Na}^+$  influx stimulates the adjacent membrane patch to generate its own action potential. The conduction velocity depends on how far ahead the depolarization of adjacent membrane area spreads, which depends on the diameter of the axon and extent of myelination.

### **1.3 Myelination and saltatory conduction**

Some axons are coated with myelin sheath to increase conduction velocity. Myelin is plasma membrane extensions of oligodendrocytes in the CNS and Schwann cells in the PNS that ensheath the axon in successive compact layers while excluding cytosol. The thickness of the myelin sheath is proportional to the axon's diameter. Neurons are typically associated with many such glial cells down the length of their axons. One region of myelin formed from a glial cell is separated from the next by an unmyelinated area known as the node of Ranvier. Electrical activity on the axon is confined to these nodes: as the myelin sheath is insulating, it is only at the nodes where the axonal membrane is in contact with extracellular fluid and ions can flow across the axonal membrane.

Impulse conduction of a myelinated axon require the impulse to jump over myelinated segments to generate action potentials only at the nodes. This process is known as saltatory conduction. Since ions can move across the axonal membrane only at the unmyelinated nodes, the passive spread of depolarization from the excess positive ions in the cytosol upon an action potential can extend to the next node with little loss; thereby triggering an action potential at the next node. Thus, myelination of an axon significantly increases conduction velocity compared to unmyelinated axons and allows for rapid neuronal signalling.

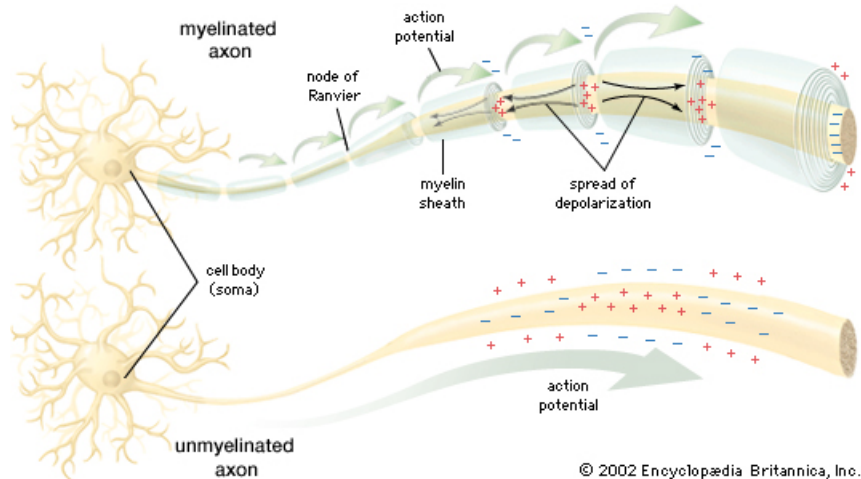


Figure 1.1: **Impulse conduction in myelinated and unmyelinated axons** (taken from 2002 Encyclopædia Britannica, Inc.)

## 1.4 Molecular view of the myelinated axon

The myelinated axon is organized into four distinct, repeating domains: the node of Ranvier, paranode, juxtaparanode, and internode (Salzer et al., 2008). These domains are interdependent for domain assembly and maintenance.

The node of Ranvier is the part of the axon that is exposed to the extracellular environment. In the CNS the node is covered by perinodal astrocyte processes (Black and Waxman, 1988) while in the PNS it is encased by interdigitating microvilli of adjacent Schwann cells and the basal lamina (Salzer et al., 2008). The node is enriched with voltage-gated ion channels ( $\text{Na}^+$  and  $\text{K}^+$  channels) necessary for impulse conduction, as well as adhesion molecules NrCAM and the 186 kDa isoform of neurofascin (NF186) (Salzer et al., 2008).

Axo-glial junctions are found at the paranodal region, where the axon and myelin are brought to their closest proximity. Under the electron microscope, these junctions are a series of loops that invaginate the axolemma and on each loop are a series of transverse bands that are also known as septate-like junctions (Peters et al., 1991). The bands were later identified to be the complex of Caspr and contactin-1 on the axonal surface and 155 kDa isoform of neurofascin (NF155) on the glial paranodal loops (Sherman et al., 2005). These junctions promote cellular adhesion and also form a barrier against the diffusion of ions between the node and internodes during action potential conduction (Rosenbluth, 1995). Furthermore, they also maintain the



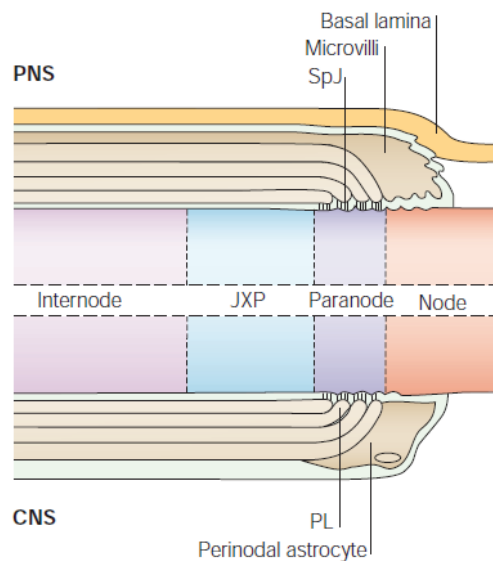


**Figure 1.2: Domains of a myelinated axon:** The axon in both the PNS and CNS is organized into four distinct domains: the internode, juxtaparanode (JXP), paranode, and node. The node is covered by interdigitating Schwann cell microvilli in the PNS and by perinodal astrocyte processes in the CNS. Paranodal loops (PL) form septate-like junctions (SpJ) with the axon for attachment. Myelinated fibres are covered by a basal lamina in the PNS. Adopted from Poliak and Peles (2003).

density of ion channels in the nodal complex by limiting lateral diffusion from the node (Rios et al., 2003), as well as avoiding the displacement of juxtaparanodal components.

The juxtaparanodal region is localized between the paranodal and internodal region just under the compact myelin. It is enriched with  $K^+$  channels that are involved in repolarization during impulse conduction (Salzer et al., 2008). There are also adhesion complexes composed axonal and glial contactin-2/TAG-1 and axonal Caspr2 (Traka et al., 2003). The internodal region is the portion that is ensheathed with compact myelin. The glial cell and the axon are separated by a periaxonal space, and their interaction involves cellular surface proteins (Yu and Bunge, 1975).

## 1.5 Neurofascin

Neurofascin is a cell adhesion molecule that is important for the formation and maintenance of nodes of Ranvier. It comprises two major isoforms upon alternative splicing: neuronal isoform NF186 and glial isoform NF155. Axonal NF186 and NrCAM interact with glial gliomedin in the PNS to cluster  $Na^+$  channels at the node of Ranvier (Feinberg et al., 2010). Glial NF155 is found at the axo-glial junctions to interact with axonal Caspr and contactin-1, forming a barrier excluding the nodal complex from the internodes (Feinberg et al., 2010). NF186 is present on the axon exclusively at the node and axonal initial segments (Zonta et al., 2008); NF155 is found at the paranodal regions, on oligodendrocytes in the CNS and Schwann cells in the PNS (Davis et al., 1996; Tait et al., 2000).

Disruption of NF function can result in defective saltatory conduction, stemming from paranodal

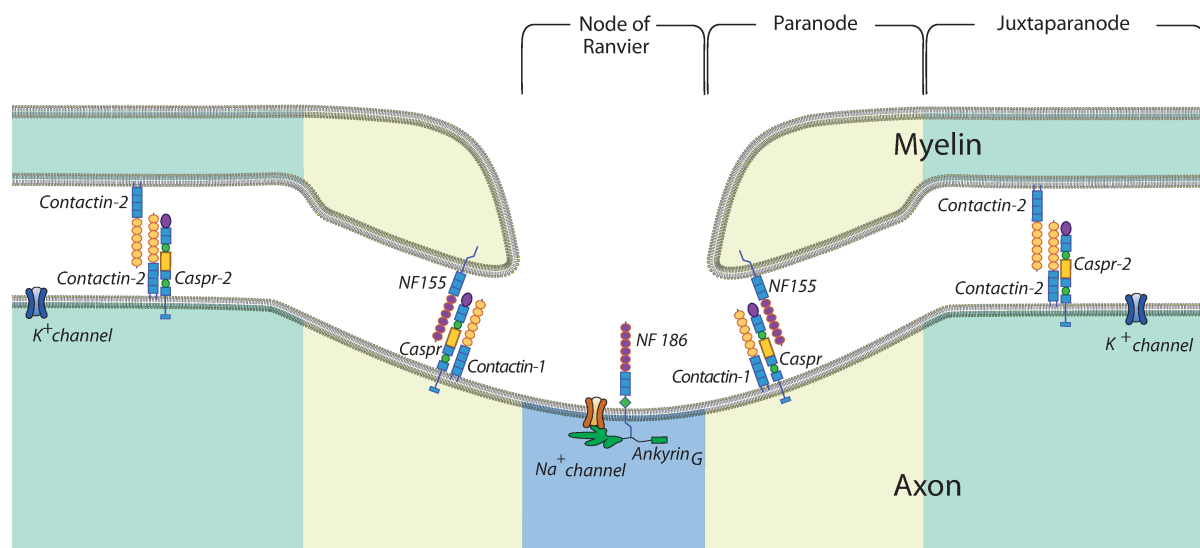


Figure 1.3: **Localization of neurofascins (NF155, NF186) at the node of Ranvier:** NF186 is localized on the axon in the nodal region anchored to ankyrin G while NF155 is found in the paranodes on the myelinating glial cell interacting with the contactin-1/Caspr complex. Other adhesion molecules (ex. Caspr-2 and contactin-2) are found in the juxtaparanode. Sodium channels are anchored to ankyrin G at the node of Ranvier while potassium channels are localized on the juxtaparanodal region. Adopted from Meinl et al. (2010).

axo-glial junction disruption and redistribution of ion channels (Thaxton et al., 2010). Pan-NF knockout mice show severe defects in node formation (Sherman et al., 2005) as well as loss of the transverse bands (Sherman et al., 2005). Reconstitution of the paranodal adhesion complex using NF155 knock-in cannot promote PNS nodal complex assembly without NF186 (Sherman et al., 2005), but in the CNS, either one of the neurofascin isoforms can rescue the node of Ranvier (Zonta et al., 2008). While there are subtle differences between the nodes of Ranvier in the CNS and PNS (Figure 1.2), NF155 and NF186 are found in both the CNS and PNS at similar sites in the nodes (Poliak and Peles, 2003) (Figure 1.3).

## 1.6 Effects of myelin disruption

The function and integrity of a myelinated axon are dependent on the organization of the specialized domains induced by myelination, and disruption of this organization due to demyelination, induced by inflammation for example, may lead to conduction block and axonal degeneration (Nave, 2010).

Conduction block upon demyelination reflects the lack of insulating properties of myelin, the localization of  $\text{Na}^+$  channels that remain at the sites of former nodes, and an inadequate presence of  $\text{Na}^+$  channels in the former internodal regions as well as the misexpression of other

ion channels that impair impulse conduction (Salzer et al., 2008). Furthermore, any impulse conduction along a demyelinated axon would require significantly more energy compared to myelinated axons due to channel redistribution (Waxman, 2006). With remyelination, conduction is restored since once more the axon is insulated in some segments and the distance between successive channel clusters is shortened (Honmou et al., 1996).

Distal axonal degeneration may also be induced by myelin disruption since myelinating glial cells modify axonal properties during myelination. Although the exact cause is unknown, some observations provide insight to possible contributing factors. Normal axonal transport in myelinated axons is impaired when axo-glial junctions in the paranodal region are defective (Martini, 2001). Impulse conduction along demyelinated axons require more energy due to channel redistribution and higher  $\text{Na}^+$  channel density, perturbing the energy balance as a result. Consequently, the  $\text{Na}^+$  - calcium ( $\text{Ca}^+$ ) exchanger function fails, leading to high  $\text{Ca}^+$  levels inside the neuron thereby trigger axonal degeneration (Nave, 2010). Loss of trophic and metabolic support from glial cells (Nave and Trapp, 2008) as well as alterations of the axonal cytoskeleton and chemistry (Salzer et al., 2008) may also contribute to the pathology.

## 1.7 Inflammatory diseases in the nervous system

The CNS and PNS are immune privileged sites: they are separated from the systemic immune compartment by the blood-brain barrier (BBB) in the CNS and the blood-nerve barrier (BNB) in the PNS. These barriers must be breached for immune factors to contribute to the myelin disruption and damage in inflammatory nerve diseases. The BBB regulate transport of solutes from blood to the CNS parenchyma (Owens et al., 2008). This barrier may be altered in an inflammatory setting; supporting evidence comes from observations of delocalized proteins at the tight junctions (Kirk et al., 2003) and metalloprotease alteration of the basal lamina (Liu et al., 2008). The BNB restricts access of soluble mediators to the peripheral nerve, though less restrictive than the BBB. The BNB is absent at the most proximal and distal parts of peripheral nerve (ex. nerve roots and terminals, dorsal root ganglia) (Kieseier et al., 2012).

Demyelination can occur in the context of inflammation; it is a feature of some autoimmune inflammatory diseases of the nervous system, such as Guillain-Barré syndrome (GBS) and chronic inflammatory demyelinating polyneuropathy (CIDP) in the PNS, and multiple sclerosis (MS) in the CNS. In these diseases, antibody and complement deposition, cellular infiltration,

and varying degrees of axonal loss have also been shown (Lassmann et al., 2007; Kieseier et al., 2012). Antibodies to myelin components may direct complement deposition and activate immune cell activity resulting in myelin destruction (Wootla et al., 2011). As the myelin membrane may protect axons from auto-reactive cytotoxic T cells, the loss of myelin may result in secondary axonal degeneration (Lassmann et al., 2007). Furthermore, reactive radicals generated by activated microglia and macrophages may diffuse into the exposed axon to disrupt mitochondria ATP generation (Nave, 2010; Smith et al., 1999), resulting in an energy imbalance in the neuron.

### **1.7.1 Inflammatory demyelinating diseases in the PNS**

Guillain-Barré syndrome is an acute inflammatory polyneuropathy of several subtypes that are differentiated based on clinical presentation and underlying pathology. There is evidence that, in some cases, infection and vaccination may trigger an aberrant immune response that subsequently lead to a breakdown of the blood nerve barrier to trigger GBS manifestation (Hughes and Cornblath, 2005). The GBS variant acute inflammatory demyelinating neuropathy (AIDP) is characterized by multifocal segmental demyelination and inflammatory infiltrates (Yuki and Hartung, 2012). Demyelinated axons are found at the spinal roots and peripheral nerves, often accompanied by axonal degeneration (Lehmann et al., 2009; Yuki and Hartung, 2012). Demyelination was shown to be induced by serum taken from a proportion of GBS patients (Harrison et al., 1984). Histological studies using patient tissue samples revealed deposition of antibodies and activated complement on Schwann cells (Hafer-Macko et al., 1996) as well as nerve infiltration of T cells and macrophages (Prineas, 1981). Furthermore, in an animal model that resembles AIDP, myelin antigen-induced experimental autoimmune neuritis (EAN), myelin protein specific T cells were found to be neuritogenic and Schwann cells were assaulted by antibody mediated cytotoxicity as well as complement dependent cytotoxicity (Spies et al., 1995; Lonigro and Devaux, 2009). Although the involvement of antibodies in the pathogenesis of AIDP is evident, the target of pathogenic autoantibodies in many patients is currently unclear.

For the axonal GBS variant acute motor axonal neuropathy (AMAN), antigenic targets are better defined. Antibodies to several gangliosides (ex. GM1, GD1a, GM1b, GalNAc-GD1a) and complexes of these gangliosides were detected in patient serum (Kaida and Kusunoki, 2010). These antibodies preferentially target the nodes of Ranvier and the motor nerve terminal. Fur-

thermore, anti-ganglioside antibodies were found to exert pathogenic effects by complement fixation and macrophage activation (Hughes and Cornblath, 2005) that could lead to conduction block and injury to Schwann cells though the myelin is mostly still intact (Lehmann et al., 2009).

Chronic inflammatory demyelinating polyneuropathy (CIDP) involves proximal and distal functional deficits (Koeller et al., 2005). It is characterized by nerve infiltration of T cells and macrophages, and deposition of antibody and complement on myelinated nerve fibres (Koeller et al., 2005). Increased levels of pro-inflammatory cytokines are found in the CSF and also in serum, and more activated macrophages and T cells are found in circulation (Lehmann and Hartung, 2011). It was suggested that some T cells activate residing macrophages, which then enhanced phagocytosis and increased production of pro-inflammatory cytokines, proteases, and reactive oxygen and nitrogen species (Lehmann and Hartung, 2011). In addition, antibody and complement deposits were found on Schwann cells and also in intraneural blood vessels (Dalakas and Engel, 1980). The involvement of antibodies in CIDP is further supported by passive transfer experiments into an animal model of peripheral neuropathy (EAN) in which antibodies from CIDP patients were shown to induce conduction block and demyelination pathology (Yan et al., 2000). However, the antigenic targets of the pathogenic antibodies are currently unknown.

### **1.7.2 Inflammatory demyelinating disease in the CNS**

Multiple sclerosis (MS) is an inflammatory demyelinating disease that is heterogeneous in pathogenesis (Lassmann et al., 2007). It is also variable in onset and progression: the majority of patients develop MS with a relapsing course that is followed by a progressive phase, while some patients enter the progressive phase from the onset (Lassmann et al., 2007). MS is characterized by demyelination with partial axonal preservation in lesions found in the CNS. These lesions occur in the context of inflammation, though active demyelination may be induced by different immune mechanisms: (1) T cell and macrophage mediated, (2) antibody and complement mediated, (3) production of reactive radicals disturbing mitochondrial function resulting in hypoxia, and (4) mild inflammation associated with oligodendrocyte degeneration (Lassmann et al., 2001). In slowly expanding lesions in progressive MS, activated microglia and rarely immune cell infiltration are present; it was hypothesized that demyelination in the progressive phase is driven by soluble factors from immune cells that became compartmen-

talized in the CNS (Lassmann et al., 2007). Besides demyelinating plaques, another hallmark of MS is the presence of oligoclonal bands in cerebrospinal fluid (Disanto et al., 2012). The involvement of autoantibodies in MS pathogenesis is further evident in patients who were unresponsive to steroids but had greatly benefited from plasma exchange (Keegan et al., 2005), where blood is separated from plasma and the plasma is exchanged with albumin prior to returning the cellular components back into the patient. (Wootla et al., 2011). Autoantibodies to myelin components (protein, lipid, carbohydrate) were found in some MS patients and some targets (ex. myelin oligodendrocyte glycoprotein, myelin basic protein, glycosphingolipids) were identified (Wootla et al., 2011). However, confirmation of the antigen specificity of pathogenic autoreactive antibodies is still lacking (Wootla et al., 2011).

## **1.8 Autoantibodies against neurofascin in inflammatory diseases in the PNS and CNS**

Neurofascin-specific autoantibodies were first detected in MS patients by Mathey et al. (2007) using a proteomic approach. They found that some MS patients show such antibodies by two-dimensional Western blot with human myelin glycoprotein. Functional studies revealed that antibody targeting of neurofascin using a pan-NF monoclonal antibody (mAb) disrupted nerve conduction in rat hippocampal slices in the presence of complement. Furthermore, in a T cell transfer experimental autoimmune encephalomyelitis (EAE) model, the pan-NF mAb exacerbated clinical disease presumably by mediating axonal injury when the blood-brain barrier of the CNS was breached (Mathey et al., 2007). Although the potential pathogenicity of anti-NF antibodies was demonstrated, the frequency of these antibodies in MS patients is unclear.

Neurofascin-specific autoantibodies were also reported in patients with GBS and CIDP by Devaux et al. (2012) and Pruess et al. (2011). Devaux et al. had found that 43% of GBS patients and 30% of CIDP patients showed IgG fixation at nodes or paranodes on teased nerve fibres from rodents. They had further investigated the specificity of these antibodies and found that a small subset (5%) of GBS/CIDP patients harbour antibodies to the extracellular domain of the rat isoforms of NF186, gliomedin, or contactin. Pruess et al. had performed ELISA using rat NF155 that is commercially produced in NS0 murine myeloma cells. They found a higher level of NF reactivity in GBS patient group compared to healthy controls. Furthermore, in an animal model of GBS, namely EAN, pathogenic antibodies against both isoforms of NF were found

upon inducing disease by myelin homogenate injection (Lonigro and Devaux, 2009).

Previous studies to detect neurofascin-specific antibodies in human serum utilized Western blotting with glycoprotein preparations from human myelin or recombinant rat NF155 from NS0 murine cells, ELISA using also the rat NF155, indirect immunofluorescence using rodent nerve fibres, and HEK293-cell-based assay using the rat isoforms of NF. There are two obvious limitations to these detection methods for potentially physiologically relevant antibodies to neurofascin. First, with Western blot the protein antigen is denatured and antibodies detected may be directed to hidden epitopes that are irrelevant for disease. Second, antibody detection assays using rodent isoforms of the antigens may not detect antibodies specific to the human isoform of the protein antigen; the species-specific sequences of the protein antigens in addition to species-specific post-translational modifications may elicit false positives against immunogenic rodent-specific differences and false negatives when a pathogenic epitope is absent or hidden by modifications. These limitations confound the significance of the results obtained, making it difficult to appreciate the disease relevance of anti-NF autoantibodies.





## **Chapter 2**

# **Objectives and Strategy**

## 2.1 Objectives

Neurofascin isoforms 155 and 186 (NF155, NF186) are implicated as autoantibody targets in demyelinating diseases in the peripheral and central nervous system, namely GBS, CIDP, and MS. However, the methods used in previous studies have inherent limitations that hinder a clear evaluation of the presence of such antibodies in these patient groups. These limitations include the display of denatured protein which may present hidden epitopes that are irrelevant for disease while masking conformationally intact relevant epitopes, and the use of rodent NF rather than human NF which introduces a cross-species difference to confound the results. The pathogenicity of antibody targeting of neurofascin in the central nervous system was shown using an experimental autoimmune encephalomyelitis model in which a monoclonal pan-NF antibody exacerbated clinical disease. However, such pathogenicity has not been shown in any peripheral nerve disease model.

Here we want to clearly determine the frequency of anti-human-neurofascin autoantibodies among patients with GBS, CIDP, and MS and characterize the reactive antibodies for functional significance. Furthermore, we evaluate the pathogenic potential of anti-NF antibodies in the context of peripheral demyelinating conditions.

## 2.2 Strategy

We developed assays to detect serum antibodies specific for human NF155 and NF186. We started by cloning human NF155 and human NF186 from human brain RNA, and recombinantly expressing the proteins in human cell lines as a cell-bound form and a soluble form. Then we established three antibody detection assays: cell-based assay by flow cytometry, ELISA, and Western blot; they were validated using two anti-NF mAbs and NF155-specific rabbit serum. The NF155 and NF186 were displayed in their native conformation on the transfectants for flow cytometry, in a denatured state on a Western blot, and in a conformation that was neither native or completely denatured when they were adsorbed onto the solid support for ELISA. We used a test cohort of patient samples to optimize the assays to maximize sensitivity and clarity of results.

We investigated the frequency of anti-human NF155 and NF186 antibodies in the serum of patients with demyelinating disease of the PNS and CNS (GBS: AIDP and AMAN, CIDP, MS) with

our optimized assays. For comparison, we included serum samples from healthy donors and from patients with other neuropathies, non-demyelinating nervous system disease amyotrophic lateral sclerosis (ALS), and other non-inflammatory neurological diseases. The positive samples that we identified were further tested for nodal or paranodal recognition on tissue sections. Since we suspected low levels of NF reactivity in relapsing-remitting MS (RRMS) patients, we purified NF-specific antibodies by affinity chromatography from plasma exchange material of these patients and tested them for reactivity in our assays.

To probe for disease relevance, we characterized the reactive antibodies of positive samples by performing serial dilution and isotyping, and by determining specific domain recognition on the NFs. Furthermore, we investigated potential pathogenicity of NF-targeting in peripheral neuropathies by inducing experimental autoimmune neuritis (EAN) in rats with P2-peptide immunization and injecting monoclonal anti-pan-NF antibodies at disease onset. To provide a coherent picture, I included experiments performed by colleagues or collaboration partners. People involved in the analyses are mentioned in the relevant sections.



## **Chapter 3**

# **Material and Methods**

## **3.1 Molecular cloning**

### **3.1.1 Molecular biological methods**

#### **3.1.1.1 Reverse-transcriptase polymerase chain reaction (RT-PCR)**

Superscript III reverse transcriptase (Invitrogen, Darmstadt, Germany) was used to synthesize cDNA (700-900 bp) from human brain RNA (prepared by Dr. Tobias Derfuss). The reaction was performed according to the protocol provided by the manufacturer using buffers provided in the kit and self-designed NF sequence specific primers directed to the cytoplasmic region and to the region between immunoglobulin-like domain-2 and -3 (Ig-2, Ig-3; primers listed in Table 3.1). For each RT-PCR reaction, 1 µg of human brain RNA was used as template, and the resulting cDNA product was used for amplification by polymerase chain reaction.

#### **3.1.1.2 Polymerase chain reaction (PCR)**

Polymerase chain reaction (PCR) was performed using a thermocycler (Biometra, Goettingen, Germany) for two main purposes: (1) amplification of DNA fragment for molecular cloning, and (2) screening of bacterial colonies for plasmid of interest. All primers were designed to have an annealing temperature between 58-64 °C and were synthesized by Metabion (Martinsried, Germany). A typical amplification reaction involved a sample of template DNA (ex. cDNA, PCR product, plasmid, bacteria cells), two oligonucleotide primers, deoxynucleotide triphosphates (dNTPs), reaction buffer, magnesium, and a thermostable DNA polymerase. Taq DNA polymerase (Roche, Penzberg, Germany) was used unless otherwise specified. The reaction involved an initial denaturing step at 95 °C for 2 min. This was followed by typically 25-40 cycles consisting of: (1) Denaturation step at 95 °C for 2 min, (2) Annealing step at between 53-62 °C for 1 min, and (3) Elongation step at 72 °C for 1-2 min. The duration of the elongation step depended on the length of the expected PCR product (1 min for 1 kbp). The elongation time of the final cycle was set to 10 min to ensure that all products were fully extended. Afterwards, it is stored at 4 °C.

Typical PCR mixture:

Molecular cloning	Colony screening	
5 $\mu$ L	2 $\mu$ L	10x Buffer with $MgCl_2$
1 $\mu$ L	0.4 $\mu$ L	10 mM dNTP
0.25 $\mu$ L	0.1 $\mu$ L	Forward primer
0.25 $\mu$ L	0.1 $\mu$ L	Reverse primer
0.5 $\mu$ L	0.2 $\mu$ L	Taq DNA polymerase
2 $\mu$ L DNA	Bacterial cells	Template
41 $\mu$ L	17.2 $\mu$ L	Water
50 $\mu$ L	20 $\mu$ L	<b>TOTAL</b>

### 3.1.1.3 Overlap-extension PCR

Overlap-extension PCR is an efficient method to generate truncation mutants when restriction endonuclease recognition sites are not available for precise cleavage and ligation. It is a simple method where initial PCR products are generated with overlapping gene segments that can then be used as templates for a subsequent PCR to create the full length construct.

Referring to Figure 3.1, AB and CD are two separate DNA fragments to be joined to form AD by overlap-extension PCR. The internal primers (B and C) contain the overlapping sequence to join AB and CD, while the outer primers (A and D) can only work together to amplify the joined DNA template. The first step is to separately generate AB and CD by PCR, and the second reaction combines the first two PCR products using outer primers A and D to amplify the hybrid product AD. KOD DNA polymerase (Novagen, Darmstadt, Germany) was used because it is a high fidelity thermostable polymerase that is superior in accuracy, yield and processivity compared to other DNA polymerases currently available. The following details the reaction conditions used:

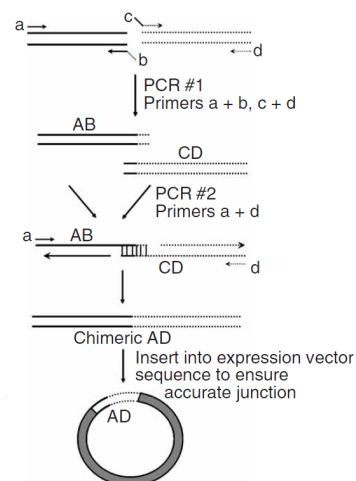


Figure 3.1: **OE-PCR schematic** from Heckman and Pease (2007)

Fragment AB	Fragment CD			
2.0 µL	2.0 µL	KOD buffer 2		
1.2 µL	1.2 µL	25mM MgCl <sub>2</sub>		
1.6 µL	1.6 µL	2 mM dNTP		
0.1 µL	0.1 µL	Forward primer A or C	1 Denaturation	94 °C 1 min
0.1 µL	0.1 µL	Reverse primer B or D	2 Denaturation	94 °C 15 sec
0.5 µL	0.5 µL	Template plasmid (5ng)	3 Annealing	55 °C 30 sec
13.5 µL	13.5 µL	Water	4 Elongation	72 °C 20 sec
1.0 µL	1.0 µL	KOD DNA polymerase	5 Elongation	72 °C 10 min
			6 Pause	4 °C ∞
20 µL	20 µL	TOTAL		

Subsequently,

Fragment AD	PCR-AB + PCR-CD			
10 µL + 10 µL	PCR-AB + PCR-CD			
3.0 µL	KOD buffer 2		1 Denaturation	94 °C 1 min
1.8 µL	25mM MgCl <sub>2</sub>		2 Denaturation	94 °C 15 sec
4.0 µL	2 mM dNTP		3 Annealing	55 °C 30 sec
0.3 µL	Forward primer A		4 Elongation	72 °C 1 min
0.3 µL	Reverse primer D		5 Elongation	72 °C 10 min
20.6 µL	Water		6 Pause	4 °C ∞
50 µL	TOTAL			

### 3.1.1.4 Cloning primers for NF155, NF186, and truncated NF variants

Table 3.1: Cloning primers for NF155, NF186, and truncated NF variants

	Description	Name	Sequence
1	RT-PCR	NFASC-RT-inlg3	ATG TCT GGT GTT GGG AC
2	RT-PCR	NFASC-RT1-Cyt	CAG AGA TGT CTG ACT GC
3	NF cloning	NFASC-Sall-for	GTC GAC ATG GCC AGG CAG CCA CCG
4	NF cloning	NFASC-IgG2/3-HindIII-rev	ACA TGA AGC TTG GTG TTC TTT C
5	NF cloning	NFASC-Fn2-Fn3-for	GGT TAC TCC GGA GAA GAT TAT C
6	NF cloning	NFASC-Fn2-Fn4-for	GGT GAA TCC GGA GAA GAT TTA CCC AG
7	NF cloning	NFASC-Bgl2-TM-Cyt-rev	AGT AGA TCT TCA GCC GCG ACT CCT CTT GAT G
8	NF with HIS tag	NFASC-soluble rev	CAG TAG ATC TTA GTG ATG GTG ATG GTG ATG GCC CTG GGT GGC GAT GTC
9	pET F1 primer	NFSC-F1 for	TAT AGT ACT ATG GGA GCC ATC GAA ATT CCT ATG
10	pET F1 primer	NFSC-F1 rev	CAG TAG ATC TTA GTG GTG ATG GTG ATG GTG ATC CAG CAC ACT GAC AAA GG
11	pET F2 primer	NFSC-F2 for	TAT AGT ACT ATG GTC AGT GTG CTG GAT GTG C
12	pET F2 primer	NFSC-F2 rev	CAG TAG ATC TTA GTG GTG ATG GTG ATG ATC TTC TCC GGA GTA ACC GAT
13	pET F3-5 primer	NFSC-155-F3 for	TAT AGT ACT ATG TCC GGA GAA GAT TAT CCC AGG
14	pET F3-8 primer	NFSC-186-F3 for	TAT AGT ACT ATG GGA GAA GAT TTA CCC AGT GC
15	sGFP forward for RSV5neo	SuperGFP-Xba1-Cla1-for	GC TCT AGA GCC ATC GAT GGC GGA GGT GGC AGC ATG GTG AGC AAG GGC GAG
16	sGFP reverse for RSV5neo	SuperGFP-Xba1-rev	GC TCT AGA GC TTA GTG ATG GTG ATG GTG ATG



17	6lg TM fragment for	NF-6lg-Sal1-Nhe1-for	A CGC GTC GAC TCT CTA GCT AGC TGA TCA GGC CAC TAA CAA CCA AGC GGA CAT CG
18	6lg TM fragment rev	NF-Cyt-Cla1-rev	GCC ATC GAT GGC GCC GCG ACT CCT CTT GA
19	Fn1Fn2 fragment 1	Fn1Fn2-Sal1-Signal-for	TAT GTC GAC ATG GCC AGG CA
20	signal seq reverse	Fn1Fn2-signal-overlap-rev	AAC GGT TAG TCG GCT GCG TCA GCT CAT TC
21	Fn1Fn2 fragment 2	Fn1Fn2-overlap-gene-for	GAC GCA GCC GAC TAA CCG TTT GGC TGC CCT
22	Fn1Fn2 fragment 2	Fn1Fn2-gene-Mro1-rev	TC TTC TCC GGA GTA ACC GAT G
23	Fn1Fn2 fragment 3	Fn1Fn2-Mro1-TM-for	GTT ACT CCG GAG AAG ATT ACA CCA ACA ACC AAG CCG
24	Fn3Fn4 fragment1	Fn3Fn4-sig-overlap-rev	AAT CTT CTC CCG GCT GCG TCA GCT CAT TC
25	Fn3Fn4 fragment2	Fn3Fn4-f3f4-overlap-for	GAC GCA GCC GGG AGA AGA TTA TCC CAG GG
26	Fn4Muc fragment1	Fn4Muc-sig-overlap-rev	AAT CTT CTC CCG GCT GCG TCA GCT CAT TC
27	Fn4Muc fragment2	Fn4muc-f4muc-overlap-for	GAC GCA GCC GGG AGA AGA TTT ACC CAG TGC
28	Fn3 fragment2	Fn3-f2-overlap-Bst-rev	TGT TGG TGT ATA CTC CTT CCG GGG TGG TG
29	Fn3 fragment2	Fn3-f3-overlap-Bst-for	GGA AGG AGT ATA CAC CAA CAA CCA AGC GGA
30	Muc fragment1	Muc-sig-overlap-rev	CTT CAT TCG GGG GCT GCG TCA GCT CAT TC
31	Muc fragment2	Muc-muc-overlap-for	GAC GCA GCC CCC GAA TGA AGC TAC TCC AAC

### 3.1.1.5 Agarose gel electrophoresis

Agarose gel electrophoresis enables visualization of the purity, yield and size of DNA molecules in a preparation. In addition, DNA molecules of different sizes are separated and can be selectively eluted from the gel. To cast an agarose gel, agarose powder (Biozyme, Hessisch Oldendorf, Germany) was dissolved in TBE buffer by heating and poured into a self assembled mold with an appropriate comb. TBE buffer (10x) consisted of 108 g of Trizma base (Sigma-Aldrich, Munich, Germany), 55 g of Boric acid (Merck, Darmstadt, Germany) and 40 mL of 0.5 M EDTA (pH 8.0) in 1 L of water. The percentage of agarose in a gel varied depending on the size of the DNA molecule of interest. In this work 0.8% to 1.5% agarose gels were used. Ethidium bromide was added into the gel mixture at 1 µg/mL to visualize DNA under UV light ( $\lambda = 254\text{-}366$  nm). The gel was placed in TBE buffer in a horizontal electrophoresis chamber and samples that were mixed with gel loading dye were loaded into the wells. Gel loading dye (6x) consisted of 50% glycerin, 0.02% bromophenol blue (Serva, Heidelberg, Germany), 0.02% xylencyanol (BioRad, Munich, Germany), and 10 mM Trizma base (Sigma-Aldrich), and

was adjusted to pH 7.5. DNA ladders (100 bp or 1 kb; New England Biolabs (NEB), Frankfurt, Germany) were included for size recognition. The electrophoresis conditions were 100 mV for 30 min to 1 h at room temperature. Afterwards, the gel were visualized in a UV light box.

#### **3.1.1.6 DNA extraction from agarose gel**

DNA molecules were eluted from agarose gel pieces cut from the whole gel with a scalpel in the UV light box. The elution was done using EasyPure kit (Biozyme) according to the protocol provided by the manufacturer for a final elution volume of 12  $\mu$ L.

#### **3.1.1.7 DNA quantification**

The amount of DNA in a solution was measured on a Nanodrop spectrophotometer (Peqlab, Erlangen, Germany). First a blank measurement was done with the DNA buffer, then 2  $\mu$ L of DNA sample was loaded onto the stage for photometric measurement at 260 nm, and the concentration and purity (from RNA and protein) of the DNA sample were measured.

#### **3.1.1.8 DNA digestion with restriction endonuclease**

Restriction digestion using endonucleases was performed on PCR products and plasmids. Both conventional (New England Biolabs and Fermentas, St. Leon-Rot, Germany) and FastDigest (Fermentas) formats were used. For a conventional restriction enzyme, 1 U is described to be the amount of enzyme required to cleave 1  $\mu$ g of substrate DNA in 60 min. For a FastDigest enzyme, 1  $\mu$ L is made to cleave 1  $\mu$ g of substrate DNA in 5-15 min. For each enzyme, the digest reaction was carried out according to the manufacturer's recommendation of buffer usage and temperature for incubation. A consideration common to all digest reactions was that the volume of enzyme used should not exceed 10% of total volume of the reaction, ensuring that the glycerol concentration of the reaction remains less than 5%. In suboptimal conditions or with prolonged incubation times, restriction enzymes are capable of star activity, which means they can cleave sequences other than their defined recognition sequence. Double digest reactions were carried out if there exists a compatible buffer and if the two recognition sequences were sufficiently far apart from each other to avoid steric hindrance. Otherwise the cleavage reactions were done sequentially, using alcohol precipitation (3.1.1.12) in between reactions to precipitate the DNA and exchange the buffer.

Table 3.2: Restriction enzymes used in this project

Enzyme	Restriction site	Manufacturer
<i>AvrII</i>	C'CTAGG	New England Biolabs
<i>BamHI</i>	G'GATCC	Fermentas
<i>BglII</i> FastDigest	A'GATCT	Fermentas
<i>BsiMI</i>	T'CCGGA	-
<i>BstZ17I</i>	GTATAC	New England Biolabs
<i>Clal</i> FastDigest	AT'CGAT	Fermentas
<i>EcoRI</i>	G'AATTC	New England Biolabs
<i>HindIII</i>	A'AGCTT	New England Biolabs
<i>MroI</i>	T'CCGGA	Roche
<i>NheI</i>	G'CTAGC	New England Biolabs
<i>PmeI</i>	GTTT'AAAC	New England Biolabs
<i>SalI</i> FastDigest	G'TCGAC	Fermentas
<i>Scal</i>	AGT'ACT	New England Biolabs
<i>SmaI</i>	CCC'GGG	New England Biolabs
<i>XbaI</i>	T'CTAGA	New England Biolabs

### 3.1.1.9 DNA blunt end synthesis

DNA polymerase I large fragment (Klenow) from *E. coli* has 5' to 3' DNA polymerase and 3' to 5' exonuclease activities. It was used here to fill in the single-strand restriction endonuclease termini to produce a double-strand blunt end. The large fragment of DNA polymerase I kit (Invitrogen) was used and reaction conditions were according to the instructions from the manufacturer.

### 3.1.1.10 DNA ligation

Fragments of DNA generated by PCR or by restriction digest were ligated to each other and to the vector to produce a plasmid. After determining the DNA concentration of each fragment or the linearized vector, a ratio of 1 (fragment) to 1 (fragment) was used to join fragments for the insert and a ratio of 1 (vector) to 4 (insert) was used to form a complete plasmid. Ligation reactions were set up as double ligation (1 insert, 1 vector) or triple ligation (2 fragments of the insert, 1 vector). T4 DNA ligase (Invitrogen) was used here and reactions were set up according to the protocol provided by the manufacturer, and incubated at room temperature for 30 min or at 16 °C overnight. After the ligation reaction, 1-2 µL of the reaction was used to transform *E. coli* cells (Section 3.1.2.1), typically DH5 $\alpha$  or TOP10 (Invitrogen).

#### **3.1.1.11 TOPO TA cloning**

TOPO TA cloning was used to amplify single DNA fragment molecules. It is an alternate method to PCR for amplifying DNA fragments of interest. TOPO TA cloning kit (Invitrogen) was used and the protocol from the manufacturer was followed. The technique involved a linear vector with DNA topoisomerase I covalently attached to both free 3' ends and PCR products with adenine overhangs at the 3' end. The free 5' end of the PCR product attacks the 3' end of the vector, and the topoisomerase facilitates its ligation to the vector. This product was then amplified by transformation into *E. coli* cells, typically TOP10 (Invitrogen).

#### **3.1.1.12 Alcohol precipitation of DNA**

Alcohol precipitation of DNA was carried out by adding 0.1 volume of 3 M sodium acetate and 2.5 volume of 100% ethanol to the mixture containing the DNA. The mixture was placed in  $-80^{\circ}\text{C}$  for at least 30 minutes. After centrifugation at 14 000 rpm for 30 min at  $4^{\circ}\text{C}$ , the DNA was pelleted and the supernatant was discarded.

An alternative technique for small scale DNA precipitation is by using the Pellet Paint Co-precipitant kit (Novagen). Pellet Paint is a non-fluorescent-dye-labelled carrier molecule that enables visualization of the DNA pellet during alcohol precipitation which does not interfere with downstream applications of the DNA. And the kit utilized the same mixture of sodium acetate and ethanol as described above, with the addition of 2  $\mu\text{L}$  of the labeling dye to each reaction. After successive wash steps with 80-100% ethanol at room temperature, the DNA was pelleted and could be used for downstream applications.

#### **3.1.1.13 DNA sequencing**

Sequencing of plasmids and PCR products was performed at the sequencing facilities provided by the MPI of Biochemistry and the LMU Biocenter (both in Martinsried, Germany).

### 3.1.2 Microbiological methods

#### 3.1.2.1 Transformation of bacterial cells

Plasmids were transformed into *Escherichia coli* (*E. coli*) cells for amplification. Typically, 10 ng of plasmid preparation or 1  $\mu$ L of ligation reaction was added into 50  $\mu$ L of electro-competent DH5 $\alpha$  cells or chemically competent TOP10 cells.

For electroporation, the bacteria/plasmid mixture was transferred into a 2 mm Gene Pulser cuvette (BioRad) and placed in the Gene Pulser electroporator (BioRad). The machine settings were 25  $\mu$ F, 200  $\Omega$ , and 1.8 kV, and the time constant was 3 - 4 msec. After electroporation, the cells were transferred into 500  $\mu$ L of Luria-Bertani (LB) medium (defined below) and incubated in a 37 °C shaker at 150 rpm for 1 h to recover. After incubation, typically 20  $\mu$ L, 50  $\mu$ L, 100  $\mu$ L of the transformed bacteria cells were plated on LB-Amp agar plates (defined below). The bacteria plates were incubated overnight at 37 °C and the rest of the unplated bacteria culture was stored at 4 °C.

Chemically competent cells were transformed by heat shock. In detail, 10 ng of plasmid preparation or 1  $\mu$ L of ligation reaction was added into 50  $\mu$ L of cells. After incubation on ice for 10 min, the cells were heated-shocked at 42 °C for 30 sec in a water bath, and then returned to ice for 2 min. For recovery, 250  $\mu$ L of SOC media (provided by Invitrogen) was added and then the cells were placed in a 37 °C shaker at 150 rpm for 30 min. Afterwards, the cells were plated on LB-Amp agar plates as explained previously.

LB medium (for 1 L in water) consisted of: 10 g Bacto-tryptone (BD Biosciences, Heidelberg, Germany), 5 g yeast extract (BD Biosciences), and 10 g NaCl (Merck); it was brought to pH 7.5 using NaOH (Merck) and sterilized by autoclaving. For LB-agar, 15 g of agar was dissolved in 1 L of LB, sterilized by autoclaving, and for LB-Amp agar, ampicillin (Sigma-Aldrich) was added to a final concentration of 100  $\mu$ g/mL; 20 mL was poured onto each 10 cm culture plate (Greiner, Frickenhausen, Germany) for casting and the plates were stored at 4 °C until use.

#### 3.1.2.2 Bacterial colony screening for plasmid identification

Bacterial colonies grown on agar plates with antibiotic selection were screened for the plasmid of interest. Colony screening was done by PCR (as described in section 3.1.1.2) with a primer combination that would only produce a product if the correct construct is present, ideally one

primer specific to the vector and the other to the insert.

### **3.1.2.3 Plasmid purification from bacterial cells**

Plasmid DNA was purified from *E. coli* cells while contaminating chromosomal DNA of the bacteria was removed. This was done using miniprep and maxiprep kits (Qiagen, Hilden, Germany). Using the protocol from the manufacturer, 20 or 500 µg of plasmid DNA may be recovered from 5 or 500 mL overnight bacterial culture in LB-Amp using the miniprep or maxiprep kits respectively. The resulting plasmid DNA was used for sequence verification, further cloning procedures, or cell transfection.

## 3.2 Recombinant protein expression

### 3.2.1 Generation of NF-expressing stable cell lines

Immortalized human cell lines were transfected with the pRSV5neo vector containing NF155TM, NF186TM, or NF-truncation mutants fused to sGFP (refer to Table 4.1). Adherent host cell lines obtained from the ATCC (Wesel, Germany) that were used here include: TE671 (human rhabdomyosarcoma cells), HEK293 (human embryonic kidney), and HeLa (human cervical adenocarcinoma).

#### 3.2.1.1 Cell culture conditions

All three wildtype cell lines were grown in complete Roswell Park Memorial Institute medium (RPMI; Gibco, Darmstadt, Germany) media, which consisted of RPMI supplemented with 10% fetal calf serum (FCS; Gibco), 1% Penicillin/Streptomycin solution (Gibco), and 1% sodium pyruvate (Gibco). They were incubated in 37 °C with 5% CO<sub>2</sub>. The cells were passaged once they reached 80-90% confluency by detachment with Trypsin-EDTA (EDTA = Ethylenediaminetetraacetic acid; PAA Laboratories, Coelbe, Germany), rescue from the protease trypsin with 3 volumes of complete RPMI media, centrifugation at 1000 rpm for 5 min at 4 °C, and suspension in complete media for plating. Cell viability was assessed by mixing the cell suspension 1 : 1 with trypan blue solution (0.4%, 1:4 in phosphate buffered saline (PBS), pH 7.4; Invitrogen) and quantifying on a hemocytometer under the microscope. The cells were typically grown in T25, T75, or T175 cell culture flasks (BD Biosciences). PBS consisted of 137 mM NaCl, 2.7 mM KCl, 10 mM Na<sub>2</sub>HPO<sub>4</sub>, and 2 mM KH<sub>2</sub>PO<sub>4</sub>, and was adjusted to pH 7.4.

#### 3.2.1.2 DNA plasmid preparation

To generate stable cell lines, the plasmids were linearized using *ScaI* restriction digest enzyme (NEB). The reaction was set up according to the instructions of the manufacturer and incubated at 37 °C for 2 h. The DNA was then alcohol precipitated (Section 3.1.1.12) and stored in -80 °C. For transfection, the precipitated plasmid sample was centrifuged at 14 000 rpm for 30 min at 4 °C to pellet the DNA. At this point the DNA preparation was sterile. Subsequent steps were performed in a cell culture hood under sterile conditions. The supernatant was discarded and the DNA pellet was left to air-dry at room temperature for 5 min.

### 3.2.1.3 Transfection protocols

Transfection of human cell lines was done using two different techniques: electroporation and by using FuGENE transfection reagent (Roche).

#### By electroporation

Transfection by electroporation typically required 5 million cells and 30 µg DNA in 1 mL of RPMI. Both the cells and DNA were added into a cold 0.5 cm Gene-Pulser cuvette and kept on ice. For electroporation, the Gene Pulser along with the Gene Pulser Capacitance extender were set to 0.280 kV and 960 µF. The time constant was 17 - 22 msec. Afterwards, the cells were transferred into 6 mL of prewarmed complete RPMI media, and divided into six 10 cm cell culture dishes containing 9 mL of prewarmed media. Antibiotics were applied 48 h after transfection (Section 3.2.1.4).

#### Using FuGENE transfection reagent

To transfect cells with FuGENE 6 Transfection reagent (Roche), 500 000 cells were plated into each well of a 6-well cell culture dish. They were left in the incubator for at least 4 h to adhere. A ratio of 6 µL Fugene to 2 µg plasmid DNA was used, and the volume was made up to 100 µL of RPMI. The mixture was allowed to sit at room temperature for 15 min, and then it was added dropwise into the culture. The cells were cultured in the transfection solution overnight, and on the following day replated with fresh media. Antibiotics were applied 48 h after transfection (Section 3.2.1.4).

### 3.2.1.4 Selection of transfected cells with antibiotics

Geneticin (Gibco) was used as a selection antibiotic with pRSV5neo plasmids. For TE671 and HEK293 cells, it was applied at three different concentrations: 1.5 mg/mL, 2.0 mg/mL, 2.5 mg/mL. For HeLa cells, the final concentrations used were: 2.0 mg/mL, 2.5 mg/mL, 3.0 mg/mL. Approximately 10-14 days later, colonies formed from single cells were visible and they were individually picked to be expanded and screened for recombinant protein expression.

For cell lines expressing the complete NF155 and NF186 on the cell surface, the expression level of the recombinant protein was determined by flow cytometry using a monoclonal anti-



pan-NF antibody (A12/18.1, Table 3.5.1; section 3.5.2.1 for details on flow cytometry). For cell lines expressing truncated versions of NF155 and NF186 fused to sGFP, the intensity of the sGFP fluorescence was measured by flow cytometry as an indirect indication of the level of truncated NF expression.

### **3.2.1.5 Maintenance of stable cell lines**

Once a transfected cell line was established, it was maintained in complete RPMI supplemented with 1 mg/mL geneticin. Each group of cell lines to be used for direct comparison were grown in synchrony, meaning that the cell lines of a particular group were passaged together using the same media and plated at the same density in a new bottle at each passage so that they were kept as similar as possible.

### **3.2.1.6 Storage of stable cell lines**

The cell lines were resuspended at 5 million cells per mL in freezing medium: FCS in 10% dimethyl sulfoxide (DMSO; Merck). DMSO is a cryoprotectant used to protect cells from damage during freezing. The suspension was transferred into a cryotube vial (NUNC) to be frozen. The freezing medium was kept cold because DMSO is toxic to cells at high concentrations. The cryotube was placed in an indirect alcohol bath (Nalgene) to be placed in  $-80^{\circ}\text{C}$  so that the cells could be slowly brought to  $-80^{\circ}\text{C}$  as the alcohol cools down. The filled cryotubes were transferred into liquid nitrogen tanks for long-term storage 24 h afterwards.

## **3.2.2 Generation of soluble NF by transient protein expression**

The extracellular domains of NF155 and NF186 were expressed in suspension HEK293-EBNA cells in serum-free conditions. HEK293-EBNA cells are human embryonic kidney cells that are stably transfected with a plasmid encoding Epstein-Barr virus nuclear antigen (EBNA) under geneticin selection. The EBNA allows for episomal amplification of plasmids that contain the viral EBV origin of replication (EBV-ori). Thus, by transfecting a plasmid containing EBV-ori into the cells, more copies will be generated which enhances the level of protein production. We used the pTT5-vector; it contains the EBV-ori as well as human cytomegalovirus (CMV) promoter, which is a strong transcription promoter. An adenovirus E1a/E1b fragment that is integrated in the genome of the HEK293 cells further enhances the CMV promoter. Thus, significant

amounts of recombinant protein may be produced. The HEK293-EBNA/pTT5-vector protein expression system was described Durocher et al. (2002) and was patented by Yves Durocher at NRC Biotechnology Research Institute in Canada (Patent nr. 20110039339).

### **3.2.2.1 Cell culture conditions**

HEK293-EBNA cells were grown in suspension in Freestyle293 Expression Medium (Gibco) supplemented with 1% Pluronic F-68 (10%) (Gibco) and 25 mg/L geneticin (Gibco) in vented flasks (Corning, Amsterdam, Netherlands) in a Multitron shaker (Infors, Einsbach, Germany) at 37 °C, 5% CO<sub>2</sub>, 70% humidity, and 90 rpm. They were passaged at 2 million cells per mL.

### **3.2.2.2 DNA plasmid preparation**

Plasmids for transfection (pTT5-NF155sol and pTT5-NF186sol) were amplified in *E. coli* and purified by maxiprep (Qiagen, refer to section 3.1.2.3). The resulting plasmid preparation was dissolved in EB buffer (provided in maxiprep kit, Qiagen) and was directly used for transfection.

### **3.2.2.3 Transfection using Polyethylenimine (PEI)**

For transfection, viable HEK293-EBNA cells were adjusted to 1 mil/mL. The transfection mixture for 100 mL of cells was made by mixing (1) 1mL Optipro SFM (Gibco) containing 100 µg of plasmid DNA with (2) another 1 mL Optipro SFM containing 200 µL of jetPEI DNA transfection reagent (Polyplus Transfection). The mixture was left at room temperature for half an hour, and then added dropwise into the cell suspension while the culture was swirled. After 24 h, a Bacto TC Lactalbumin hydrolysate (BD Biosciences) solution was added to the culture to 0.5% final concentration.

### **3.2.2.4 Harvesting of supernatant**

After 96 h, the cell culture was harvested: the cells and cell debris were separated from the supernatant that contained soluble neurofascin first by centrifugation at 1 500 rpm for 5 min at 4 °C, and then by ultracentrifugation at 10 000 rpm for 15 min at 4 °C. The resulting supernatant was filtered using a 0.22 µm pore-size ExpressPLUS Stericup (Millipore), and the pH

was adjusted to pH 8.0.

### 3.2.2.5 Purification and preparation of soluble NF

The HEK293-EBNA cells secreted recombinant soluble NF with a C-terminal His-tag into the supernatant. The His-tag exhibits binding affinity to several types of metal ions, such as nickel and cobalt. For purification, our resin of choice was Ni-NTA agarose (Qiagen): a resin with immobilized Ni<sup>2+</sup> ions. Typically 1 L of supernatant was loaded onto the 20 mL column by gravity flow at 4 °C overnight. The column was eluted using a fast protein liquid chromatography (FPLC) setup (Pharmacia). The protein purification procedure using Ni-NTA matrix on the FPLC is explained in detail in Section 3.3.1.1. The eluted protein was concentrated and buffer-exchanged with PBS using Ultracel 10 k spin tubes (Millipore) according to the manufacturer's instructions. The resulting protein preparation was stored as 1 mL aliquots at -20 °C. The concentration of the protein preparation was measured photometrically at 280 nm by Nanodrop (Peqlab) or by bicinchoninic acid (BCA) assay (details in Section 3.3.4).

### 3.2.3 Protein expression in bacterial cells

Fragments of the extracellular domains of NF155 and NF186 were produced in Rosetta *E. coli* (Novagen). The Rosetta strain is a derivative of BL21 that is modified for enhanced expression of eukaryotic proteins that contain codons rarely used in *E. coli*. We used pET21c(+)-vector so that the transgene is expressed under the control of strong bacteriophage T7 transcription and translation signals. T7 RNA polymerase expression is induced in the host cell by isopropyl  $\beta$ -D-1-thiogalactopyranoside (IPTG) addition, and only with IPTG induction is the transgene expressed.

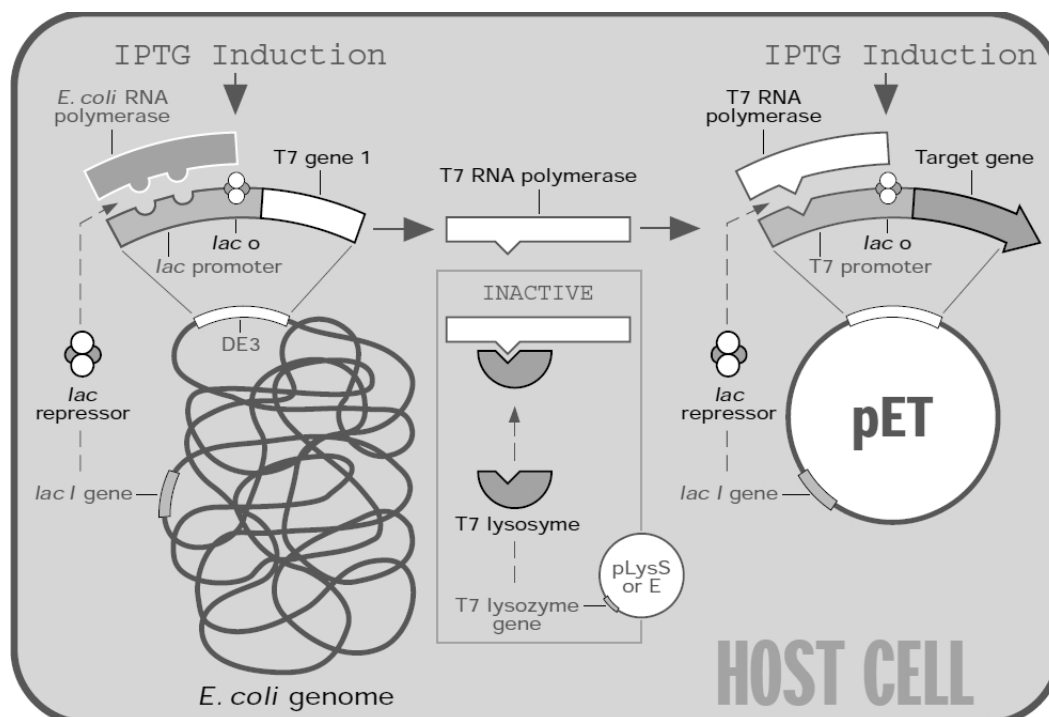


Figure 3.2: **Double induction by IPTG:** The Rosetta cell  $\lambda$ DE3 lysogen encodes the T7 RNA polymerase. When IPTG is absent, the *lac I* gene is constitutively expressed and the *lac* repressor inhibits transcription of both the T7 RNA polymerase and the transgene of the plasmid. In the presence of IPTG, T7 RNA polymerase is expressed as the *lac* repressor is inhibited and it can transcribe the transgene for recombinant protein production. Taken from Novagen, Innovations, vol. 1, number 1, 1994.

### 3.2.3.1 Transformation of Rosetta cells

To transform the chemically competent Rosetta *E. coli* cells, 10 ng of plasmid was mixed with 50  $\mu$ L of cells, and then the cells were heat shocked as described in Section 3.1.2.1. Afterwards, they were grown in 20 mL LB-Amp overnight in a 37 °C shaker at 150 rpm.

### 3.2.3.2 Protein expression by IPTG induction

Rosetta cells transformed with a pET21c(+)-vector containing the transgene of interest were induced to express the recombinant protein with IPTG addition. In detail, 1 mL of the overnight culture was used to inoculate 250 mL of LB-Amp. The culture was grown in the 37 °C shaker at 150 rpm. The rate of cell growth was monitored hourly by photometric measurement of bacterial cell density at 600 nm. When  $OD_{600}$  reached 0.4, IPTG (Invitrogen) was added to a final concentration of 1 mM. The culture was allowed to grow until the  $OD_{600}$  reaches 2. Then the culture was harvested by centrifugation at 5 000 rpm to pellet the Rosetta cells. The

supernatant was removed and the pellet was frozen at  $-20^{\circ}\text{C}$  until purification.

### 3.2.3.3 Protein purification

To recover the recombinant protein, the cell pellet was first resuspended in lysis buffer (50 mM  $\text{NaH}_2\text{PO}_4$ , 300 mM NaCl, 10 mM imidazol; Merck) supplemented with 100 mg/mL lysozyme (Sigma-Alrich), 50  $\mu\text{g}/\text{mL}$  deoxyribonuclease I (DNase I; Sigma-Alrich), 10 mM  $\text{MgCl}_2$  (Merck) and 100  $\mu\text{M}$  phenylmethylsulfonyl fluoride (PMSF; Sigma-Alrich). The cell pellets varied from 5 g to 8 g; 4 mL of lysis buffer was used per gram. The cell suspension was incubated on ice for 30 min, and sonicated on ice using the sonicator (Bransen Sonifier 450) set at 50% duty and 20% power for 10 bursts of 10 sec sonification followed by 10 sec rest. The sonicator produces high frequency sounds waves to shear cells. Afterwards, the cell lysate was centrifuged at 10 000 rpm for 30 min at  $4^{\circ}\text{C}$  to separate the cell debris from the soluble protein in the supernatant. At this point, a proportion of the recombinant protein was found in the supernatant while the rest remained in the pellet. The supernatant was kept at  $4^{\circ}\text{C}$  and the pellet was resuspended in 20 mL of solubilization buffer containing 8 M Urea (Merck) and 150 mM NaCl by vortexing and incubated at room temperature for 1 h. Afterwards, the pellet suspension was centrifuged for 30 min at 10 000 rpm at  $4^{\circ}\text{C}$  to separate the solubilized protein from cell debris.

The next step was to separate the target protein from other contaminating proteins present in the supernatant. Since the target protein was designed with a His-tag in the C-terminus, it was purified from the supernatant using Ni-NTA agarose (Qiagen). The supernatant was loaded onto a 5 mL Ni-NTA agarose column by gravity flow, washed extensively with lysis buffer and then with PBS, and the target protein was eluted with PBS containing 500 mM imidazol. The amount and purity of the target protein eluate was visualized on an SDS-PAGE gel (Section 3.3.2.1).

### **3.3 General protein analytics**

#### **3.3.1 Protein purification by fast protein liquid chromatography**

To separate a target protein from a protein mixture, fast protein liquid chromatography (FPLC) was used. It is a machine that uses medium pressure to separate proteins based specific properties of the target protein such as size (gel filtration), hydrophobic interactions, affinity to a ligand, and charge distribution (ion exchange). The present work utilized affinity chromatography based on the affinity of histidine to specific metal ions (section 3.3.1.1), antibody Fc fragment to protein G (section 3.3.1.2), and antibody to its antigen (section 3.5.8). The columns were eluted at the FPLC setup (Pharmacia) which consisted of two pumps connected to a central controller, an absorbance monitor set to 280 nm, and a pen-recorder to record the absorbance readings.

##### **3.3.1.1 Immobilized metal affinity chromatography**

The soluble recombinant proteins produced for this study were extended by a polyhistidine tag (His-tag) at the C-terminus. The His-tag is an amino acid motif consisting of at least 5 histidine residues; this motif is capable of binding to several types of immobilized metal ions, including nickel, cobalt and copper. Beaded agarose supports are produced with chelating groups such as nitrilotriacetic acid (NTA) that can immobilize metal ions; NTA-agarose may be charged with  $\text{Ni}^{2+}$  to form Ni-NTA agarose (Qiagen).

Ni-NTA agarose was packed into a column bed, and the solution containing the target protein was first adjusted to pH 8.0 before it was passed through. Unspecific protein binding was washed off using PBS containing 20 mM imidazol (Merck). To recovery the target protein, the column was eluted with PBS containing 250 mM imidazol. Both wash and elution steps were monitored on the absorbance reader at 280 nm. Subsequently, the eluted protein was further concentrated and dialyzed against PBS.

##### **3.3.1.2 Affinity purification of antibodies using Protein G**

To purify IgG antibodies from serum or cell culture supernatant, affinity chromatography on columns of gels derivatized with bacterial protein G was used. Protein G is a protein from

group G *Streptococci* that can bind antibody Fc region of mainly IgGs from various species (ex. human, mouse, rat, rabbit, bovine). The naturally occurring form of protein G also bind albumin; however, it is commercially available as a recombinant protein with the albumin-binding region deleted. This recombinant protein is covalently coupled to sepharose to form Protein G sepharose (GE Healthcare).

Protein G sepharose was packed into a column bed, and the antibody solution at neutral pH was passed through. Unspecific binding of protein onto the matrix was washed off with PBS until the absorbance reading at 280 nm was back to baseline. The antibodies were eluted with 100 mM glycine-HCl buffer with 150 mM NaCl, adjusted to pH 2.7. The acidic eluate was immediately neutralized by 100  $\mu$ L of 1 M Tris-HCl at pH 9.0 that was previously added to each fraction tube. The eluted antibodies were dialyzed against PBS in 12-16 kDa cutoff dialysis tubing cellulose membrane (Sigma-Alrich) and stored in PBS at  $-20^{\circ}\text{C}$ .

### **3.3.2 Protein separation and analysis**

Proteins may be separated according to their electrophoretic mobility, which is a function of the length of the polypeptide chain and its charge. In most cases, sodium dodecyl sulfate (SDS) is applied to the polypeptide chain to render an even charge distribution so that proteins are separated specifically by size. SDS polyacrylamide gel electrophoresis (SDS-PAGE) is a very convenient way to visualize the purity of a protein preparation and to estimate the size of a protein relative to the molecular size markerr on the gel. To visualize the separated proteins, the gel may be stained by Coomassie blue or by silver. Coomassie blue staining is much less sensitive than silver staining and its main purpose is only simple protein verification. By silver staining, as little as 5 ng of protein may be detected and it was done to monitor the purity of a protein preparation.

#### **3.3.2.1 Gel electrophoresis**

Precast 4-12% Bis-Tris gels (Invitrogen) were used in this study. As the protein sample travel through the gel, the narrowing pores exert a sieving effect so that the smaller proteins can travel faster through the matrix while the larger proteins slower. The gel was fitted into an XCell electrophoresis chamber (Invitrogen) filled with NuPAGE MOPS SDS running buffer (Invitrogen). NuPAGE LDS sample buffer (Invitrogen) was mixed with the protein sample and incubated at

95 °C for 5 min prior to loading into the gel. For sample preparation in reducing conditions,  $\beta$ -mercaptoethanol (Merck) was added to 5% final concentration before the heat incubation step. A full-range rainbow molecular weight marker (GE Healthcare) was used as a reference to estimate the size of proteins on the gel. Electrophoresis was performed typically for 1 h at 200 V.

### **3.3.2.2 Protein staining by Coomassie brilliant blue**

The protein gel was incubated for 20 min in Coomassie blue solution (0.1% (w/v) Coomassie brilliant-blue R-250, 40% methanol, 10% acetic acid) and then 1 h in destain solution (50% methanol, 7% acetic acid) on a shaker at room temperature. The destain solution was changed several times in that hour. To further remove background staining and enhance the contrast to visualize the protein bands, the gel was then incubated in 10% acetic acid solution overnight at 4 °C on a shaker.

### **3.3.2.3 Protein staining by silver**

The protein gel was fixed in 50% methanol with 5% acetic acid for 20 min at room temperature and then washed for 10 min with 50% methanol followed with another 10 min with water. Then the gel was sensitized with 1 min incubation in 0.02% sodium thiosulfate. After rinsing with water, the gel was submerged in a cold 0.1% silver nitrate solution for 20 min at 4 °C. After washing with water, the gel was developed in a solution containing 0.04% formalin and 0.2% sodium carbonate. The gel was gently shaken in the developing solution, which was discarded when yellow to reduce background staining of the gel and was replaced by fresh solution. After the desired intensity of protein staining was achieved, the reaction was terminated by addition of 5% acetic acid. For storage, the stained gels were kept in 1% acetic acid solution at 4 °C.

### **3.3.3 Mass spectrometry**

Protein bands of interest may be identified by mass spectrometry. The protein band was cut from the stained gel with a scalpel, chopped into smaller fragments and stored in 50  $\mu$ L of water. Afterwards, it was sent to the mass spectrometry service at the MPI of Biochemistry (Martinsried, Germany).



### 3.3.4 Measurement of protein concentration

#### 3.3.4.1 Bicinchoninic acid assay

The bicinchoninic acid assay (BCA assay) was used to measure the total amount of protein in a solution. The concentration of protein is estimated colourmetrically when the solution changes from green to purple in proportion to protein concentration.

In detail, the assay is based on two chemical reactions. The first step is the biuret reaction: the peptide bonds reduce  $\text{Cu}^{2+}$  ions from cupric sulfate to  $\text{Cu}^+$  ions in an alkaline medium to produce a faint blue-violet colour. The amount of reduction is proportional to the amount of protein present. The second step involves the chelation of two molecules of BCA with the  $\text{Cu}^+$  ions to produce the intense purple colour that has a strong linear absorbance at 562 nm. This assay is compatible with the presence of detergents, but not reducing agents and chelators.

For each sample, the concentration was measured in duplicates or triplicates using the BCA protein assay reagent kit (Pierce, Rockford, USA) according to the instructions of the manufacturer. A standard curve of known concentrations of bovine serum albumin (BSA; Serva, Heidelberg, Germany) was used to estimate the concentration of test samples. The reaction mixture was incubated for 30 min at 37 °C and absorbance at 550 nm was measured.

#### 3.3.4.2 UV spectrophotometry by Nanodrop

The concentration of a protein sample was also measured using Nanodrop 1000 (Peglab). Between 0.5  $\mu\text{L}$  to 2.0  $\mu\text{L}$  of sample was used to make absorbance at 280 nm. It is a fast and convenient method, requiring no additional reagents, incubation time, or standard curves. However, as amino acids with aromatic rings (phenylalanine, tryptophan, histidine and tyrosine) are responsible for the absorbance peak at 280 nm, different proteins will exhibit different absorption characteristics. Furthermore, the absorption characteristics of each protein are dependent on environmental factors that can affect the structure, like pH and ionic strength.

### 3.3.5 Circular dichroism spectroscopy

The conformation of the soluble recombinant proteins generated from HEK293-EBNA cells was analyzed by circular dichroism spectroscopy (CD spectroscopy). CD spectroscopy measures

differences in absorption of left-handed polarized light versus right-handed polarized light that arise from structural asymmetry. Thus, this method is based on the optical activity of protein from the chiral  $\alpha$ -carbon atom of all amino acids except glycine, and especially secondary structures such as alpha-helices and beta-sheets. A CD spectra between 250-195 nm was analyzed for secondary structures like alpha-helix, beta-sheet, turn and unordered structures.

CD spectroscopy was performed in the Microchemistry Core Facility at the MPI of Biochemistry using J-715 spectrometer (Jasco, Gross-Ulmstadt, Germany). The spectra was recorded at 25 °C at a speed of 50 nm/min. Duplicates were done for each protein sample.

### **3.4 Patient material**

Serum and plasma exchange material from patients and serum from healthy donors were used in this project. In some rare cases, cerebrospinal fluid was also analyzed. Material from multiple sclerosis patients came from the following donors: Prof. Dr. Frank Weber and Dr. Philipp Saemann of the MPI of Psychiatry (Munich, Germany), Prof. Dr. Tomas Olsson and Dr. Mohsen Khademi of the Karolinska Institute (Stockholm, Sweden), and the staff doctors at the Institute for Clinical Neuroimmunology at Klinikum Großhadern (Munich, Germany). Material from patients with peripheral inflammatory neuropathies came from the following donors: Prof. Dr. Nobuhiro Yuki and Dr. Masaaki Odaka of Dokkyo Medical University (Mibu, Japan), Dr. Bjoern Tackenberg of Philipps University (Marburg, Germany), Dr. Harald Pruess, Dr. Jan Schwab, and Prof. Dr. Lutz Harms of Charité (Berlin, Germany), Dr. Hendrik Harms of St. Josef-Krankenhaus (Potsdam, Germany) and Dr. Sommer of the University Hospital of Wuerzburg (Wuerzburg, Germany). Material from patients with amyotrophic lateral sclerosis came from Dr. Johannes Brettschneider of University of Ulm (Ulm, Germany) and Prof. Dr. Harms. Control patients with other neurological diseases came from the Prof. Dr. Olsson and Dr. Pruess. Serum from healthy donors were provided by Prof. Dr. Yuki, Dr. Pruess, Prof. Dr. Olsson, and my colleagues at the MPI of Neurobiology. Details are listed in Table 3.3.

#### **3.4.1 Ethical standard and patient consent**

These studies were approved by the local ethical committee of each sample source and the donors gave their informed consent.

#### **3.4.2 Storage and handling of patient material**

All patient material were stored at  $-20^{\circ}\text{C}$ , and were regarded as hazardous and treated as potentially infectious specimens. Working aliquots of typically 50  $\mu\text{L}$  were made with serum samples for screening and characterization. Working volumes of between 200 mL and 1 L of plasma exchange material was thawed for antibody purification, and the column flow through was bottled, labelled and refrozen for future studies.

## 3.4.3 Patient material list

Table 3.3: Patient material list

	Source	Disease	Volume	Number	Age	Male:Female	
<b>Multiple Sclerosis</b> Serum	MPI-Psychiatry	RR-MS	500 µL	74	22-63	23:51	
		PP-MS	500 µL	6	38-72	4:2	
		SS-MS	500 µL	9	34-74	2:7	
		MS-unclassified	500 µL	2	58		
		CIS	500 µL	5	35-44	1:4	
	Karolinska Institute	RR-MS	100 µL	124	17-69	46:88	
		PP-MS	100 µL	4	44-63	0:4	
		SP-MS	100 µL	2	57, 67	0:2	
		MS-unclassified	50 µL	4	-	-	
	Plasma exchange	Klinikum Großhadern	RR-MS	1 mL	17	22-52	6:11
NMO			1 mL	3	31-51	1:2	
RR-MS			200-1000 mL	8	22-52	5:3	
<b>Peripheral Neuropathy</b> Serum	Dokkyo University	CIDP	100 µL	50	9-87	40:10	
		AIDP	100 µL	50	1-84	33:17	
		AMAN	100 µL	50	14-83	29:21	
	Philipps University	CIDP	500 µL	30	20-90	23:7	
	Charité	CIDP	100 µL	2	45, 61	2:0	
		AIDP	100 µL	4	23-53	1:3	
	St. Josef-Krankenhaus	CIDP	500 µL	37	13-85	27:10	
		AIDP	500 µL	11	20-58	8:3	
		ALS	500 µL	16	35-80	7:9	
		ON	500 µL	20	20-78	19:1	
	University of Ulm	ALS	500 µL	55	26-88	31:24	
	Plasma exchange	University of Wuerzburg	CIDP	1 mL	40	28-83	30:10
	<b>Control donors</b> Serum	Karolinska Institute	OND	100 µL	57	21-80	13:44
Charité		OND	100 µL	1	34	-	
Karolinska Institute		HC	100 µL	5	20-35	3:2	
MPI Neurobiology		HC	500 µL	21	21-55	9:12	
Dokkyo University		HC	100 µL	50	14-84	17:33	

**RR-MS** = relapsing-remitting multiple sclerosis; **PP-MS** = primary progressive multiple sclerosis; **SP-MS** = secondary progressive multiple sclerosis; **CIS** = clinically isolated syndrome; **NMO** = neuromyelitis optica; **CIDP** = chronic inflammatory demyelinating polyneuropathy; **AIDP** = acute inflammatory demyelinating polyneuropathy; **AMAN** = acute motor axonal neuropathy; **ALS** = amyotrophic lateral sclerosis; **ON** = other neuropathies (including diabetic polyneuropathy, monoclonal gammopathy, polyneuropathy from vitamin B12 deficiency, and polyneuropathy with unclear origins); **OND** = other neurological (non-inflammatory) diseases (including sensory symptoms, headache, migraine, vertigo, neurasthenia, pain, cancer, and vascular problems); **HC** = healthy controls

### 3.5 Antibody detection assays

#### 3.5.1 List of primary and secondary antibodies used in this project

Table 3.4: List of primary and secondary antibodies used in this project

Specificity	Conjugate	Clone	Species/Isotype	Concentration	Dilution	Source
pan-NF	-	A12/18.1	mouse IgG2a	1-2 mg/mL	1:1000	in-house hybridoma
pan-NF	-	A4/3.4	mouse IgM	2 mg/mL	1:1000	Genovac
pan-NF	-	L11A/41	mouse IgG1	-	1:200	NeuroMab
NF155	-	polyclonal	rabbit IgG	serum	1:100	in-house
Caspr	-	polyclonal	rabbit IgG	serum	1:1000	Peles et al. (1997)
Oligodendrocyte marker O4	-	MAB345	mouse IgM	1.05 mg/mL	1:100	Chemicon
Galactocerebroside	-	MAB342	mouse IgG3	1 mg/mL	1:100	Chemicon
Olig-2	-	polyclonal	rabbit IgG	-	1:200	Millipore
polyHistidine	Peroxidase	HIS-1	mouse IgG2a	5-11 mg/mL	1:2000	Sigma-Aldrich
mouse IgG	HRP	polyclonal	goat F(ab') <sub>2</sub>	0.8 mg/mL	1:7000	JacksonImmuno
	R-PE	polyclonal	goat IgG	-	1:200	Dako
	Alexa488	polyclonal	donkey IgG	2 mg/mL	1:200	Molecular Probes
mouse IgM	HRP	polyclonal	donkey F(ab') <sub>2</sub>	0.8 mg/mL	1:7000	JacksonImmuno
	Alexa594	polyclonal	goat IgG	2 mg/mL	1:1000	Invitrogen
	R-PE	polyclonal	rat Ig	0.2 mg/mL	1:100	BD Biosciences
mouse IgG2a	FITC	polyclonal	goat IgG	0.4 mg/mL	1:100	Abd Serotec
rat IgG,IgM	HRP	polyclonal	goat IgG	0.8 mg/mL	1:1000	JacksonImmuno
	Alexa594	polyclonal	goat IgG	2 mg/mL	1:1000	Molecular Probes
rabbit IgG	biotin	polyclonal	donkey IgG	1.1 mg/mL	1:1000	JacksonImmuno
	Alexa568	polyclonal	donkey IgG	2 mg/mL	1:1000	Invitrogen
human IgA,IgG,IgM	biotin	polyclonal	goat F(ab') <sub>2</sub>	1.2 mg/mL	1:1000	JacksonImmuno
	HRP	polyclonal	goat IgG	0.8 mg/mL	1:7000	JacksonImmuno
	R-PE	polyclonal	goat F(ab') <sub>2</sub>	0.1mg/mL	1:150	SouthernBiotech
	DyLight488	polyclonal	goat IgG	1.5 mg/mL	1:150	JacksonImmuno
	DyLight649	polyclonal	goat IgG	1.5 mg/mL	1:150	JacksonImmuno
	-	polyclonal	goat IgG	2.4 mg/mL	-	JacksonImmuno
human IgG	HRP	polyclonal	goat IgG	0.8 mg/mL	1:7000	JacksonImmuno
	DyLight488	polyclonal	goat IgG	1.5 mg/mL	1:100	JacksonImmuno
	R-PE	polyclonal	goat F(ab') <sub>2</sub>	0.5 mg/mL	1:150	JacksonImmuno
	DyLight649	polyclonal	goat F(ab') <sub>2</sub>	1.5 mg/mL	1:150	JacksonImmuno
human IgA	biotin	polyclonal	goat F(ab') <sub>2</sub>	1.2 mg/mL	1:1000	JacksonImmuno
	DyLight488	polyclonal	goat IgG	1.5 mg/mL	1:100	JacksonImmuno
	R-PE	polyclonal	goat IgG	0.5 mg/mL	1:50	JacksonImmuno
	PerCP	polyclonal	goat IgG	0.5 mg/mL	1:50	JacksonImmuno
human IgM	HRP	polyclonal	goat IgG	0.8 mg/mL	1:7000	JacksonImmuno
	DyLight 488	polyclonal	goat IgG	1.5 mg/mL	1:100	JacksonImmuno
	R-PE	polyclonal	donkey F(ab') <sub>2</sub>	0.5 mg/mL	1:100	JacksonImmuno
	DyLight649	polyclonal	donkey F(ab') <sub>2</sub>	1.5 mg/mL	1:100	JacksonImmuno
human IgG1	biotin	4E3	mouse IgG1	0.5 mg/mL	1:1000	SouthernBiotech
	R-PE	4E3	mouse IgG1	0.1 mg/mL	1:1000	SouthernBiotech
human IgG2	biotin	31-7-4	mouse IgG1	0.5 mg/mL	1:1000	SouthernBiotech
	R-PE	31-7-4	mouse IgG1	0.1 mg/mL	1:1000	SouthernBiotech
human IgG3	biotin	HP6050	mouse IgG1	0.5 mg/mL	1:1000	SouthernBiotech
	R-PE	HP6050	mouse IgG1	0.1 mg/mL	1:1000	SouthernBiotech
human IgG4	biotin	HP6025	mouse IgG1	0.5 mg/mL	1:1000	SouthernBiotech
	R-PE	HP6025	mouse IgG1	0.1 mg/mL	1:1000	SouthernBiotech
isotype control	-	polyclonal	human IgG	11.2 mg/mL	-	Sigma Aldrich
isotype control	-	eBM2a	mouse IgG2a	-	-	eBioscience
isotype control	-	eB121-15F9	mouse IgM	-	-	eBioscience
isotype control	-	polyclonal	rabbit IgG	-	-	Dako

### **3.5.2 Serum screening**

#### **3.5.2.1 Cell-based assay by flow cytometry**

Cell-bound recombinant protein antigens in native conformation were used to probe for reactive autoantibodies in human serum. For each serum sample, TE671 cells expressing human NF155 and human NF186, and also cells transfected with the empty vector were stained. The 3 cell lines (TE-RSV0, TE-NF155, TE-NF186) were plated at 200 000 cells per well. After pelleting by centrifugation, the cells were stained with antibodies.

Initial experiments to set up a staining protocol utilized pan-NF mAbs (A12/18.1, A4/3.4) and secondary detection antibodies conjugated to fluorescent molecules. The initial staining protocol was the following: 100  $\mu$ L of 1:100 diluted primary antibody or 1:100 diluted human serum was used to resuspend the cell pellet and this was incubated on ice for 1 h. Following 2 washes with 200  $\mu$ L PBS/1% FCS, 100  $\mu$ L secondary detection antibody solution (1:200 anti-mouse-Ig-PE (Dako, Eching, Germany) or 1:100 anti-human-IgG-DyLight488 (JacksonImmuno, Newmarket, UK)) was applied and the cells were incubated on ice for 45 min. After 3 washes, the cells were resuspended in 100  $\mu$ L PBS with TO-PRO3 (1:4000; Invitrogen). The stained cells were acquired on FACS Calibur (BD Biosciences), and the data was analyzed on FlowJo (Tree Star Inc., Ashland, USA). The fluorescence intensity measured on the NF-expressing cells was divided by the intensity measured on cells with the empty vector to normalize for background staining.

The optimized protocol contained the following modifications: serum samples were diluted 1:50 in PBS/1% FCS and 100  $\mu$ L was used to stain cells in each well, this was incubated for 1 h on ice; after 2 washes with 200  $\mu$ L PBS/1% FCS, 100  $\mu$ L secondary antibody solution (1:150 anti-human-IgG-PE or 1:150 anti-human-Ig-PE, both from JacksonImmuno) was added and incubated on ice for 35 min. Following 3 washes, the cells were again resuspended in PBS with TO-PRO3 iodide for analysis as in the previous protocol. It was found to be important to keep the cells cold during the entire procedure.

#### **3.5.2.2 ELISA**

Soluble recombinant human NF155 and NF186 were immobilized on a solid surface to be displayed in random orientation for antibody detection. The optimized protocol was the fol-

lowing: 5 µg/mL of human NF155 and NF186, rat NF155 (R&D Systems, Abingdon, UK), and BSA (Serva) were used for coating in 0.1 M carbonate buffer at pH 9.5 (maxisorp) or 1 x PBS (Ni-NTA) at 4 °C overnight. After washing with PBS, the plate was blocked with 200 µL of PBS/0.05% Tween-20 (PBST) with 3% BSA (Serva) at 37 °C for 1 h. The plate was then washed with PBST. To each well, 100 µL of sera diluted 1:100 or 0.2 µg/mL mAb (A4/3.4) in blocking buffer was applied to wells coated with BSA, human NF155 and NF186 and rat NF155; this was incubated for 1 h at 37 °C. After washing with PBST, 100 µL of anti-human-Ig-horseradish peroxidase (HRP; 1:7000; JacksonImmuno) or anti-mouse-IgM-HRP (JacksonImmuno) was added into each well and the plate was incubated at 37 °C for 30 min. After washing with PBST, 100 µL of TMB solution (eBioscience) was added to each well and 50 µL of 2 N sulfuric acid was used to stop the reaction once sufficient colour change was observed. The optical density was measured at 450 nm, and the data was analyzed using Prism Graphpad (Graphpad software, La Jolla, USA). For antigen crossreactivity experiments, human contactin-2 and human oligodendrocyte myelin glycoprotein (OMgp) (both from R&D systems) were incorporated to the panel of test antigens used for screening.

### 3.5.2.3 Western blot

To screen human serum for NF reactivity by Western blot, we blotted NF155 and NF186 onto polyvinylidene fluoride (PVDF) membrane, and stained each blot with a diluted serum sample. In detail: 1 µg of each neurofascin and 3 µL of Protein Rainbow Marker (GE Healthcare, Munich, Germany) were loaded for every 3 lanes on a 4-12% BIS-TRIS gel (Invitrogen). The gel was subjected to electrophoresis at 200 V for 1 h. Hybond-P PVDF-membrane (GE Healthcare) was cut to the size of the gel, activated by methanol, washed with water and then incubated in cold transfer buffer (20x NuPAGE transfer buffer, Invitrogen). When the gel electrophoresis was completed, the 'blot sandwich' was built and placed between the electrode-plates of a semi-dry transfer apparatus. The 'blot sandwich' from cathode to anode consisted of 3 sheets of 3 mm Whatman filter paper pre-soaked in transfer buffer, the gel on top of the membrane, and then another 3 sheets of pre-soaked filter paper. The semi-dry transfer set at 0.8 mA/cm<sup>2</sup> for 90 min. Afterwards, the membrane was cut into strips where each strip contain the protein marker, NF155, and NF186. These strips were blocked in 5% skim milk in PBST for 1 h at room temperature. After washing with PBST, each strip was incubated in diluted human serum (1:400 in blocking solution) overnight at 4 °C on a shaker. These strips were washed with PBST for 1 h

at room temperature, and anti-human-Ig-HRP (1:7000; JacksonImmuno) was applied for 1 h at room temperature on a shaker. After washing with PBST, enzymatic chemiluminescence (ECL) solution was applied for 1 min. The ECL solution was a mixture of 10 mL ECL-A (0.25% (w/v) luminol in 1M Tris/HCl), 100  $\mu$ L ECL-B (0.11% (w/v) para-hydroxycoumarin acid in DMSO), and 3.1  $\mu$ L of 30% H<sub>2</sub>O<sub>2</sub>. Then the strip was exposed onto autoradiography film (GE Healthcare) for 3 sec to 1 min. Visual analysis was done on a lightbox for presence of bands where each neurofascin isoform was blotted.

### 3.5.3 Epitope mapping by cell-based assay

TE671 cell lines stably transfected with truncated forms of NF155 or NF186 were used to elucidate the immunogenic region within the multi-domain protein. The truncation mutants were made to express (1) immunoglobulin-like (Ig)1-Ig2-Ig3-Ig4-Ig5-Ig6 domains, (2) fibronectin type III (Fn)1-Fn2 domains, (3) Fn3-Fn4 domains, (4) Fn3 domain, (5) Fn4-Mucin-Fn5 domains, and (6) Mucin-Fn5 domains. To monitor the level of transgene expression, each truncated version of NF was tagged with super-GFP (sGFP) in the cytoplasmic region. NF155 or NF186 reactive samples identified by flow cytometry were diluted 1:100 in PBS/1% FCS for staining. Secondary anti-human-Ig conjugated to Dylight649 (1:200, JacksonImmuno) was used for detection. The fluorescence intensity of sGFP was plotted against Dylight649, and the staining was scored positive if (1) the mean fluorescence intensity in the FL4-channel (for Dylight649) was higher than that measured on control cells and (2) there was a strong direct correlation between the level of sGFP expression and the amount of staining observed.

### 3.5.4 Epitope mapping by Western blot

Recombinant truncated forms of NF155 and NF186 expressed in Rosetta *E. coli* cells were: (1) Ig1-Ig2-Ig3-Ig4, (2) Ig5-Ig6-Fn1-Fn2, (3) Fn3-Fn4, and (4) Fn4-Mucin-Fn5. These 4 fragments along with the complete NF155 and NF186 were blotted onto PVDF membrane and probed with diluted serum as described in Section 3.5.2.3.

### 3.5.5 Isotyping

For isotyping of NF reactivity by flow cytometry or ELISA, the procedures described in Sections 3.5.2.1 and 3.5.2.2 were modified at the step of primary human antibody detection. In-



stead of using anti-human-Ig conjugated with either PE or HRP for detection of all antibodies indiscriminantly, the following secondary antibodies were used: anti-human-IgG1, anti-human-IgG2, anti-human-IgG3, anti-human-IgG4, anti-human-IgM, or anti-human-IgA (JacksonImmuno, SouthernBiotech).

### **3.5.6 Serial dilution**

Serum samples were diluted 1:100, 1:500, 1:1000, and 1:10 000 to probe for reactivity using the same procedure as described in Sections 3.5.2.1 and 3.5.2.2

### **3.5.7 Immunohistochemistry**

Fresh rat spinal cord was embedded in tissue freezing medium (Leica, Wetzlar, Germany) and 10 µm thick longitudinal sections were cut using a cryotome. The tissue was stored at -20 °C. Prior to staining, sections were fixed for 7 min in ice cold methanol and blocked with goat IgG (Sigma-Aldrich) diluted in antibody diluent (Dako) for 3 h at room temperature. Human serum was diluted 1:100 and purified human antibodies were diluted to 2 µg/mL in PBS/10% FBS, and applied to a tissue section for overnight incubation at 4 °C. ivIG (Intratect; Biotest Pharma, Dreieich, Germany) was adopted as healthy control immunoglobulin preparation. After PBS wash, anti-human-IgG-Alexa488 secondary antibody (1:100; Invitrogen) and DAPI (1:1000 Thermo Scientific) were applied. Subsequently Caspr-specific rabbit serum antibody (1:1000; Peles et al. (1997)) was incubated with the tissue sections for 1 h at room temperature. The sections were washed and secondary antibody (anti-rabbit-IgG-Alexa594, 1:1000; Invitrogen) was added to the section for 45 min at room temperature. They were then washed and mounted with coverslips using fluoromount (Invitrogen).

### **3.5.8 Antibody purification by antibody-antigen affinity chromatography**

Recombinant neurofascin (human NF155, NF186, or rat NF155-NS0) was covalently conjugated to N-hydroxysuccinimide (NHS)-activated sepharose (GE Healthcare, Munich, Germany) at 0.5 mg/mL according to the protocol provided by the manufacturer. The NF-conjugated matrix was then packed into a column bed (Sigma-Aldrich) and stored in PBS with 10 mM NaN<sub>3</sub> (Merck, Darmstadt, Germany) and 0.1 mM PMSF (Sigma-Aldrich) at 4 °C. Human samples were stored in -20 °C. Sample preparation was as follows: centrifugation at 4000 rpm for 10

min, filtration through a 0.22  $\mu\text{m}$  Stericup (Millipore, Schwalbach, Germany), 1:1 dilution with PBS and the pH was adjusted to 7.0.  $\text{NaN}_3$  and PMSF were added to final concentrations of 10 mM and 0.1 mM respectively. The column was loaded with the sample at 4 °C. After loading, elution was done at an FPLC setup (Pharmacia, Uppsala, Sweden) at pH 5, pH 4, pH 3, and pH 11, while bringing the pH up to neutral in between each pH step. The buffers used were: PBS at pH 7.2, 100 mM citrate with 150 mM NaCl at pH 5, 100 mM acetate with 150 mM NaCl at pH 4, 100 mM glycine with 150 mM NaCl at pH 2.7, and 100 mM ethanolamine with 150 mM NaCl at pH 11.2. Elution was monitored by absorbance at 280 nm. The eluted fractions were concentrated and dialyzed with PBS using Amicon Ultra centrifugation filters (Millipore) according to the protocol provided by the manufacturer. ivIG (Intratect; Biotest Pharma, Dreieich, Germany) was adopted as healthy control immunoglobulin for these experiments. A sample of each fraction was analyzed on a reducing SDS-PAGE gel for visualization of antibodies and contaminants.

### 3.5.9 Antibody quantification by ELISA

Human antibodies (purified Abs, serum, cerebrospinal fluid) were quantified by ELISA. In detail, affinity-purified anti-human-IgG, IgM, IgA polyclonal goat IgG (JacksonImmuno) was coated on a maxisorp plate (Nunc) at 2  $\mu\text{g}/\text{mL}$  in 0.1 M carbonate buffer (pH 9) at 4 °C overnight. After blocking with 3% BSA in PBST, 100  $\mu\text{L}$  of diluted antibody samples may be added. Serum was normally diluted 1:1000 000, and then further diluted 1:10 and 1:100. Purified antibodies were diluted 1:1000, and then further diluted 1:10, 1:100, 1:1000. CSF samples were diluted 1:1000, and then 1:100, 1:1000, 1:10 000. Protein concentration estimates were made using a standard curve of known concentrations of intravenous immunoglobulin (ivIG; pooled human antibodies). The ivIG standard curve was the following (in  $\text{pg}/\text{mL}$ ): 0, 8, 16, 32, 64, 128, 256, 512, 1024, 2048, 4096, and 8192. The diluted antibody samples and ivIG solutions were incubated for 1 h at 37 °C. Secondary anti-human-IgG, IgM, IgA polyclonal goat IgG conjugated to horseradish peroxidase (JacksonImmuno) was diluted 1:7000 and applied to the ELISA plate for 30 min at 37 °C. Afterwards, TMB substrate solution (eBioscience) was added, followed by 2 N sulfuric acid to stop the colorimetric reaction, and then optical density at 450 nm was measured. The data was analyzed on Prism Graphpad (Graphpad software, La Jolla, USA) and estimates of antibody concentration in a complex protein mixture was inferred from the standard curve.

### **3.6 Experimental autoimmune neuritis animal experiments**

P2-peptide (AA 53-78; Uyemura et al. (1982)) was synthesized by the Core Facility in the Max Planck Institute of Biochemistry (Martinsried, Germany). To induce EAN, Lewis rats were immunized subcutaneously on both hind limbs with 100 µg of P2-peptide emulsified in Complete Freund's Adjuvant (CFA; Difco, Lawrence, USA). Clinical scores and body weight were monitored daily. Clinical scores were evaluated as follows: 0 = normal; 0.5 = loss of tail tonus; 1 = tail paralysis; 2 = gait disturbance; 3 = hind-limb paralysis. Upon initial signs of clinical disease approximately 2 weeks after peptide immunization, anti-NF antibodies (A12/18.1, A4/3.4) or their respective isotype controls (mouse IgG2a, mouse IgM; eBioscience) were injected intravenously into the EAN rat at 500 µg per rat. The animals were followed until full recovery was seen in all four groups, and then they were sacrificed. (Dr. Naoto Kawakami, from the Institute of Clinical Neuroimmunology, performed the animal experiments and provided the information for this text)



## **Chapter 4**

# **Results**

## 4.1 Cloning and recombinant expression of neurofascin

### 4.1.1 Construction of expression plasmids

The complete DNA templates of human NF155 and human NF186 were constructed piecewise using human brain RNA and a commercially available cDNA clone. All other constructs were derived from these DNA templates.

#### 4.1.1.1 Complete transmembrane form of NF155 and NF186

All self-designed oligonucleotide primers were produced by Metabion (Martinsried, Germany). Primers were designed according to the following criteria: annealing temperature near 60 °C (summation of each A/T=2 °C and C/G=4 °C), 20 nt in length, and C/G at the 3' end.

The complete DNA of human NF155 and NF186 were generated stepwise according to the cloning strategy devised by Dr. Klaus Dornmair. First, cDNA from RNA of human brain was prepared with RT-primers specific to the cytosolic region (primer-1; Table 3.1) and to the third immunoglobulin domain (primer-2). Next three fragments were amplified by PCR: Fragment 1 that spans the signal sequence and immunoglobulin-like domains (Ig)-1 and -2 using primer-3 and -4, Fragment 2 that spans fibronectin type III domains (Fn)-3 and -4 and the transmembrane domain with primer-5 and -7, and Fragment 3 that spans Fn-4, Mucin, Fn-5 and the transmembrane domain using primer-6 and -7. Fragment 1 is common to both isoforms while Fragment 2 is NF155-specific and Fragment 3 is NF186-specific. For the cDNA fragment containing Ig-3,-4,-5,-6 and Fn-1,-2 domains that are common to both isoforms, it was excised from cDNA clone IRAKp961P2270Q (GenomeCube, Nottingham, UK) using restriction sites *HindIII* and *AvrII*. (Figure 4.1)

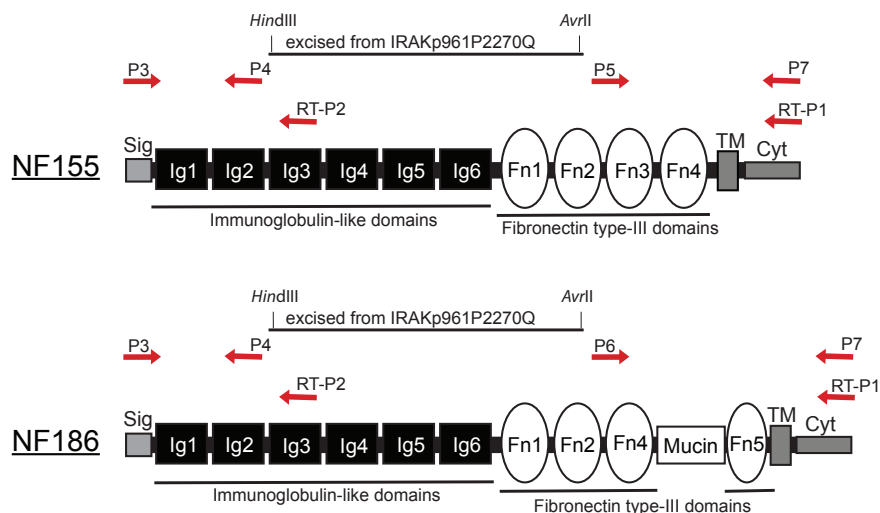


Figure 4.1: **Amplification and digestion for fragments of NF155 and NF186:** NF155 and NF186 both contain a signal sequence, 6 immunoglobulin-like domains (Ig; black), fibronectin type-III domains (Fn; white), transmembrane domain (TM) and cytoplasmic region (Cyt). NF186 has a mucin domain. Primers used for amplification are indicated with red arrows (P = primer; RT = reverse transcription). The region covered by the fragment excised using *HindIII* and *AvrII* restriction enzymes from the cDNA clone IRAKp961P2270Q is indicated.

To assemble the fragments, pcDNA6.1v5 His C (Invitrogen) was used as a surrogate vector. First, the vector and Fragment 1 were cut with *EcoRI* and *HindIII*, and they were ligated together. Next this ligation product was cut with *HindIII* and *NheI*, and ligated with the cDNA fragment digested with *HindIII* and *AvrII*. This plasmid containing both fragments was cut with *Bsi*MI and *Bgl*II, and either Fragment 2 or Fragment 3 was inserted, producing essentially the cDNAs of the entire NF155 and NF186 (Figure 4.2). Both full-length NFs were excised from the pcDNA plasmid using *Sal*I and *Bgl*II, and ligated into a plasmid vector appropriate for each expression system used. For each construct, full-length sequencing was done to confirm the sequence identity. For cell surface expression of the full-length neurofascins on TE671 cell line, the full NF cDNA was inserted into pRSV5neo (Long et al., 1991) using *Sal*I and *Bam*HI sites (example in Figure 4.3). This cloning work was done together with Joachim Malotka.

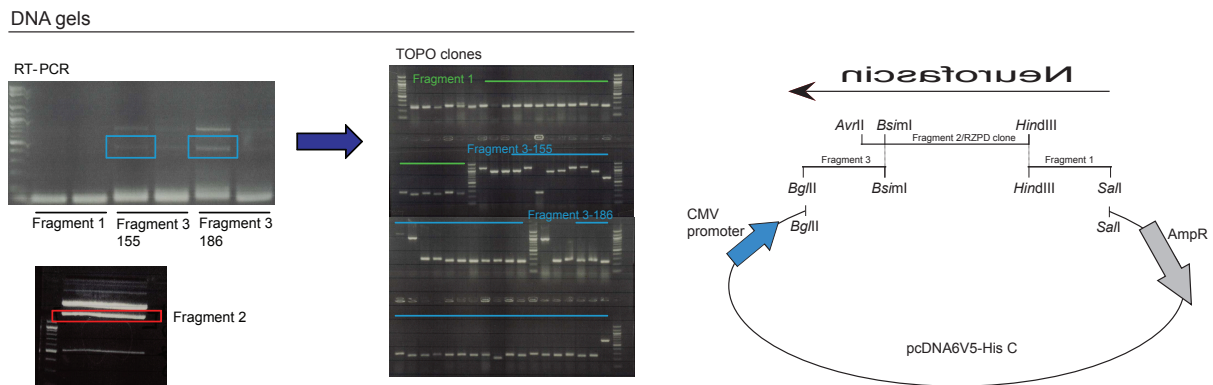


Figure 4.2: **Schematic of NF155 and NF186 cloning strategy:** Left panel: DNA gels used in the cloning process. cDNA generated from the RT-PCR reaction was reamplified by PCR for Fragment 1, Fragment 3-155 and Fragment 3-186. Fragment 2 was cut from the RZPD clone plasmid using restriction enzymes, and it was purified from the resulting mixture of DNA fragments by gel separation and subsequent purification from the gel. TOPO cloning was used to further amplify the scarce material obtained from PCR amplification of Fragment 1, Fragment 3-155 and Fragment 3-186. Right panel: Fragment 1, Fragment 2, and Fragment 3-155/186 were assembled using pCDNA6V5-His C vector. Fragment 1 and Fragment 2 were joined through the *HindIII* restriction site, Fragment 2 and Fragment 3 were joined through the *BsiI* site. The neurofascin gene insert was in reverse orientation in the pcDNA vector; it was cut out using *Sall* and *BglII* to be subcloned into an appropriate expression vector.

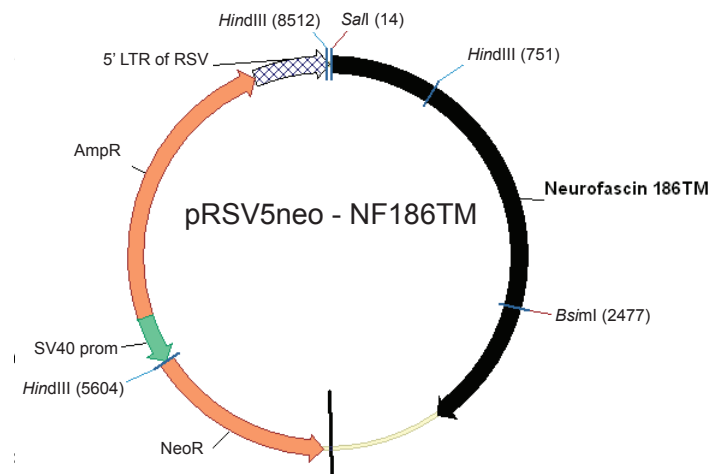


Figure 4.3: **pRSV5neo with transmembrane NF186:** NF186TM was cut from pcDNA vector with *Sall* and *BglII* and ligated into pRSV5neo vector digested with *Sall* and *BamHI* in correct orientation for mammalian expression using the rous sarcoma virus (RSV) promoter within the 5' long terminal repeat (LTR). There are also a neomycin resistance gene (NeoR), simian virus promoter (SV40 prom), and an ampicillin resistance gene (AmpR). Vector map was generated on VectorNTI (Life Technologies, USA)



#### 4.1.1.2 Soluble form of NF155 and NF186

For secreted soluble NF155 and NF186, primer-7 was replaced by primer-8 to generate new Fragment 2 (for NF155) and Fragment 3 (for NF186) in which the transmembrane domain was substituted with a polyhistidine tag. They were assembled with Fragment 1 and the excised cDNA fragment as described in Section 4.1.1.1. For soluble NF production in HEK293-EBNA1 (293E) cells, both NF constructs containing the polyhistidine tag were inserted into pTT5 digested with *PmeI* and *BamHI* by first making the *SalI* site of the insert blunt-ended and then cutting with *BglII*.

#### 4.1.1.3 Transmembrane form of truncated NF variants

We produced six truncated variants of NF155 and NF186 that were fused to superGFP (sGFP) at the C-terminus for cell surface expression. First, we constructed a cassette vector with sGFP inserted into plasmid pRSV5neo by PCR-amplifying sGFP from another plasmid using primer-15,-16. We cut this PCR product and pRSV5neo with *XbaI*, ligated them, and identified a clone containing the insert in the correct orientation for expression. The pRSV5neo vector containing sGFP was referred to as pRSV5neo-sGFP (Figure 4.4).

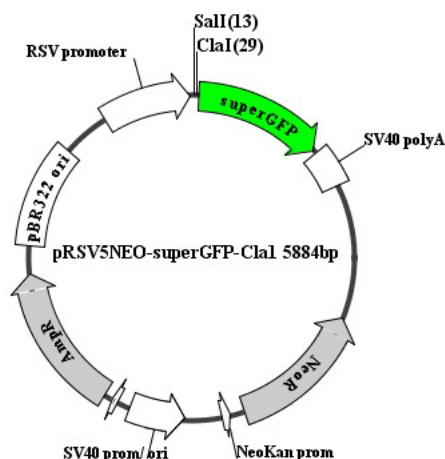


Figure 4.4: **Schematic of pRSV5neo-sGFP cassette vector:** The vector contains the RSV promoter driving the sGFP (or sGFP-fusion protein) expression, the polyA sequence of simian virus 40 (SV40 polyA), neomycin resistance (NeoR), origin of replication and promoter of SV40 (SV40 prom/ori), ampicillin resistance (AmpR), origin of replication (pBR322 ori), and the cloning sites *SalI* and *ClaI*. Vector map generated on DNADynamo (BlueTractor, UK).

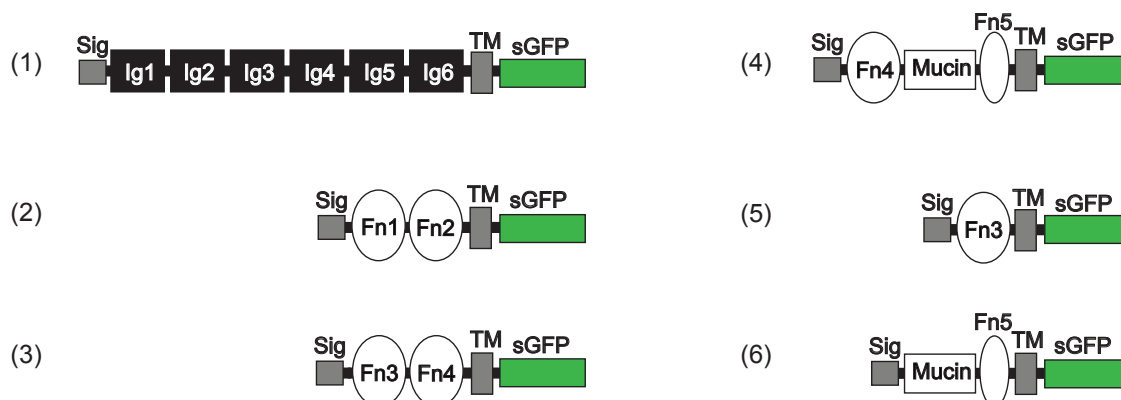


Figure 4.5: **Schematic of sGFP fusion truncated NF variants for cell surface expression:** Sig = signal sequence; Ig = immunoglobulin-like domain; Fn = fibronectin type-III domain; TM = transmembrane domain; sGFP = super GFP. Details of the fragments in text (as numbered).

To generate the truncated NF constructs, a combination of restriction enzymes and overlap-extension-PCR amplification (Heckman and Pease, 2007) was used. Each construct contained a signal sequence and a transmembrane domain to ensure cell surface expression, and they were fused to sGFP in the cytosolic region. (Figure 4.5)

(1) For **NF-Ig** construct spanning the six Ig-domains, a fragment with the signal sequence and the six Ig-domains was excised from the complete NF155 construct using *Sall* and *NheI*. The transmembrane domain fragment was PCR-amplified with primer-17 and -18. The PCR product and the pRSV5neo-sGFP vector were both digested with *Sall* and *Clal*, and ligated together. The ligation product was then cut with *Sall* and *NheI*, and the fragment with the Ig-domains was inserted. (2) For **NF-Fn1Fn2** construct covering Fn1-Fn2 domains, three PCR products were produced to separately cover the signal sequence, the Fn1-Fn2 domains, and the transmembrane domain, using primer-19,-20, primer-21,-22, and primer-23,-18 respectively. The Fn1-Fn2 domains and transmembrane domain were ligated through a *MroI* site. This ligation product was PCR-amplified, and then joined with the signal sequence fragment by overlap-extension PCR. The PCR product was inserted into the pRSV5neo-sGFP vector through *Sall* and *Clal* restriction sites, as it was for the following inserts described. (3) The **NF-Fn3Fn4** construct required overlap-extension PCR to join the signal sequence PCR product (primer-19 and -24) and the Fn3-Fn4 domains, and transmembrane domains PCR product (primer-25 and -18). (4) The **NF-Fn4MucFn5** insert also required overlap-extension PCR to join the PCR product for the signal sequence (primer-19 and -26) and the PCR product for Fn4-Muc-Fn5, and transmembrane domains (primer-27 and -18). (5) The NF155-specific **NF-Fn3** fragment

was produced by joining 3 PCR products: the signal sequence (primer-19 and -24), the Fn3 domain (primer-25 and -28), and the transmembrane domain (primer-29 and -18). The Fn3 domain fragment was joined to the transmembrane domain through a *Bst*Z17I restriction site, and this ligation product was joined with the signal sequence by overlap-extension PCR. (6) For the fragment **NF-MucFn5**, two PCR fragments were joined by overlap-extension PCR: the signal sequence fragment (primer-19 and -30) and the fragment containing Muc-Fn5 and the transmembrane domain (primer-31 and -18).

#### 4.1.1.4 Soluble form of truncated NF variants

For soluble truncated NF variants, we made four constructs containing C-terminus polyHis-tags by PCR amplification using the complete NF constructs as template: 1) **Ig1-Ig2-Ig3-Ig4** using primer-9 and -10; 2) **Ig5-Ig6-Fn1-Fn2** using primer-11 and -12; 3) **Fn3-Fn4** using primer-13 and -8; 4) **Fn4-Muc-Fn5** using primer-14 and -8 (Figure 4.6). These inserts were all digested with *Sca*I and *Bgl*II, and the vector was digested with *Nhe*I, made blunt-ended, and subsequently digested with *Bam*HI. The four ligated pET21c(+) constructs were then transformed into Rosetta competent cells for protein production.



Figure 4.6: **Schematic of soluble truncated NFs:** Sig = signal sequence; Ig = immunoglobulin-like domain; Fn = fibronectin type-III domain; TM = transmembrane domain; sGFP = super GFP; 6xHis = polyhistidine tag. Details of the fragments in text (as numbered).

## 4.1.1.5 List of plasmids generated for this study

Table 4.1: Plasmid list

	<b>Vector</b>	<b>Insert</b>	<b>Expression</b>	<b>Intended host cell line</b>
1	pRSV5neo	-	-	TE671, HeLa
2	pRSV5neo	NF155TM	cell surface	TE671, HeLa
3	pRSV5neo	NF186TM	cell surface	TE671, HeLa
4	pRSV5neo	NF155sol	soluble	HEK293
5	pRSV5neo	NF186sol	soluble	HEK293
6	pRSV5neo	sGFP	cytosolic	TE671
7	pRSV5neo	6lg-sGFP	cell surface	TE671
8	pRSV5neo	Fn1Fn2-sGFP	cell surface	TE671
9	pRSV5neo	Fn3Fn4-sGFP	cell surface	TE671
10	pRSV5neo	Fn3-sGFP	cell surface	TE671
11	pRSV5neo	FN4MucFn5-sGFP	cell surface	TE671
12	pRSV5neo	MucFn5-sGFP	cell surface	TE671
13	pTT5	NF155sol	soluble	HEK293-EBNA
14	pTT5	NF186sol	soluble	HEK293-EBNA
15	pET21c(+)	Ig1Ig2Ig3Ig4	soluble	Rosetta E. coli
16	pET21c(+)	Ig5Ig6Fn1Fn2	soluble	Rosetta E. coli
17	pET21c(+)	Fn3Fn4	soluble	Rosetta E. coli
18	pET21c(+)	Fn4MucFn5	soluble	Rosetta E. coli

## 4.1.2 Recombinant expression of complete NFs and truncated variants

### 4.1.2.1 Cell lines expressing complete NF155 and NF186

TE671 human rhabdomyosarcoma cells were transfected with linearized pRSV5neo-NF155 and -NF186 to produce cell lines with stable expression of the gene of interest. Individual colonies were picked from single cells that were successfully transfected and that had expanded during the subsequent two weeks of incubation. The expression profiles of the cell lines with the best expression that were employed for antibody detection assays are shown in Figure 4.7 as compared to cells transfected with only the mock vector.

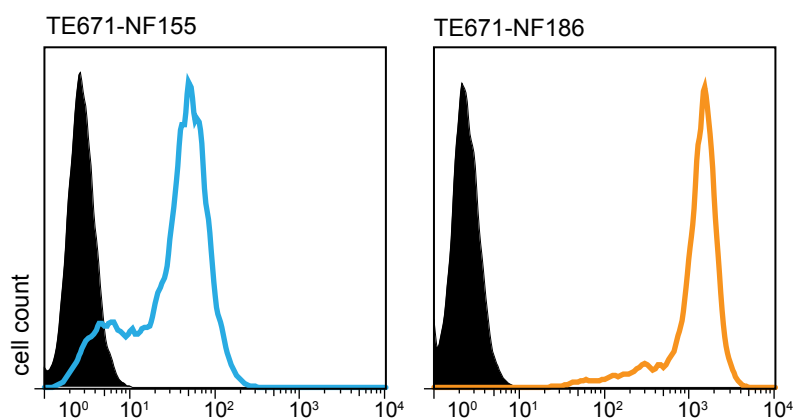


Figure 4.7: **Expression profile of TE671 cells transfected with NF155 and NF186:** TE671 cells transfected with the pRSV5neo vector only (black), with pRSV5neo-NF155 (blue), and with pRSV5neo-NF186 (orange). The 3 cell lines were stained with anti-pan-NF mAb A12/18.1, which recognizes the Fn4 domain that is present in both isoforms of NF.

### 4.1.2.2 Cell lines expressing truncated NF variants

TE671 cells were also transfected with linearized pRSV5neo-sGFP containing 6lg, Fn1-Fn2, Fn3-Fn4, Fn3, Fn4-Muc-Fn5 and Muc-Fn5 to produce cell lines with stable transgene expression as indicated by the intensity of sGFP fluorescence. Individual colonies were picked and individually expanded. All the cell lines were analyzed by flow cytometry to evaluate expression levels. The expression profiles of the cell lines used for epitope mapping are shown in Figure 4.8.

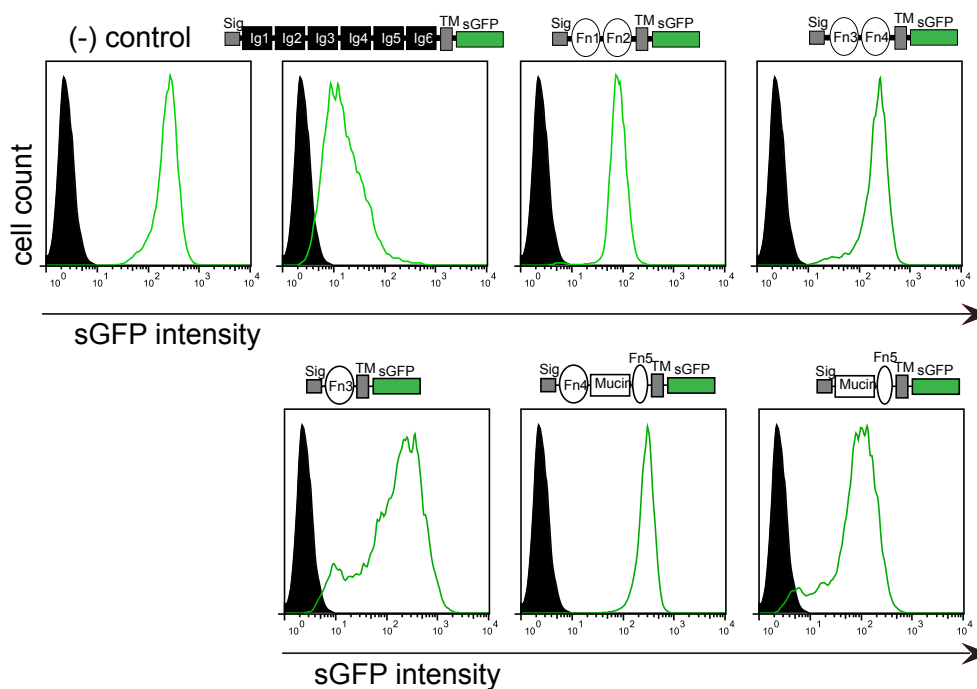


Figure 4.8: **Expression profile of sGFP fusion truncated NF variants compared to TE671 mock transfected cells:** (from left to right) sGFP only, 6Ig, Fn1-Fn2, Fn3-Fn4, Fn3, Fn4-Muc-Fn5 and Muc-Fn5.

#### 4.1.2.3 Soluble complete NF155 and NF186

Soluble complete NF155 and NF186 were produced in HEK293-EBNA cells by transient transfection. Typically from 1 L of cell culture, up to 20 mg of protein could be purified from the supernatant by Ni-NTA chromatography through the His-tag. Purity of the eluted fractions of NF155 and NF186, as well as recognition by pan-NF mAb (A12/18.1) and anti-His-tag mAb are shown in Figure 4.9.

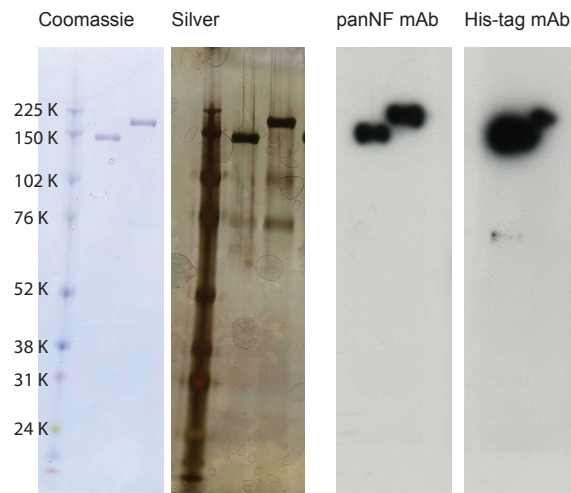


Figure 4.9: **Soluble NF155 and NF186 by SDS-PAGE and Western blot:** (Left) Coomassie blue and silver stained SDS-PAGE show NF155 and NF186 at around 150 kDa and just below 225kDa, and the purity achieved for the preparation; (Right) Western blots detected with antibodies against NF (using A12/18.1) and the His-tag showed bands for NF155 (left band) and NF186 (right band) at the expected positions.

### CD spectroscopy analysis of protein conformation

CD spectroscopy was performed to analyze the conformation of the soluble neurofascins. A CD spectra between 250-195 nm was measured for each protein. For both NF155 and NF186, the spectra were dominated by the presence of beta-sheet structure, consistent with the structure of neurofascins predicted by bioinformatics tool NextProt ([www.nextprot.org](http://www.nextprot.org)).

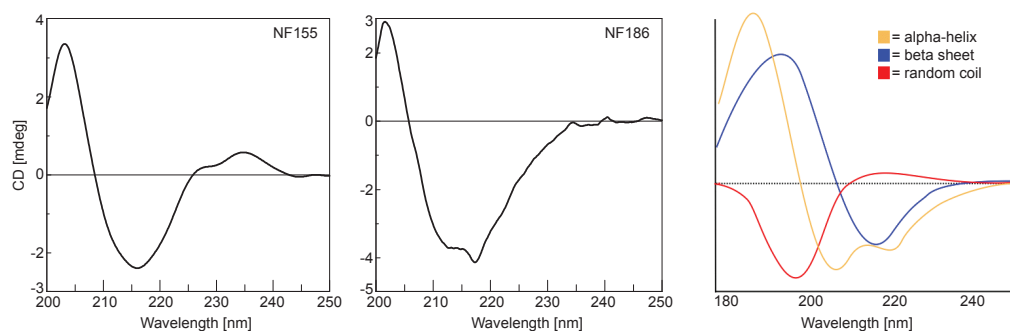


Figure 4.10: **CD-Spectra of soluble NF155 and NF186:** (Left) NF155; (Middle) NF186; (Right) Reference absorption graphs show the absorbance curve of alpha helices, beta sheets, and random coils (adapted from lecture notes of Dr. Ramy Farid, USA).

#### 4.1.2.4 Soluble truncated NF variants

Soluble truncated NF variants were produced in Rosetta *E. Coli* cells and found in the inclusion bodies. The His-tagged truncated NFs (1) Ig1-Ig2-Ig3-Ig4, (2) Ig5-Ig6-Fn1-Fn2, (3) Fn3-Fn4, and (4) Fn4-Muc-Fn5 were solublized and then purified using Ni-NTA chromatography. Their sizes were visualized by SDS-PAGE and identified using anti-His-tag antibody by Western blot (Figure 4.11).

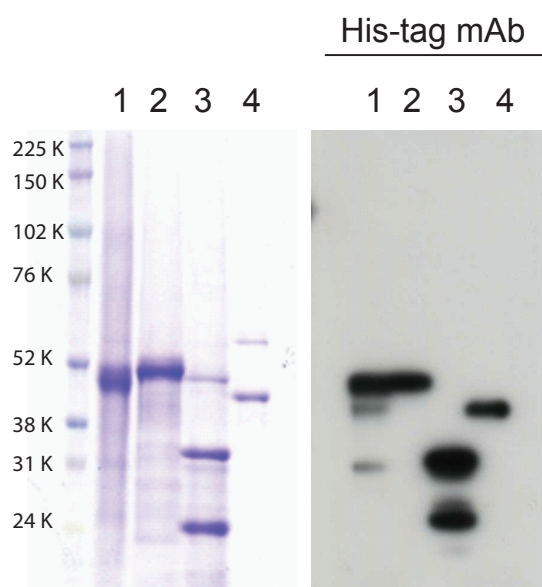


Figure 4.11: **Soluble NF truncation variants by SDS-PAGE and Western blot:** (Left) A Coomassie blue stained SDS-PAGE gel of protein preparation; (Right) Western blot using an antibody against the His-tag shows bands for all 4 fragments at the expected positions. Lane 3 shows the Fn3-Fn4 fragment in the upper band and a degradation product of the fragment in the lower band.



## 4.2 Establishment of anti-NF antibody detection assays

Three assays were established to detect anti-neurofascin autoantibodies in human serum: cell-based assay by flow cytometry, ELISA, and Western blot. Using cell-based assay, we detected antibodies against NF in its the native conformation. By ELISA, we could detect antibodies against NF that was not completely denatured, but it was also not in its native conformation. With Western blot, we detected antibodies against continuous epitopes of NF.

### 4.2.1 Cell-based assay by flow cytometry

Detection of NF-specific antibodies on NF-transfected cells relied on the ability to distinguish the signal specific to the over-expressed NF on the cell surface from the background signal coming from antibodies staining something inherently present on the surface of the TE671 cells. With every serum sample, we stained the NF-overexpressing cell lines (TE-NF155 and TE-NF186) and cells harbouring only the empty vector (TE-RSV0). The signals (mean fluorescence intensity; MFI) measured on TE-NF155 and TE-NF186 were then divided by the signal from TE-RSV0 to normalize for background staining. A negative control staining should give a MFI ratio of approximately 1.

The first step was to make the three cell lines comparable. Initially, the background signal of the cell lines did not give an MFI ratio of 1, which means that only very strong signals were detected and weak signals were masked. We cultured the three cell lines in the same medium with supplements and antibiotic selection, passaged them together, and used new cell culture bottles every time to avoid influence of residual protein left on the bottle surface after trypsinization. After several passages, the cell lines showed comparable background signal, then they could be used for screening (Figure 4.12 A).

The serum samples were initially diluted 1:100 in PBS/1% FBS and a FITC-conjugated anti-human IgG secondary antibody was used for detection. Optimization of this staining protocol was complicated by the lack of anti-NF Ab positive serum samples. We screened 80 serum samples and found one to with NF186 reactivity. We used this positive sample to optimize the screening procedure. The modifications included: dilution of serum 1:50 and detection with anti-human-IgG or anti-human-Ig secondary antibody conjugated with PE (Figure 4.12 B). The established protocol is outlined in Section 3.5.2.1.

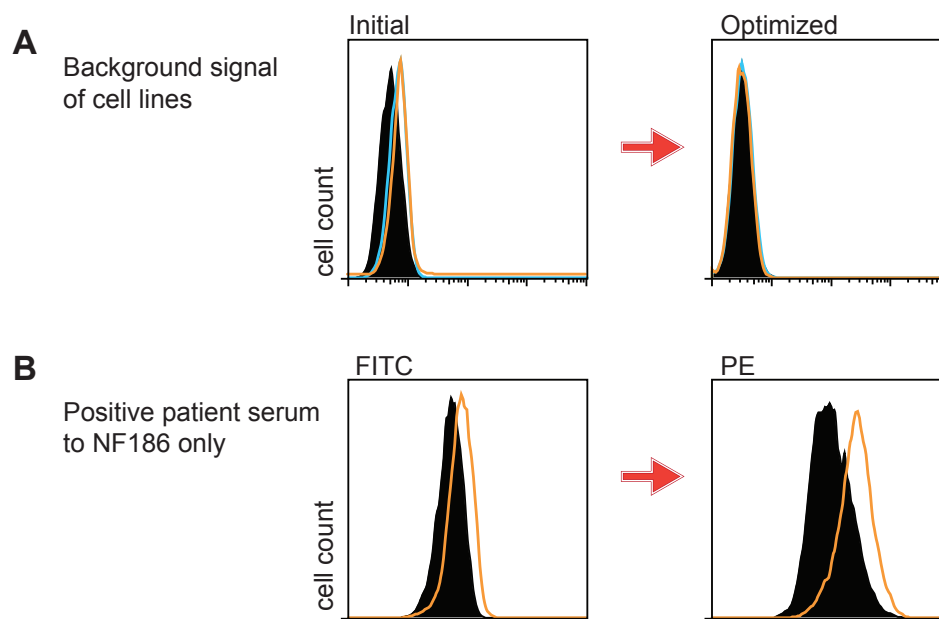


Figure 4.12: **Optimization of cell-based assay by flow cytometry:** TE-RSV0 (black, filled), TE-NF155 (blue line), and TE-NF186 (orange line) stained with only the secondary anti-human-IgG antibody (**A**) before and after optimization. TE-RSV0 and TE-NF186 were stained with anti-NF186 reactive patient serum and detected by anti-human-IgG conjugated with FITC and PE (**B**). The cell lines became comparable for background signal and signal-to-noise ratio was improved after optimization.

#### 4.2.2 ELISA

For ELISA detection of NF-specific autoantibodies in human sera, we considered how the antigen was displayed, the optimization of signal-to-noise ratio, and the reproducibility of the results.

To choose a suitable solid support for the assay, we compared maxisorp plates and nickel-chelate (Ni-NTA) coated plates. While maxisorp plates involve mainly hydrophilic binding of the glycosylated protein antigen, Ni-NTA coated plates utilize C-terminus His-tag to bind the antigen, thus theoretically conferring orientation to the displayed antigen. We compared the utility of the two different supports using monoclonal anti-NF antibodies, serum from rats immunized with human NF155, and serum from a human donor. We noted that although pattern of reactivity to human NF155 and NF186, and rat NF155 in each staining was essentially identical in both types of plates, the signals observed were consistently stronger on the maxisorp plates (Figure 4.13 B and C). In addition, reproducibility using maxisorp plates was superior compared to Ni-NTA plates. This could be due to leakage of the antigen from the Ni-NTA beads and interference from unknown factors present in the serum that produce an inconsistent level

of background. An additional consideration for our choice to use maxisorp plates for screening of serum samples was the economy of the procedure.

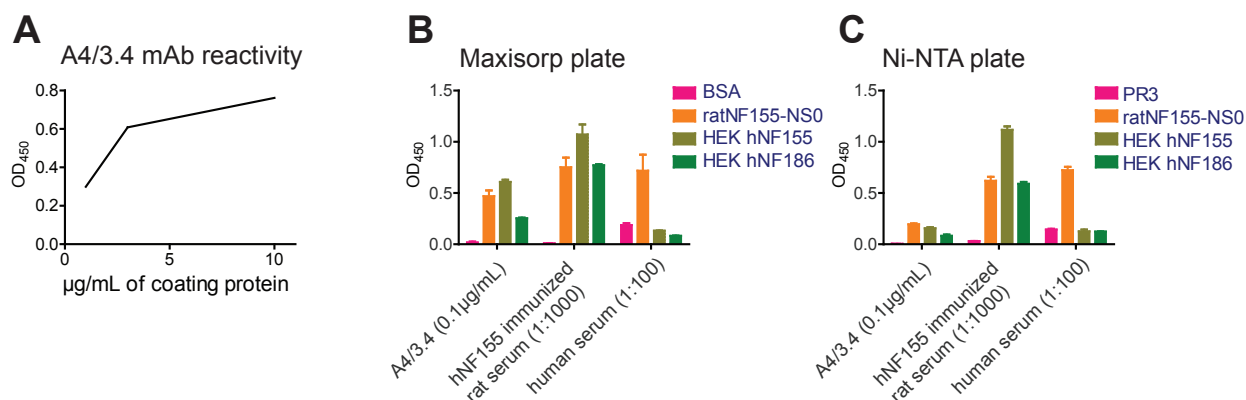


Figure 4.13: **Optimization of the ELISA protocol:** Level of reactivity of A4/3.4 mAb towards hNF155 coated at 1 µg/mL, 3 µg/mL and 10 µg/mL is shown (A). Reactivities of A4/3.4 mAb (0.1 µg/mL), serum from a rat immunized with HEK NF155 (1:1000), and control human serum (1:100) against ratNF155-NS0, hNF155 and hNF186 from HEK cells, and negative control (BSA for maxisorp plates, PR3 for Ni-NTA plates) were compared between maxisorp plates (B) and Ni-NTA plates at 3 µg/mL (C). ELISA reactivity is shown here as the raw OD<sub>450</sub> value.

Sensitivity of the assay was essential to the screening protocol. We coated maxisorp plates with protein antigen at concentrations of 1, 3, and 10 µg/mL and then found the optimal concentration for antigen coating to be between 3 and 10 µg/mL (Figure 4.13 A). So we subsequently tested ELISA reactivity at 5 µg/mL. In addition, we tested human serum samples diluted 1:50, 1:100, and 1:400, and found that 1:100 dilution gives the best signal-to-noise ratio. The optimized protocol that was used for serum screening is described in Section 3.5.2.2.

#### 4.2.2.1 ratNF155-NS0 is not a specific antigen to detect anti-NF reactivity

We also compared the utility of human NF155 and NF186 (self-generated) with rat NF155 (commercially available from R&D Systems) since ratNF155 was used as the antigen to detect human antibodies to NF in previous studies (Mathey et al., 2007; Pruess et al., 2011). RatNF155-NS0 was produced in NS0 murine myeloma cells while the human NFs were produced in HEK293 cells.

We found that while in total only very few donors showed low reactivity to HEK293-produced human NF155 and NF186 (Figure 4.23, ELISA screening of serum from MS patients and controls shown), virtually all donors of the same cohort showed some response against ratNF155-NS0. To investigate this large discrepancy, we affinity-purified antibodies from four RR-MS donors

using a ratNF155-NS0-conjugated column. With these purified antibodies, we probed for reactivity against HEK293-EBNA-derived NF155 and NF186, ratNF155-NS0, and irrelevant NS0-derived antigens: human contactin-2/TAG-1 and human OMgp. We found by ELISA that the affinity-purified anti-ratNF155-NS0 antibodies did not bind NF155 and NF186, but recognized the irrelevant NS0-derived antigens. By Western blot, a faint HEK293-derived NF155 band was detected along with NS0-derived antigens, signifying that a small proportion of the purified antibodies indeed recognize neurofascin. This was seen with all four donors (one example shown in Figure 4.14 B and C). The mAb A4/3.4 recognized ratNF155-NS0 along with NF155 and NF186, and as expected, not contactin-2 or OMgp (Figure 4.14 B). Thus, we show that although the ratNF155-NS0 was detected by some antibodies to NF, it was also recognized by other Igs that were not NF-specific.

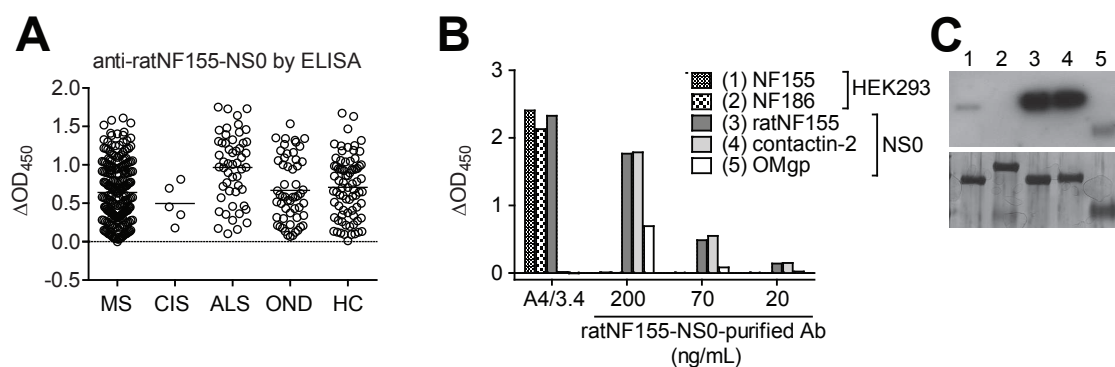


**Figure 4.14: ratNF155-NS0 was not a specific antigen to detect antibodies to human neurofascin in human serum:** Serum screening by ELISA using ratNF155-NS0 (**A**) included samples from patients with MS (n=225), CIS (n=5), ALS (n=52), and controls OND (n=55), HC (n=77). The delta OD (response to ratNF155-NS0 minus BSA reactivity) is shown. Most of the patients and control donors show a response against this antigen. The mean of each group is shown. Antibodies purified over rat NF155-NS0 conjugated column were tested by (**B**) ELISA and (**C**) Western blot for reactivity against HEK293-EBNA derived NF155 and NF186, ratNF155-NS0, and unrelated NS0-derived antigens: human contactin-2/TAG-1 (hTAG1) and human oligodendrocyte myelin glycoprotein (hOMgp). The number above each lane in (**C**) corresponds to the antigen with the same number in (**B**). Anti-pan-NF mAb (A4/3.4) was also tested by ELISA and recognized NF155, NF186 and ratNF155-NS0 (**B**).

#### 4.2.3 Western blot

The protocol for NF-specific antibody detection by Western blot is described in Section 3.5.2.3. The procedure used was essentially the standard protocol for immunoblots. A drawback to this approach was the high background signal observed when diluted serum was incubated with the blotted membrane, which confounded our ability to detect an NF-specific signal. The

advantage of performing Western blots is that we knew exactly where the NF-specific signal should be in relation to the molecular weight ladder. For screening, we diluted human serum 1:400 in a blocking buffer (5% skim milk in PBST; filtered). Example blots are shown in Figure 4.24.

#### **4.2.4 Reactivity of pan-NF monoclonal antibodies and NF155-specific rabbit serum in the assays**

The three anti-NF antibody detection assays were tested using pan-NF mouse monoclonal antibodies (A4/3.4 and A12/18.1) and rabbit serum that was generated against a peptide specific to NF155. The mouse mAb A4/3.4 recognized both NF155 and NF186 strongly by flow cytometry, ELISA and Western blot (Figure 4.15 A). The other mouse mAb A12/18.1 recognized both isoforms strongly by flow cytometry, only the NF186 and hardly the NF155 by ELISA, and only the NF186 by Western blot (Figure 4.15 B). The rabbit serum was unreactive to the NFs by flow cytometry, but was strongly reactive to NF155 by ELISA. By immunohistochemistry using longitudinally cut spinal cord sections, antibodies purified from the rabbit serum stained paranodes, where NF155 was located, and the A12/18.1 stained nodes, where NF186 was found (Figure 4.15 C).

We further analyzed the specificity of the mAbs using truncation variants of NF155 and NF186 by Western blot (Figure 4.15 A and B right) and flow cytometry (Figure 4.16 B). We did not detect reactivity by Western blot nor by flow cytometry with A4/3.4 using truncation variants. With A12/18.1, we saw strong reactivity to Fn3-Fn4 (NF155 specific fragment) and also its degradation product by Western blot, and by flow cytometry reactivity to Fn3-Fn4 and Fn4-Muc-Fn5 fragments. Considering that A12/18.1 recognized both isoforms by flow cytometry, evidence would indicate that the reactivity was directed to the Fn4 domain, which was common to both isoforms.

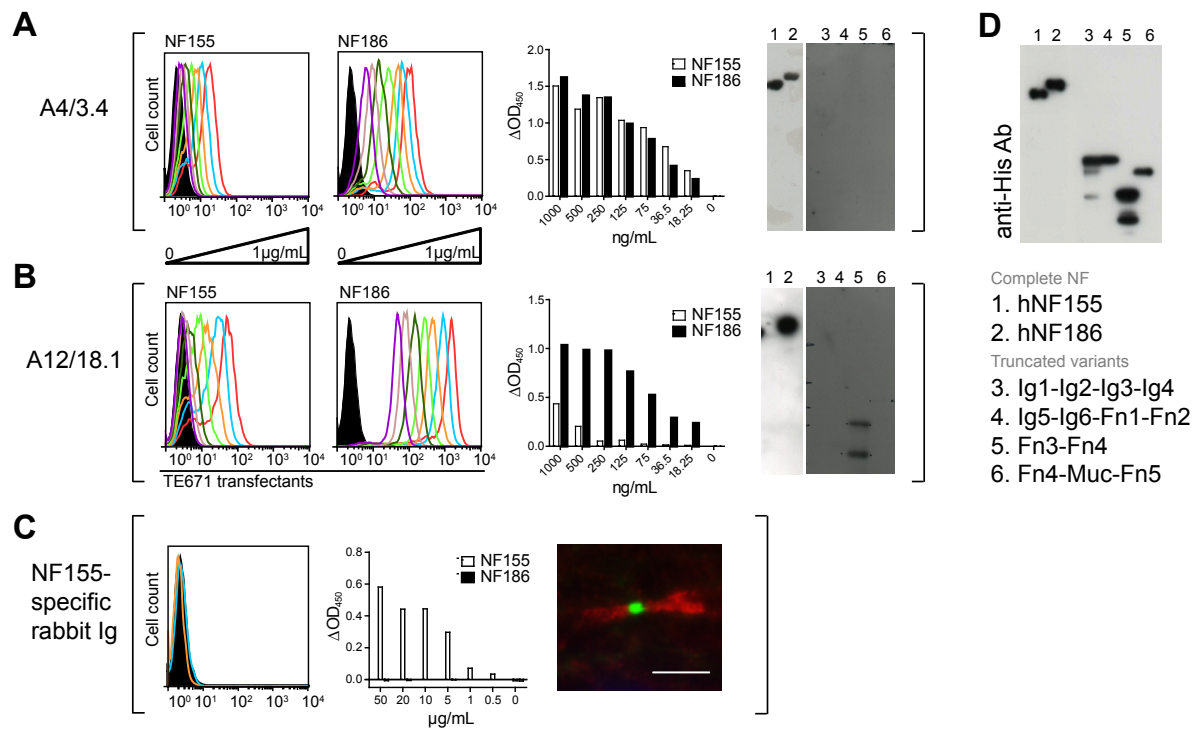


**Figure 4.15: Reactivity of pan-NF mAbs and NF155-specific rabbit serum in the assays:** Reactivity of mAbs A4/3.4 (**A**) and A12/18.1 (**B**), and rabbit serum (**C**) by flow cytometry (left), ELISA (middle), Western blot (right; upper 2 panels), immunohistochemistry on longitudinally cut spinal cord section (right; lower panel). Flow cytometry results are depicted in histograms for antibody staining intensity. ELISA results are shown as  $\Delta OD_{450}$ . The section was stained with antibodies purified from the rabbit serum (red) and A12/18.1 (green). Serial dilution (in ng/mL: 1000, 500, 250, 125, 75, 38.5, 18.25) was done for mAbs by flow cytometry and for all three antibodies by ELISA. The antigens employed in Western blot analysis are shown in a blot using anti-His tag antibody (**D**): complete extracellular regions of (1) hNF155 and (2) hNF186 produced in HEK293 cells, and truncated variants (3) Ig1-Ig2-Ig3-Ig4, (4) Ig5-Ig6-Fn1-Fn2, (5) Fn3-Fn4, and (6) Fn4-Muc-Fn5 produced in *E. coli*.

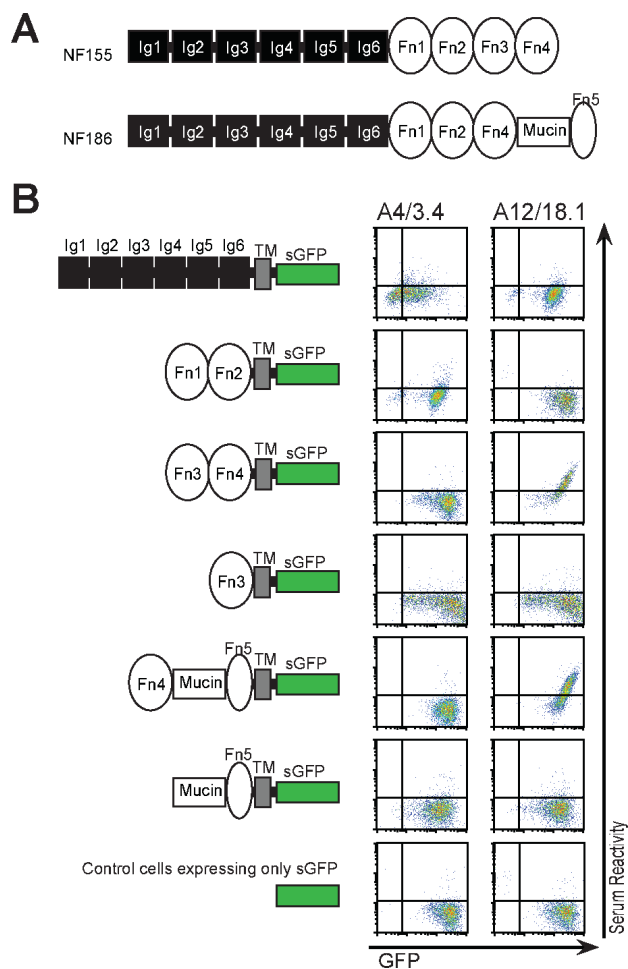


Figure 4.16: **Domain specificity of pan-NF mAbs by flow cytometry:** (A) A scheme of the extracellular domains of NF155 and NF186 are shown. The six Ig-like domains and fibronectin domains 1, 2 are common between the two isoforms. NF155 has Fn3 before Fn4 while NF186 lacks the Fn3, has Fn4 and additionally a Mucin domain and Fn5 domain. (B) The reactivities of the two mAbs (A4/3.4 and A12/18.1) to each truncation variant are shown next to a scheme depicting each truncated NF variant.

### 4.3 Neurofascin-specific autoantibodies in Guillain-Barré syndrome and chronic inflammatory demyelinating polyneuropathy

In this study, we asked if anti-NF antibodies are present in serum of patients with peripheral neuropathies. We screened serum samples from patients with different variants of inflammatory neuropathies, mainly GBS variants acute inflammatory demyelinating polyneuropathy (AIDP) and acute motor axonal neuropathy (AMAN), and chronic inflammatory demyelinating polyneuropathy (CIDP). Then we characterized samples with anti-NF reactivity by isotyping, serial dilution, domain mapping, and for staining of nodal structures on tissue sections. Since we found NF-reactivity in a small proportion of patients with AIDP and CIDP, we investigated possible *in vivo* effects of anti-NF antibodies in a neuritis animal model, experimental autoimmune neuritis (EAN), and report that anti-NF antibodies enhance and prolong disease in this model.

#### 4.3.1 Serum screening for anti-NF antibodies

We have tested a total of 394 serum samples by both ELISA and cell-bound assay using flow cytometry with human NF155 and NF186. Using ELISA, we found reactivity in 8/254 (3%) patients with inflammatory neuropathies (5 CIDP, 3 AIDP, 0 AMAN), but in none of 140 controls (Figure 4.17 A and B). Among these eight anti-NF positive patients, six (5 CIDP, 1 AIDP) recognized only NF155, one (AIDP) recognized only NF186, and one (AIDP) recognized both isoforms (Figure 4.17 A and B). In addition, six of the patients showed clear reactivity while two were at the detection limit.

Using our cell-based assay, we found very strong reactivity to NF155 in two CIDP patients (Figure 4.17 C). These two patients had also exhibited reactivity to NF155 by ELISA (Figure 4.17 A). In addition, four controls (1 other neurological disease (OND) with sensory symptoms, 3 healthy (HC)) exhibited reactivity to one NF isoform expressed on the cell surface, but did not react by ELISA (Figure 4.17).

To further investigate the prevalence of human NF reactivity in CIDP patients, we tested an additional cohort of 40 patient samples taken from plasma exchange material (Figure 4.17). We found one donor with clear NF155 reactivity by ELISA, but not in the cell bound assay.



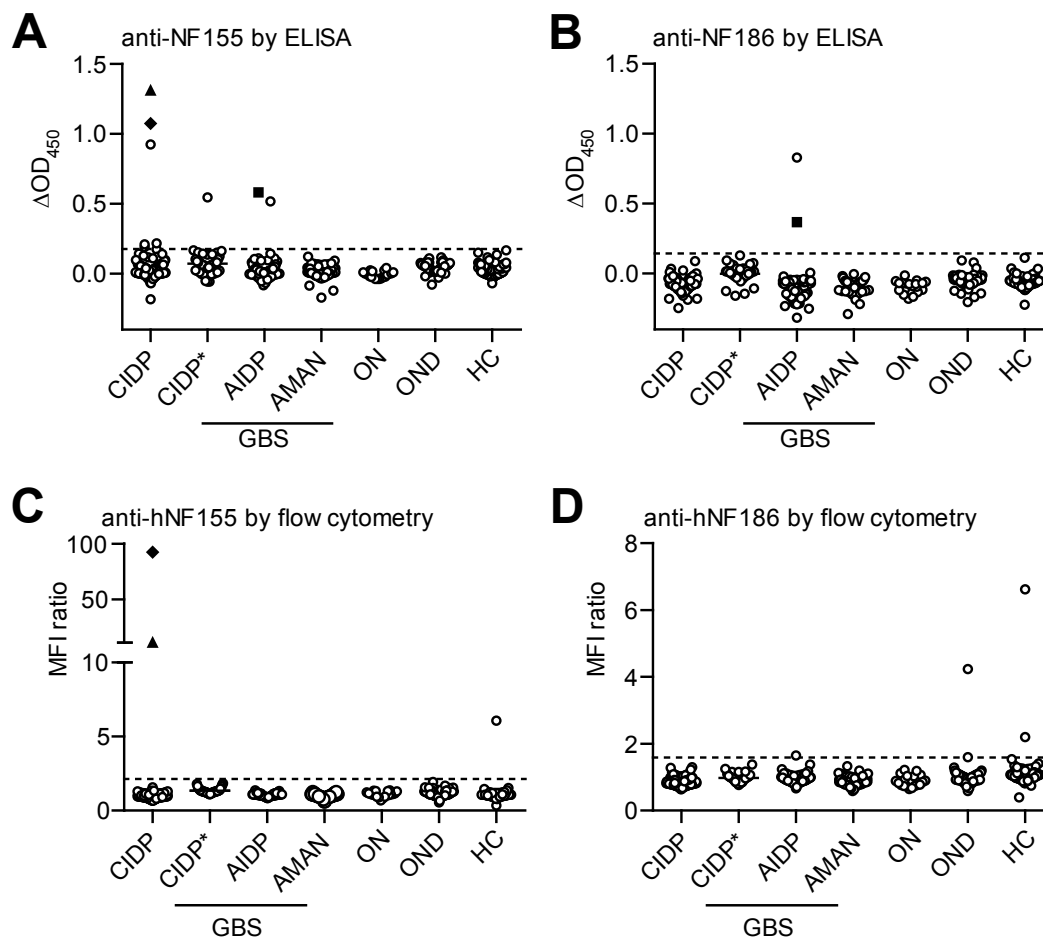


**Figure 4.17: Autoantibodies to NF155 and NF186 detected by ELISA and flow cytometry:** Serum samples from patients with CIDP ( $n = 118$ ), AIDP ( $n = 65$ ), AMAN ( $n = 50$ ), ON ( $n = 20$ ), and controls OND ( $n = 61$ ), HC ( $n = 77$ ) were tested for autoantibodies to NF155 and NF186 by ELISA (**A,B**) and flow cytometry (**C,D**). Plasma exchange material from an additional cohort of CIDP patients (CIDP\*;  $n = 40$ ) were tested. ELISA reactivities to NF155 (**A**) and NF186 (**B**) are shown as baseline-subtracted optical density reading at 450 nm ( $\Delta OD_{450}$ ; response to NF minus BSA reactivity). Reactivity by flow cytometry is shown as mean fluorescence intensity (MFI) ratio (reactivity to NF transfectants divided by reactivity to control cells). The cutoff (dashed line) represents the mean of OND group plus four standard deviations. The special symbols are each representative of one serum sample.

Since a previous report (Pruess et al., 2011) found a higher average reactivity to ratNF155-NS0 by ELISA in GBS patients compared to healthy controls, we also used this antigen for serum screening in parallel with the HEK293-derived protein. As in that report, we found broad reactivity to ratNF155-NS0. However, we did not observe a significant difference between the GBS group (AIDP and AMAN;  $n = 115$ ) compared to the control group (OND and HC;  $n = 138$ ). The patients who showed reactivity to the NF155/NF186 by ELISA were not conspicuous with ratNF155-NS0 (gray symbols; Figure 4.18). Nonetheless, as shown earlier in Section 4.2.2.1, we believe that ratNF155-NS0 is not a specific antigen to identify antibodies against human

NFs and would consider data obtained with this antigen with caution.

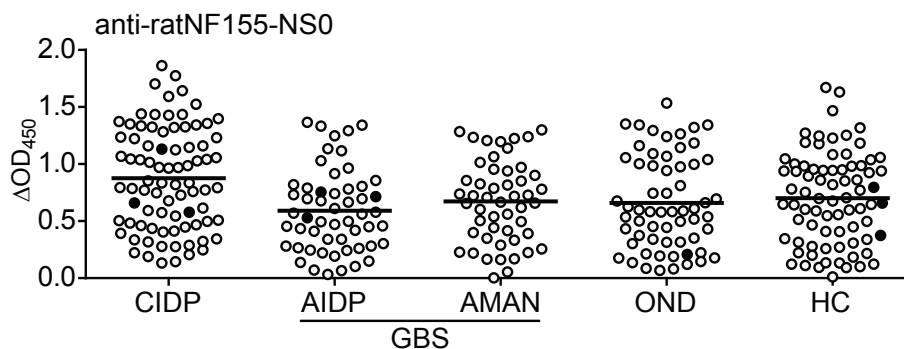
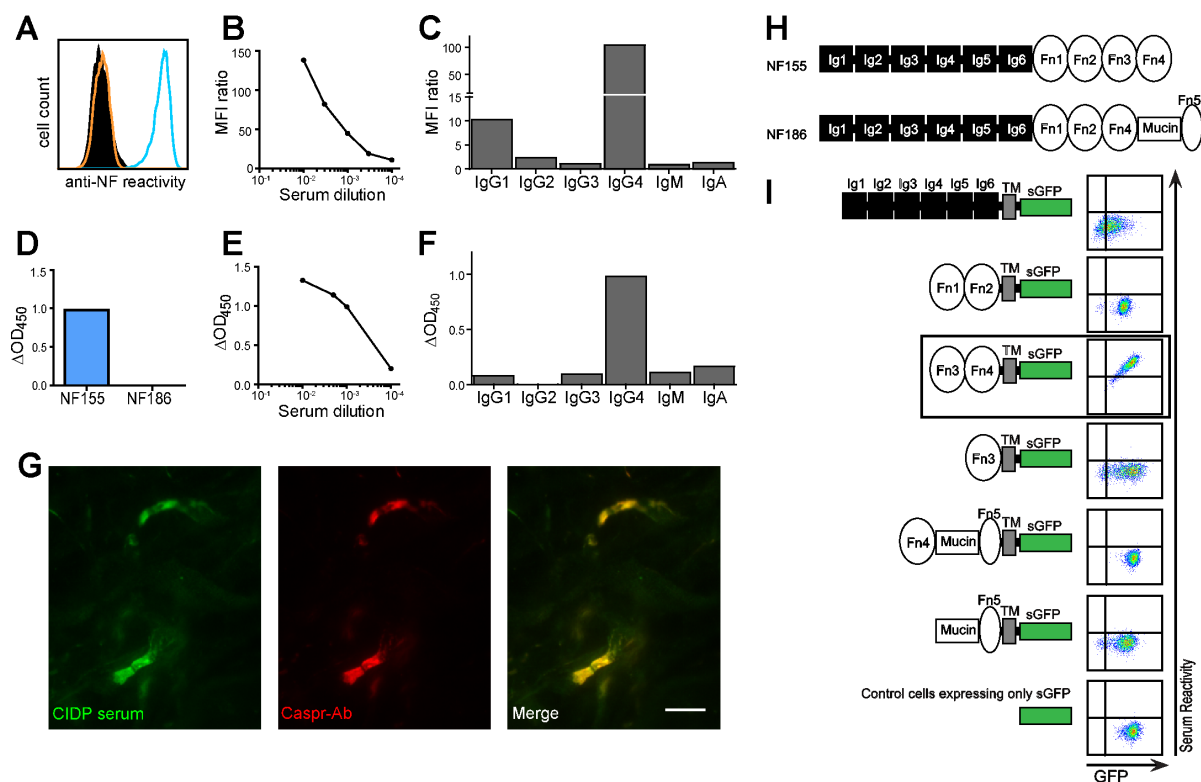


Figure 4.18: **ELISA screening with ratNF155-NS0:** Serum screening by ELISA using ratNF155-NS0 (A) included samples from patients with CIDP ( $n = 82$ ), AIDP ( $n = 54$ ), AMAN ( $n = 50$ ), and controls OND ( $n = 61$ ), HC ( $n = 77$ ). The delta OD (response to ratNF155-NS0 minus BSA reactivity) is shown. Most of the patients and control donors show a response against this antigen. The mean of each group is shown. Filled circles represent positive samples from ELISA or flow cytometry using NF155 and NF186.

### 4.3.2 Detailed analysis of NF-reactive serum samples

We further characterized the anti-NF reactivities detected in the two patient samples by both assays and the four highest by only ELISA, as well as four control samples by flow cytometry (Figure 4.17).

Two CIDP patients (43 yr old Japanese female and 76 yr old German female) showed high IgG reactivities to NF155 by both ELISA and cell-based assay (Figure 4.17 A and C). In both patients, the anti-NF155 reactivities were detected at serum dilutions of 1:1000 up to 1:10 000 in both assays (Figure 4.19 B and E, Figure 4.20 B and E). In one of the two patients, we also tested cerebrospinal fluid and found NF155 reactivity (Figure 4.20 D). The dominant IgG subclass was IgG4 in both cases, with minor contribution from IgG1, IgG2, IgG3, and IgM, IgA (Figure 4.19 C and F, Figure 4.20 C and F). To identify the domains that were recognized by these autoantibodies, we expressed truncated variants of NF155 and NF186 on the surface of TE671 cells. Autoantibodies from both patients recognized only one fragment unique to NF155 spanning the Fn3-Fn4 domains (Figure 4.19 I, Figure 4.20 I). We further analyzed whether these autoantibodies also recognized NF155 on tissue sections. NF155 is known to be localized in the paranodes in both the CNS and PNS (Poliak and Peles, 2003). Serum from both patients stained paranodes on rat tissue sections that are marked by anti-Caspr antibody staining as a paranodal marker (Peles et al., 1997) (Figure 4.19 G, Figure 4.20 G).



**Figure 4.19: A Japanese CIDP patient with high NF155 reactivity:** Reactivity to NF155 was seen by flow cytometry (**A,B,C**) up to a dilution of 1:10 000 (**B**). (**A**) Reactivity to NF155 (blue line) was compared with reactivity to NF186 (orange line) and to control cells (black, filled). (**C**) The NF155 reactivity was mediated by IgG4 with minor contribution from IgG1. Reactivity to NF155 was also seen by ELISA (**D,E,F**) up to a dilution of 1:10 000 (**E**) by IgG4 and weakly by IgG1, IgG3, IgM, and IgA (**F**). Serum staining (**G**, left) colocalizes with Caspr staining (**G**, middle) on longitudinally cut rat spinal cord sections. The scale bar represents 10 $\mu$ m. (**H**) NF186 differs from NF155 by substitution of Fn3-Fn4 with Fn4-Mucin-Fn5. (Ig = immunoglobulin-like domain; Fn = fibronectin type III domain) (**I**) A scheme of super green fluorescent protein (sGFP) fusion truncated NF variants is shown beside the corresponding serum reactivity by flow cytometry. Reactivities to truncated NF variants and to negative control cells are shown as sGFP intensity versus serum reactivity. The fragment recognized by both NF155-reactive serum samples is boxed.

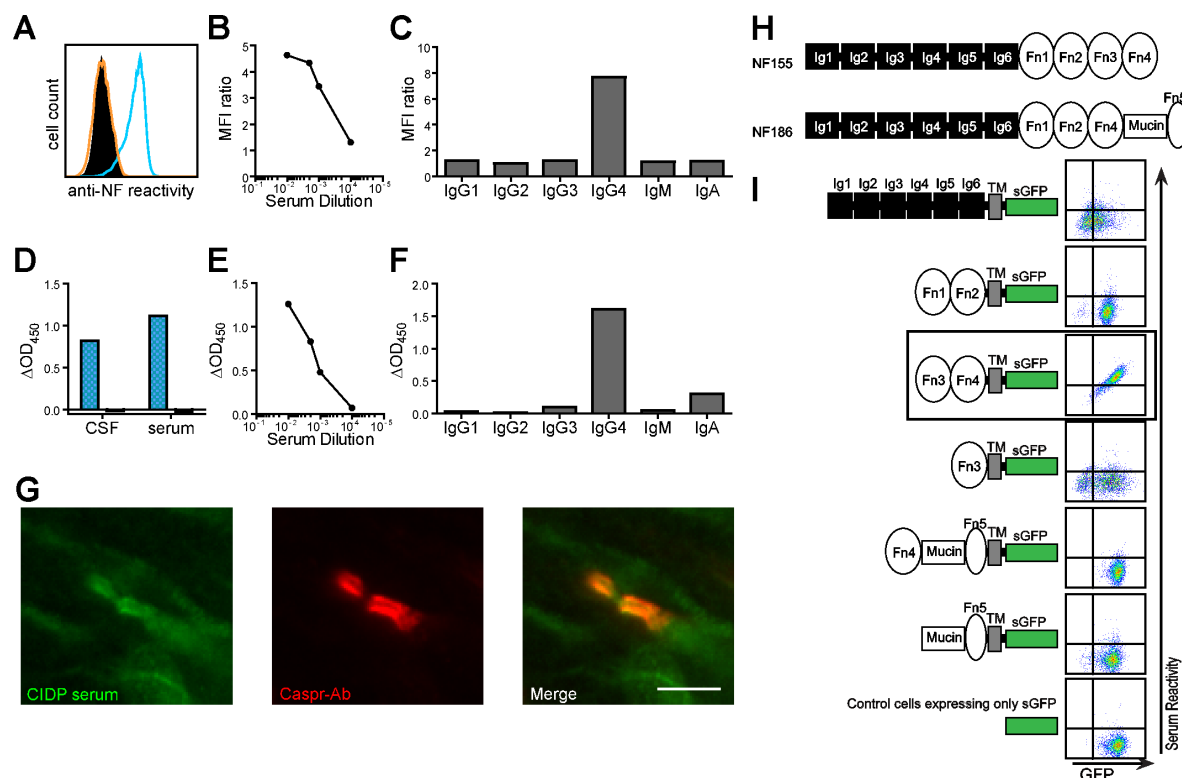


**Figure 4.20: A German CIPD patient with high NF155 reactivity:** Reactivity to NF155 was seen by flow cytometry (**A,B,C**) up to a dilution of 1:10 000 (**B**). (**A**) Reactivity to NF155 (blue line) was compared with reactivity to NF186 (orange line) and to control cells (black, filled). (**C**) The NF155 reactivity was mediated by IgG4. Reactivity to human NF155 was also seen by ELISA in serum and cerebrospinal fluid. Serum reactivity by ELISA (**D,E,F**) was seen up to a dilution of 1:10 000 (**E**) by IgG4 and weakly by IgG3 and IgA (**F**). Serum staining (**G**, left) colocalizes with Caspr staining (**G**, middle) on longitudinally cut rat spinal cord sections. The scale bar represents 10  $\mu$ m. (**H**) NF186 differs from NF155 by substitution of fibronectin (Fn) domains Fn3-Fn4 with Fn4-Mucin-Fn5. (Ig = immunoglobulin-like domain; Fn = fibronectin type III domain) A scheme of super green fluorescent protein (sGFP) fusion truncated NF variants is shown beside the corresponding serum reactivity by flow cytometry (**I**). Reactivities to truncated NF variants and to negative control cells are shown as sGFP intensity versus serum reactivity. The fragment recognized by both NF155-reactive serum samples is boxed.

A patient fulfilling clinical and electrophysiological criteria of motor-dominated CIPD (44 yr old German male) had antibodies to NF155 as detected by ELISA. Extensive antibody tests for onconeural, rheumatologic, autoimmune, neuronal surface antigen and neuropathy-related antibodies were negative in this patient. In detail, this patient tested negative for antibodies against Hu, Yo, Ri, amphiphysin, GAD65, MOG, TPO, TG, aquaporin-4, gangliosides (GM1, GM2, GM3, GD1a, GD1b, GT1b, GQ1b), AChR, ANA, ENA, cANCA, pANCA, VGKC, VGCC, MuSK, Ma1, Ma2, CV2, NMDA, GABA<sub>B</sub>, AMPA, Lgi1, and Caspr2. He developed progressive relapsing paralysis in his distal arm and hand. During the first 6 months, he completely responded to treatment with high-dose steroids and intravenous immunoglobulin (ivIG). Sural

nerve biopsy indicated demyelination. The paralysis progressively worsened to tetraparesis including facial and respiratory muscles, and he became unresponsive to steroids and ivIG. By electromyography (EMG) he showed multiple conduction blocks. Plasma exchange (PE) was found to be very efficient to rapidly and completely relieve paralysis, but frequency of PE increased from once a month to 3-4 times a week. Remarkably, with PE the patient regained reflexes within a few days, suggesting a functional disturbance rather than structural damage. Three years after initial presentation, he received an autologous stem cell transplant in 2010. Several months afterwards, frequency of PE was reduced to once a week, and he was finally weaned without recurrence of paralysis. We were able to monitor the anti-NF reactivity throughout the disease course. The NF155 reactivity persisted throughout this observation period while showing a progressive decline after the 2009 time point (Figure 4.21 A). The anti-NF antibodies were predominantly IgG3 by ELISA (data not shown). We affinity purified anti-NF antibodies against both NF155 and NF186 from plasma exchange material, and eluted IgG3, as well as small amounts of IgG1, IgM, and IgA (data not shown). These antibodies were reactive to NF155 by ELISA and also by cell-based assay, and additionally a low reactivity to NF186 in both assays (Figure 4.21 B-D).

Another CIDP patient (64 yr old German male) who benefited from plasma exchange also showed NF155-specific antibodies which were IgM, IgA, IgG3, IgG2, IgG1 (in the order of contribution to the reactivity observed by ELISA). Three patients with AIDP (83, 59, 34 yr old Japanese males) showed reactivities to NF at serum dilution of up to 1:1000 by ELISA. They tested negative for anti-ganglioside antibodies. The first exhibited antibodies to only NF155 with IgG1, the second to only NF186 with IgG1, and the third to both NFs with IgG1 and IgG3 (data not shown).

Four control samples also showed NF reactivities at serum dilution 1:1000 by flow cytometry and not by ELISA. These samples were from a patient (33 yr old Swedish female) with sensory symptoms (classified OND), and three healthy controls (46, 47, 47 yr old Japanese females). The OND control patient had anti-NF186 IgG3 antibodies, one healthy control had anti-NF155 IgG1, and the other two healthy controls had anti-NF186 IgG1 (data not shown). The NF155-reactive samples showed reactivity only to the NF155-unique truncation mutant expressing Fn3-Fn4 domains while NF186-reactive samples recognized NF186-unique fragments spanning Fn4-mucin-Fn5, and also mucin-Fn5 alone (data not shown). The other 62 OND control donors and 74 healthy controls were tested negative for NF reactivity by both assays. All the

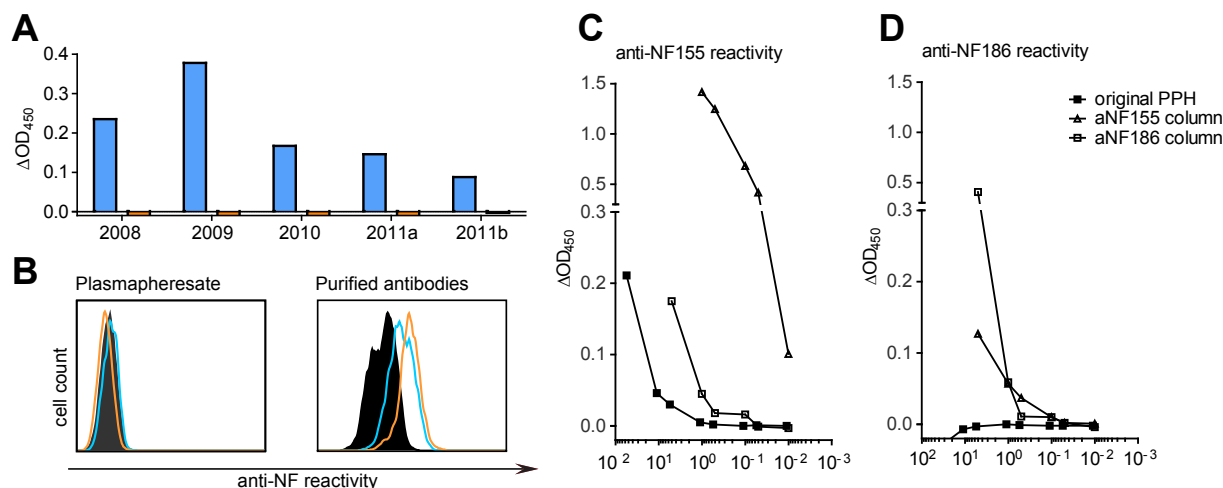


**Figure 4.21: NF155 reactivity in a CIDP patient benefiting from plasma exchange:** Anti-NF155 reactivity by ELISA persisted over years in one CIDP patient, and after affinity purification, low level reactivity was seen by ELISA and flow cytometry to both NF155 and NF186. **(A)** By ELISA, reactivity to NF155 (blue), but not NF186 (orange) was found in samples taken from 2008, 2009, 2010, and two time points (February (a) and October (b)) in 2011. Reactivities were measured at the same Ig concentration for each time point. **(B-D)** Anti-NF antibodies were purified from plasma exchange (PE) material from 2011a against NF155 and NF186. By flow cytometry **(B)**, original PE material was not reactive to either NF (NF155, blue line; NF186, orange line), but NF155-purified antibodies showed binding to both isoforms. By ELISA **(C,D)**, serial dilution of PE material and purified antibodies was done **(C)** NF155 was recognized by the original PE material and by antibodies from both NF columns. **(D)** NF186 was recognized by only purified antibodies from both NF columns but not by the original PE material.

positive samples found by either assay were tested for nodal or paranodal binding on tissue sections by immunohistochemistry, only the two highly reactive CIDP patients showed a clear paranodal staining pattern (Figures 4.19 and 4.20).

### 4.3.3 Effects of anti-NF antibodies on experimental autoimmune neuritis

We investigated possible *in vivo* effects of NF targeting by antibodies in peripheral nerve by utilizing an EAN rat model. EAN was induced by active immunization with P2-peptide and clinical disease was observed 14 days later. We tested two different anti-pan-NF mAbs (A12/18.1 mouse IgG2a and A4/4.3 mouse IgM) separately. At disease onset 500  $\mu$ g of mAb or the respective isotype control was injected intravenously. Both anti-NF mAbs rapidly increased disease severity and prolonged disease duration compared to isotype controls (Figure 4.22). Rats treated with mouse IgG2a anti-NF mAb A12/18.1 showed a clinical score of  $2.4 \pm 0.4$  (mean  $\pm$  SEM;  $n = 6$ ) at the peak of disease, compared to  $1.1 \pm 0.3$  (mean  $\pm$  SEM;  $n = 6$ ) in rats treated with isotype control. Disease duration in rats injected with anti-NF mIgG2a was 26 days compared to only 11 days with isotype control treatment. Rats treated with mouse IgM anti-NF

mAb A4/3.4 showed a clinical score of  $2.4 \pm 0.3$  (mean  $\pm$  SEM;  $n = 6$ ) at the peak of disease, compared to  $1.3 \pm 0.2$  in rats treated with isotype control. Disease duration after anti-NF mIgM injection was 24 days, compared to 17 days with the isotype control. Naïve rats injected with either anti-NF mAb without prior P2-peptide immunization ( $n = 3$  per antibody treatment) did not show any signs of clinical disease during an observation period of 15 days, implying that antibody treatment alone is not enough to cause disease. (Dr. Naoto Kawakami performed the experiments and collected the data.)

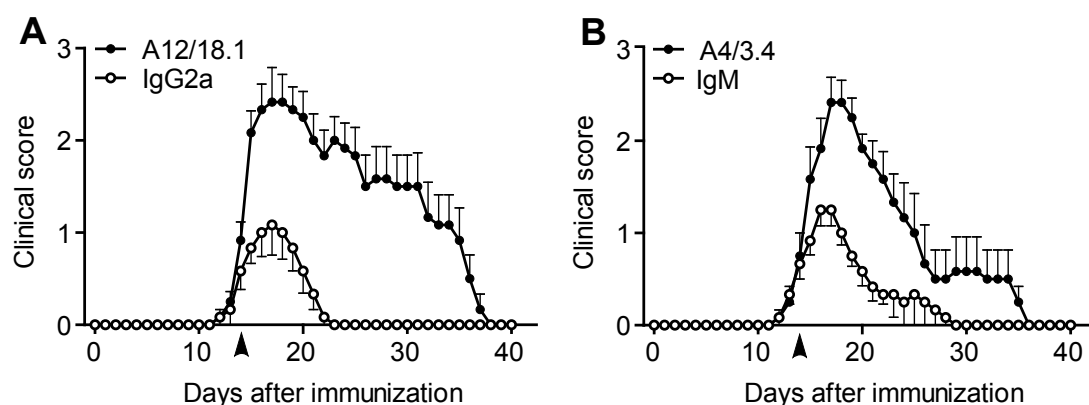


Figure 4.22: **Two different mAbs to NF enhance experimental autoimmune neuritis:** Lewis rats immunized with P2-peptide were injected with either anti-pan-NF mAb A12/18.1 mouse IgG2a (**A**) or A4/3.4 mouse IgM (**B**) (closed symbols) or their respective isotype controls (open symbol) at disease onset (day 14 after EAN induction, indicated by arrowhead). They were scored daily for EAN disease severity. Values (mean  $\pm$  SEM) represent EAN clinical scores from 6 rats per group, pooled from 2 independent experiments.

## 4.4 Neurofascin-specific autoantibodies in multiple sclerosis

In this study, we asked if anti-NF antibodies are present in serum of patients with MS. We included patients with relapsing-remitting MS as majority, and patients with primary and secondary progressive MS. In addition, we used serum from a few patients with clinically isolated syndrome (CIS). For comparison we included as controls a cohort of patients with non-demyelinating disease amyotrophic lateral sclerosis (ALS), patients with other neurological diseases, and healthy controls. The serum samples were analyzed by flow cytometry, ELISA and, to a limited extent, Western blot. Afterwards, the NF-reactivity of positive samples was further characterized by isotyping, serial dilution, domain mapping, and for staining of nodal structures on tissue sections. The control samples included in this study were from the same cohort that was reported in the peripheral inflammatory neuropathy study. To increase the sensitivity of anti-NF antibody detection, we performed affinity-purification using plasma exchange material from 8 RR-MS patients and tested the eluted antibodies for NF reactivity in our assays.

### 4.4.1 Serum screening for anti-NF antibodies

We have tested a total of 429 serum samples by both ELISA and cell-bound assay using flow cytometry with human NF155 and NF186. Using ELISA, we found 4/225 MS and 2/68 ALS samples with low reactivity to NF155, but not to NF186, and no reactivity was observed in 5 CIS, 61 OND, and 77 HC donors (Figure 4.23 A and B). By flow cytometry, we found NF-reactivity in 3/225 MS patients, 1/61 OND controls and 3/77 healthy controls (Figure 4.23 C and D). In detail, 2 MS patients (one is at the detection limit) showed reactivity to NF155, and the other to NF186; 1 healthy donor also showed NF155 reactivity while another 2 healthy donors and 1 OND donor showed reactivity to NF186.

We also screened a random selection of 44 MS (43 RR-MS and 1 PP-MS), 36 OND samples and 4 healthy controls by Western blot to the denatured human NF155 and NF186. We found 57% reactivity in the MS group and 53% reactivity in the OND group, indicating that by Western blot screening there was no significant difference (Figure 4.24).



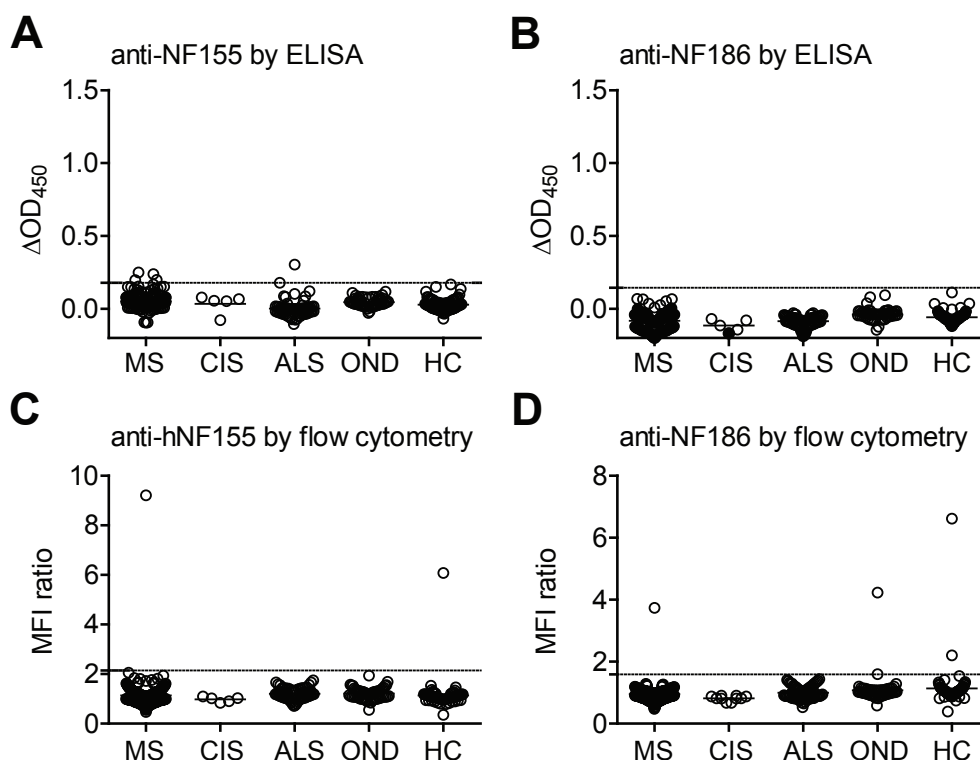


**Figure 4.23: Autoantibodies to NF155 and NF186 detected by ELISA and flow cytometry:** Serum samples from patients with MS (n=225), CIS (n=5), ALS (n=68), and controls OND (n=61), HC (n=77) were tested for autoantibodies to NF155 and NF186 by ELISA (**A,B**) and flow cytometry (**C,D**). ELISA reactivities to NF155 (**A**) and NF186 (**B**) are shown as baseline-subtracted optical density reading at 450 nm ( $\Delta OD_{450}$ ; response to NF minus BSA reactivity). Reactivity by flow cytometry is shown as mean fluorescence intensity (MFI) ratio (reactivity to NF transfectants divided by reactivity to control cells). The cutoff (dashed line) represents the mean of OND group plus four standard deviations.

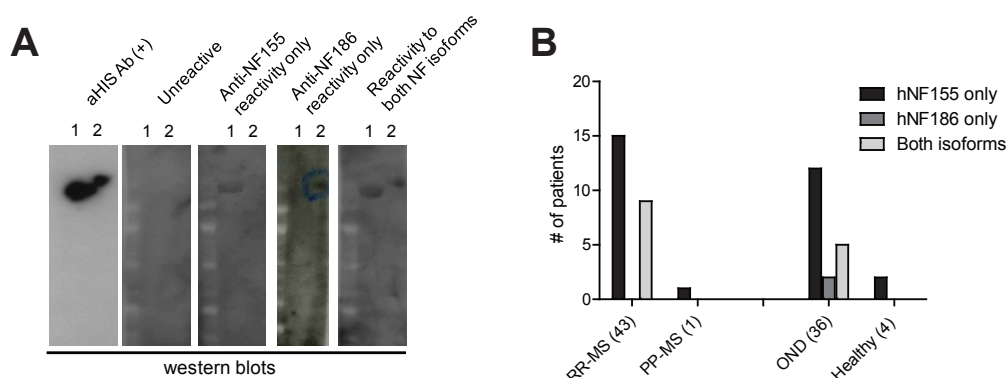


**Figure 4.24: Autoantibodies to NF155 and NF186 detected by Western blot:** (**A**) Example blots containing NF155 (lane 1) and NF186 (lane 2) stained with anti-HIS mAb and serum that were non-reactive, reactive to only NF155, NF186, or both isoforms are shown. Serum samples were diluted 1:400. (**B**) Total number of serum samples from MS groups and control groups that showed reactivity to either NF155 or NF186, or to both isoforms. The total number of samples investigated is indicated next to the patient group.

#### 4.4.2 Characterization of serum samples showing anti-NF reactivity

We further characterized the anti-NF reactivities detected by ELISA and FACS in the MS and ALS patient serum samples by performing serial dilutions, isotyping, epitope mapping by flow cytometry, and immunohistochemistry on longitudinal spinal cord sections.

One sample (from 43 yr old Swedish female) showed NF155-reactivity up to 1:1000 dilution using IgG, however the reactivity was not detected with IgG subclass specific antibodies (Figure 4.25 A and B). The observation indicated that the sensitivity for detecting human IgGs was higher using polyclonal goat anti-human IgG secondary antibody that were specific for multiple epitopes on the antibodies compared to mouse monoclonal antibodies against their specific epitope on specific IgG subclasses. The other NF155-reactive sample (34 yr old Swedish male) showed low reactivity to NF155 (barely detectable at 1:300 dilution) using IgG1. We obtained follow-up serum taken from this patient 3 years afterwards, and found that the NF reactivity had disappeared (Figure 4.25 C and D). We noted that this patient had received a bone marrow transplant within this period and did not require MS treatment afterwards.

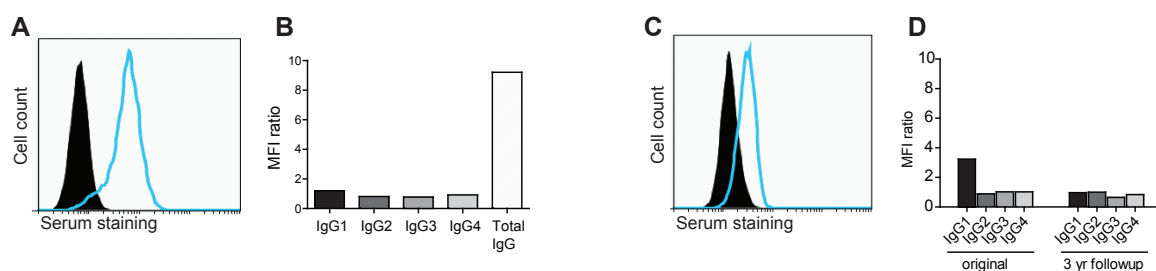
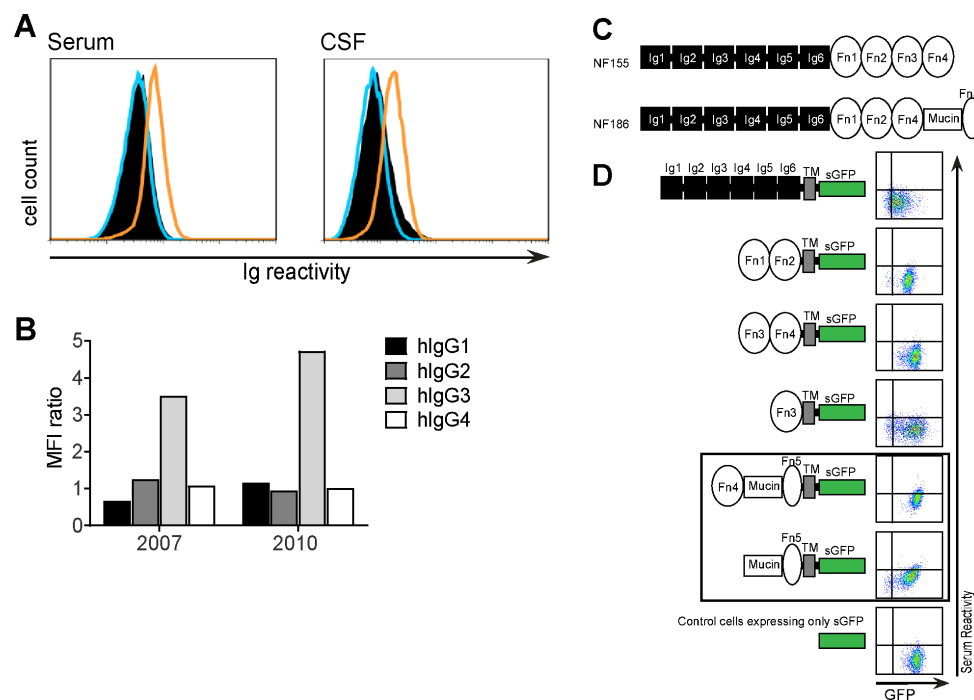


Figure 4.25: **Anti-NF155 reactivity in 2 RR-MS patients:** (A, C) Serum reactivities to only NF155 were seen by flow cytometry. (B, D) The reactivities, shown as mean fluorescence intensity (MFI) ratio, were isotyped for specific IgG subclasses. In D, reactivities of the original sample and a followup sample taken 3 yrs afterwards are shown.

A third RR-MS patient (33 yr old Iranian male) showed NF186-reactivity by IgG3 which could be detected up to 1:3000 dilution (data not shown). This reactivity was directed against the Mucin-Fn5 region of NF186 (Figure 4.26 C and D). From this patient we also found NF186 reactivity in CSF at a comparable level as in serum (Figure 4.26 A). In addition, we obtained follow-up serum, confirmed the persistence of anti-NF186 reactivity, and were able to affinity purify approximately 25  $\mu$ g of antibodies from 12 mL of serum using a NF186-conjugated sepharose column. Despite the presence of IgM and IgA in addition to IgG, reactivity to NF was mediated only by IgG and was detected only by flow cytometry directed only against NF186. These reactive antibodies were IgG3, and we confirmed that they weakly recognize the Mucin-Fn5

region of NF186 (Figure 4.26 B). We had also tested these antibodies for nodal binding on rat spinal cord sections, but we did not find a clear nodal staining pattern.



**Figure 4.26: Anti-NF186 reactivity in an RR-MS patient:** (A) In both serum and CSF, reactivity to NF186 (orange line) but not to NF155 (blue line) was shown by flow cytometry when compared to mock transfectants (black, filled). (B) IgG3 reactivity was found by flow cytometry in serum taken in 2007 and in 2010. (C,D) Staining of truncated NF variants for epitope mapping. (C) Scheme of the extracellular domains of NF155 and NF186. NF186 differs from NF155 by substitution of Fn3-Fn4 with Fn4-Mucin-Fn5. (Ig = immunoglobulin-like domain; Fn = fibronectin type III domain) (D) A scheme of super green fluorescent protein (sGFP) fusion truncated NF variants is shown beside the corresponding serum reactivity by flow cytometry. Reactivities are shown as sGFP intensity versus serum reactivity. Weak reactivity to (Fn4-)Mucin-Fn5 region was observed (boxed), and no reactivity was seen against the other fragments of NF.

By ELISA, 4 RR-MS patient samples (46, 52, 55 yr old female, 47 yr old male) showed low reactivity to NF155. Two of these samples show anti-NF IgM and IgA. Another showed low IgA reactivity only and the last exhibited reactive IgG3 in addition to IgM and IgA (data not shown). Two ALS patient samples (58, 75 yr old German females) showed low reactivity to NF155. They both had IgM and IgA antibodies, and in addition IgG3 in one sample (data not shown). Reactivity to NF found in the control groups were previously discussed in section 4.3.2. All the positive samples were additionally tested for nodal or paranodal staining by immunohistochemistry on tissue sections and we did not observe such staining patterns in these samples.

### 4.4.3 Affinity purification of anti-NF antibodies from RR-MS plasma exchange material

We asked if anti-NF antibodies are perhaps present in the serum of MS patients at a level that is beyond the lower detection limit of our screening assays. We purified antibodies by affinity chromatography using sepharose columns conjugated with either NF155 or NF186. The purified antibody preparations were then tested for binding to NF155 and NF186 by ELISA and flow cytometry, and the isotype of NF-reactive Igs were determined.

#### 4.4.3.1 Purification of anti-NF antibodies from plasma exchange material

Antibodies to NF155 and NF186 were purified in parallel from plasma exchange material collected from 8 RR-MS patients by affinity chromatography (described in Section 3.5.8). From 200 mL of plasma exchange, between 30 - 275  $\mu$ g of antibodies (pooled from different pH elution fractions) were eluted against each isoform of NF. Details are found in Table 4.2. ivIG was used as to control for the antibody purification experiments.

Table 4.2: Plasma exchange material from RR-MS patients: unpurified original material, purified anti-NF155 and anti-NF186 antibodies

Sample ID	Gender	Age	Response to PE	Antibody amount		
				Unpurified total (mg)	NF155-purified ( $\mu$ g)	NF186-purified ( $\mu$ g)
MS-010	F	39	n.a.	1680	276	30
MS-011	M	32	Yes	1000	120	120
MS-012	M	52	Yes	1520	75	82
MS-028	F	50	Yes	1200	120	93
MS-029	M	22	No	1480	132	175
MS-030	F	42	Yes	900	143	41
MS-031	F	48	Yes	1390	150	100
MS-032	F	30	Yes	1700	250	200
ivIG	-	-	-	500	40	77

Each purified antibody preparation was visualized by gel electrophoresis and bands of interest were identified by mass spectrometry. By SDS-PAGE, IgM was the most abundant, followed by IgG and IgA for all preparations made. In addition, a low amount of albumin was also found. An example gel is shown in Figure 4.27.

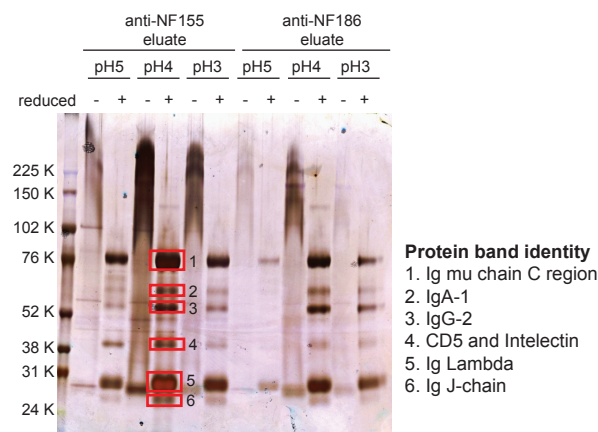
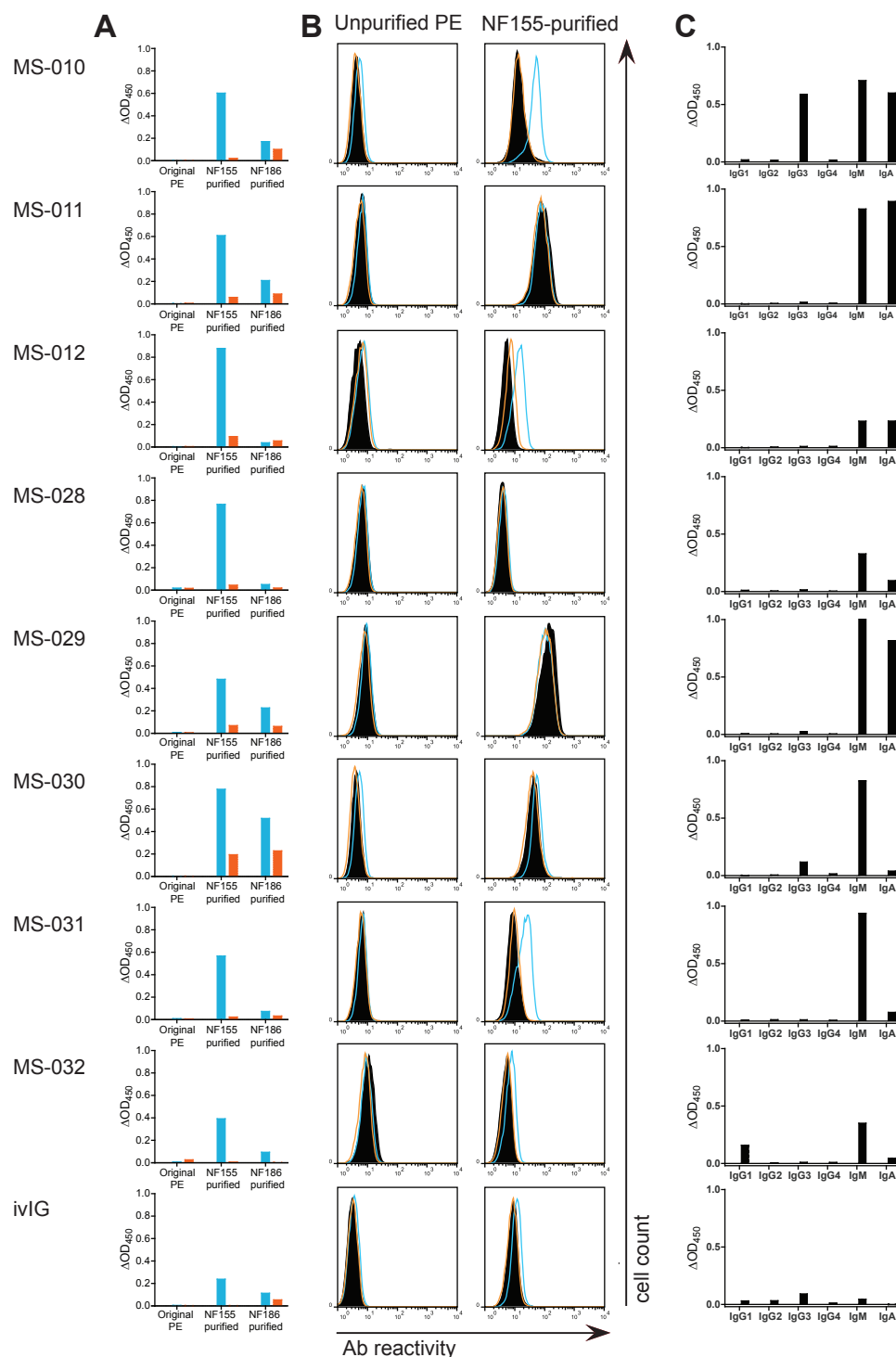


Figure 4.27: **Purified antibodies visualized by silver-stained SDS-PAGE:** Antibodies purified from one RR-MS patient plasma exchange material (MS-030) against NF155 and NF186. Antibodies were eluted at pH 5, pH 4, and pH 3, and separated using SDS-PAGE in reducing and non-reducing conditions. Red boxes indicate bands (1-6) that were cut out for identification by mass spectrometry. The identity of each numbered band is listed on the right of the gel.

#### 4.4.3.2 Reactivity of purified antibodies by ELISA and flow cytometry

The antibodies eluted from the NF155 and NF186 columns were tested for reactivity by ELISA and by flow cytometry (Figure 4.28). At 5  $\mu\text{g/mL}$ , all 8 antibody preparations from patient PE material and antibodies isolated from ivIG using the NF155 column showed clear reactivity to NF155 ( $\Delta\text{OD}_{450} > 0.1$ ), and only one patient preparation (MS-030) additionally showed clear reactivity to NF186. With antibodies purified from the NF186 column, we observed clear NF186 reactivity in only 2 of the 8 patients (MS-010, MS-030), weak reactivity in another (MS-010), and not in ivIG; in 4 of the 8 patients (MS-010, MS-011, MS-029, MS-030) we found reactivity to NF155 (Figure 4.28 A). The reactivities seen with antibody preparations from RR-MS patients were mediated predominantly by IgM and to a lower extent IgA, IgG3 antibodies were further detected in two of these patients and IgG1 antibodies in another one (Figure 4.28 C). A strong reactivity ( $\Delta\text{OD}_{450} > 0.5$ ) mediated by IgG was seen in 1 of 8 patient samples, by IgM in 5 of 8, and by IgA in 3 of 8 (Figure 4.28 C).



**Figure 4.28: NF-reactivity of purified antibodies:** Unpurified PE material and antibodies purified against NF155 and NF186 from 8 RR-MS PE material were tested for reactivity to NF155 (blue) and NF186 (orange) at 5  $\mu\text{g}/\text{mL}$  by ELISA (**A**) and flow cytometry (**B**). Antibodies purified from ivIG were additionally tested as a control. (**A**) ELISA reactivities of the unpurified PE and purified antibodies from both the NF155-column and NF186-column are shown as  $\Delta\text{OD}_{450}$  (reactivity to NF minus reactivity to BSA). Our cutoff criteria is  $\Delta\text{OD}_{450} = 0.1$ . (**B**) We show the reactivities observed by flow cytometry of the original PE material and antibodies purified from NF155 column. The fluorescence intensities measured on NF55- and NF186-expressing cell lines are compared to mock transfectants (black; filled). In (**A**) and (**B**), reactivities of total Ig are shown. (**C**) The isotype of antibodies responsible for the NF reactivity was analyzed by ELISA.

By flow cytometry, 3 of the 8 RR-MS patient antibody preparations (MS-010, MS-012, MS-031) from the NF155 column showed reactivity to NF155, another one (MS-032) showed weak anti-NF155 reactivity (Figure 4.28 B), and none showed reactivity to NF186 (data not shown). The anti-NF155 reactivities observed were directed against an epitope on the Fn3Fn4 fragment (Figure 4.29 B and C). Interestingly, the dominant Ig-isotype conveying this reactivity was different between these four preparations, one used IgG1, two others used IgM, and the last IgA (Figure 4.29 A). Antibodies purified from ivIG also showed very faint signal on NF155 cells (Figure 4.28 B). Antibodies purified over the NF186 column did not show reactivity by flow cytometry.

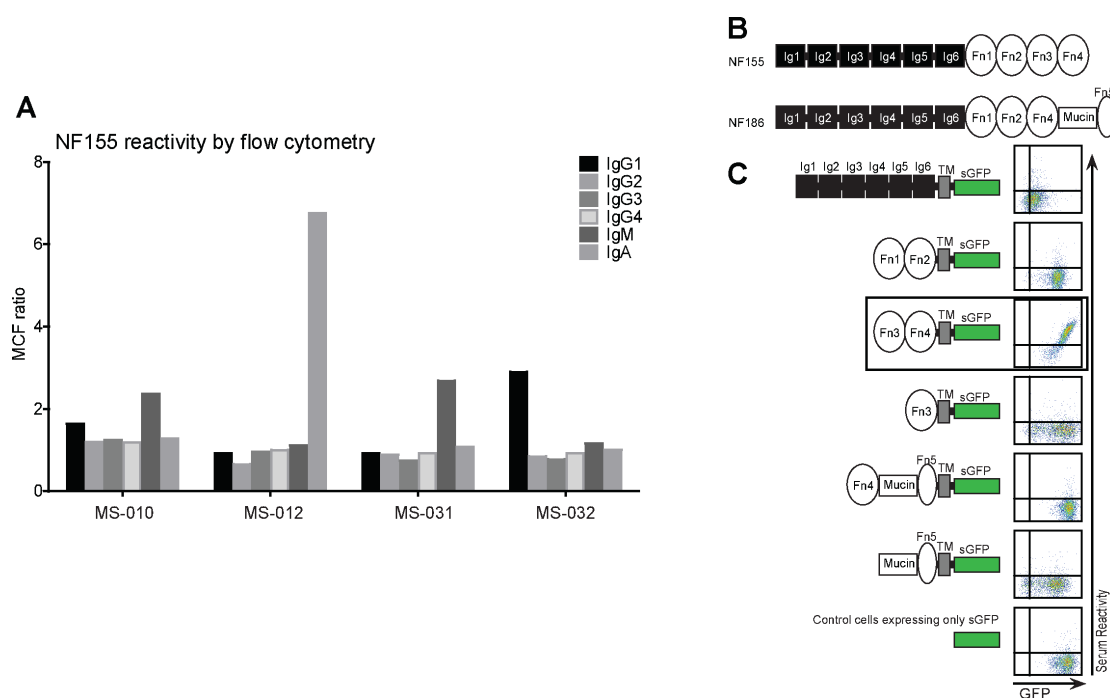


Figure 4.29: **Characterization of NF155-specific antibodies reactive by flow cytometry:** (A) NF155-column purified antibody preparations that showed NF155-reactivity were isotyped. (B) A scheme of the extracellular domains of the complete NF155 and NF186 is shown. NF186 differs from NF155 by substitution of Fn3-Fn4 with Fn4-Mucin-Fn5. (Ig = immunoglobulin-like domain; Fn = fibronectin type III domain) (C) The specific domain reactivity of MS-012 is shown. A scheme of super green fluorescent protein (sGFP) fusion truncated NF variants is shown beside the corresponding reactivity by flow cytometry. Reactivities are shown as sGFP intensity versus serum reactivity. The specific domain recognition of the NF155 reactivity was mapped to the Fn3Fn4 fragment (boxed).





## **Chapter 5**

### **Discussion**

## 5.1 Summary of findings

We cloned and recombinantly expressed human neurofascin 155 and 186 in human cell lines. Using the recombinant NFs, we developed assays to detect antibodies against human NF: cell-based assay by flow cytometry, ELISA and Western blot. We also demonstrated that ratNF155-NS0, an antigen used in previous studies for detection of NF-autoantibodies, is not a suitable antigen due to immunogenic post-translational modifications from the host cell line NS0. Antibodies against NF were found by ELISA in a small proportion (3%; 8/254) of patients with inflammatory neuropathies and none of the controls. Two strongly ELISA-reactive CIDP samples were also reactive by flow cytometry to NF155. Another CIDP patient who benefited from plasma exchange showed anti-NF155 reactivity by ELISA, and after affinity purification additional reactivity to NF186 and also by flow cytometry. We tested the pathogenic potential of antibody targeting of NF in a peripheral inflammatory nerve disease setting using mAbs, and found that the mAbs could exacerbate disease although they could not induce disease on their own. Anti-NF reactivity was detected in a small proportion of MS patients (3%; 7/225) by flow cytometry and ELISA. To increase detection sensitivity of NF antibodies in RR-MS patients, we affinity-purified NF-reactive antibodies from plasma exchange material, and found antibodies reactive to NF155, and to a lesser extent to NF186. Serum reactivities observed against NF by flow cytometry and ELISA were isoform-specific and assay-specific in most cases, and using mainly IgG subclasses. Using truncated variants of NF, we mapped the antibody specificity of NF155-reactive antibodies to the Fn3-Fn4 region and the Muc-Fn5 region for NF186-reactive antibodies.

## 5.2 Assay comparison and evaluation

Human cell lines were employed to recombinantly express human isoforms of NF155 and NF186 to detect anti-NF antibodies in patients with autoimmune diseases of the nervous system. That the antigens were as similar as possible to what are physiologically seen by antibodies was crucial for our approach. By using our human protein antigens, we avoided detecting antibodies against non-human amino acid sequences and non-human cell-specific post-translational modifications. To illustrate the importance of this aspect, we compared the utility of our human NFs to a commercially available rat isoform of NF155 that was produced in NS0

mouse myeloma cells in an ELISA format. While about 3% of all patients showed reactivity by ELISA to the human NFs, virtually every sample showed clear reactivity (at various levels) to the rat NF155. Upon further examination using antibodies purified against rat NF155, we discovered that the post-translational modifications imposed onto the protein antigen by the murine host cells is likely a major contributing factor to the reactivities detected in patient sera. It is known that the murine NS0 cells produce abnormally glycosylated proteins that are potentially immunogenic depending on culture conditions (Walsh and Jefferis, 2006). Furthermore, potentially relevant human NF epitopes may be absent or masked by such modifications. Together, it is evident that the ratNF155-NS0 is not a suitable antigen for anti-NF antibody detection studies, and this highlights the importance of using human antigens that are expressed in appropriate cell lines, as requested by Willison (2011) in a reply to the NF-antibody study published by Pruess et al. (2011).

For this project, we developed antibody detection assays: ELISA, cell-based assay by flow cytometry, and Western blot. Each assay has inherently unique properties that determine how the antigen is displayed. The properties that directly influence antibody binding include the conformation of the protein antigen, the orientation, and the density.

For flow cytometry, NFs were expressed on the surface of human cell lines in presumably its native conformation and correct orientation at a density determined by transfection efficiency. The advantage of this method is that the antigen was unlikely to be unfolded and is properly oriented and could be used to detect physiologically relevant antibodies, although its physiologically relevant binding partners necessary for complex formation were absent.

The antigen was theoretically denatured (and, in some experiments, reduced) for the Western blot assay. This implies that only linear epitopes were presented to antibodies. Such linear epitopes were in a conformation that was likely different from that of the corresponding region in the intact protein (van Regenmortel, 2000). The density of the antigen depended on the amount of protein used for blotting and also blotting conditions.

In the ELISA, the protein antigen was immobilized according to the surface chemistry of the solid support at a density defined by the user. We chose a matrix that preferentially binds hydrophilic molecules (ex. protein surface carbohydrate moieties) instead of hydrophobic surfaces (ex. inner core of a folded protein) to avoid completely denaturing the protein antigen. However, we could not exclude that the NFs were manipulated in a way that their native conformation was altered to expose hidden epitopes or to mask antigenic epitopes rendering false-positive

or -negative result. In addition, the antigen density in an ELISA assay was dependent on the concentration of coating solution and efficiency of the coating process.

Each method has advantages and disadvantages. They reflect our current understanding of immunoassays and illustrate the utility of the current available methods of detection. We screened a collection of patient serum from patients with GBS, CIDP, and MS along with other controls with our ELISA and flow cytometry assay. For a small subset, we also performed Western blot analysis. Interestingly, the majority of NF-reactive samples were positive only by ELISA but not flow cytometry, or vice versa. This was true in both the patient group and the control group. Only in 2 samples did we find (strong) reactivity in both assays. It is difficult to elucidate the reason for this disparity because we do not know the exact epitope(s) on the antigen responsible for the reactivities observed. Evidence suggesting the potential pathogenicity of antibodies that were identified by ELISA but not by flow cytometry came from work using rabbit antibodies generated against a peptide of NF155. These rabbit antibodies were reactive by ELISA but not flow cytometry, stained paranodes on tissue sections, and caused complement-dependent demyelination in an *in vitro* myelination culture model (unpublished data from Dr. Chris Lington). Our initial Western blot analysis revealed broad reactivity in both MS patient group and controls; in only one patient sample showing reactivity against NF186 did we also find reactivity by flow cytometry. Endogenous antibodies against denatured proteins, which may be found in necrotic cellular debris such as degenerating myelin, have been shown to accumulate at sites of nerve injury and has a role in promoting repair by clearance of cell debris; these antibodies were thought to recognize degenerate tissue as non-self (Vargas et al., 2010). Considering this point, antibodies reactive only towards denatured nerve antigens may not have a direct role in disease pathogenesis. However, as seen with pathogenic mAbs (ex. A12/18.1 and A4/3.4) that recognize NF by Western, flow cytometry, ELISA and also *in vivo*, antibodies that are not exclusively detected by Western blot may have a pathogenic role (Mayer and Meinel, 2012).

We performed immunohistochemistry with the NF-reactive serum samples and some negative samples chosen at random using longitudinally-cut frozen rat tissue sections. On the sections, NF155 and NF186 were in complex with their binding partners and presented at natural densities. We found clear paranodal staining for NF155 in only CIDP patient samples that also showed reactivity by ELISA and flow cytometry. With the other samples identified by either ELISA or flow cytometry, however, no nodal staining pattern was observed. This may be due to

alteration of NFs by the fixation procedure, the lower density of NFs presented compared to the other assays, or lack of crossreactivity directed to rodent NFs. Furthermore, the signal-to-noise ratio was evidently worse compared to the assays using recombinant NF. For these reasons, we also did not employ immunohistochemistry as a method for serum screening.

In addition, we isolated anti-NF antibodies by affinity chromatography from patient material where we suspected antibody presence that exceeds the lower detection limit of our assays. The isolation procedure and subsequent storage conditions can affect antibody structure, ergo its function and specificity (Omersel et al., 2010). The elution procedure was determined by optimizing a balance between purity, yield, and preservation of the natural immunoreactivity of the antibodies. Antibody-antigen binding is a combination of ionic and hydrophobic interactions, hydrogen bonds, and van der Waal forces. Elution of bound antibodies involves breaking such interactions through altering the ionic strength, pH, temperature, and by using organic solvents (Howard, 1981). We performed successive elutions with buffers at pH 5, pH 4, pH 3, and pH 11, while neutralizing the column between each step. We found higher reactivity in fractions eluted at pH 5 and pH 4 compared to pH 3, and still lower reactivity at pH 11. The small amounts of eluted antibodies were concentrated and Ig-free BSA was added as a stabilizer to prevent loss through surface adsorption. When we tested these isolated antibodies that come from unreactive original plasma exchange samples, we found NF-reactivity by ELISA (higher than  $\Delta OD_{450} = 0.2$ ) in all of the preparations and reactive by flow cytometry in a few. The reactivity observed was likely due to the much higher concentration of NF-reactive antibodies, however, we cannot exclude that some of these antibodies may harbour subtle structural alterations which make them additionally more reactive in our assays.

### **5.3 Anti-NF antibodies in peripheral inflammatory neuropathies**

Autoantibodies were implicated in disease pathogenesis in patients with GBS and CIDP, but the antigenic target is unknown. We propose that in a small proportion of patients NF155 and/or NF186 may be a target. Our anti-NF ELISA is evidently suitable for identifying subjects with anti-NF antibodies among patients with inflammatory neuropathy and for distinguishing them from controls.

We made the unexpected observation that in two CIDP patients the anti-NF155 autoantibodies were largely IgG4 with an additional contribution of IgG1, IgG2, IgG3, and IgA. Anti-NF155

IgG4 in these CIDP patients may have an antigen blocking function to impair myelination and thereby nerve conduction, as IgG4 is generally known not to be complement-activating and it does not bind Fc receptors on effector cells (Nirula et al., 2011). This blocking effect of IgG4 antibodies may be pathogenic. For example, in endemic pemphigus foliaceus, a blistering skin disease, IgG4 antibodies against desmoglein 1 cause a direct disruption of the epithelial layer leading to blister formation (Rock et al., 1989). In this case, the pathogenic role of IgG4 is through antigen blocking, disrupting the normal function of the target protein, and not through antibody-mediated effector functions or complement activation (Rock et al., 1989; Nirula et al., 2011). Apart from IgG4, low level reactivity was found from IgG1, IgG2, IgG3, IgM, and IgA in the two CIDP patients with the remarkably high anti-NF reactivity. These isotypes can activate the complement cascade, and can recruit and amplify immune effector cell function.

One CIDP patient who benefited remarkably from plasma exchange had antibodies to NF, but no reactivity to a broad range of onconeuronal, autoimmune and neuropathy-related antibodies. This patient had largely anti-NF155 antibodies, and in addition, anti-NF186 antibodies which were detectable after affinity purification. With escalation of immunotherapy, which involved frequent plasma exchange therapy and an autologous bone marrow transplant in 2010, the patient eventually remitted completely over the course of four years. Initially we saw an increase of NF155 reactivity in this patient's serum between 2008 and 2009, and it was followed by a progressive decline of titers. It is tempting to speculate that the reduced anti-NF antibody levels may be linked to the reduced dependence on PE, but we must consider that our EAN animal studies showed that the antibodies alone are not pathogenic; rather they are one of several distinct pathogenic components. Another CIDP patient that benefited from plasma exchange also showed anti-NF155 antibodies and we may speculate a role of these antibodies in pathogenesis. However, due to the insufficient amount of purified patient antibodies against NF, we were not able to perform passive transfer experiments into our EAN model to test for the functional significance of such antibodies.

#### **5.4 Anti-NF antibodies in multiple sclerosis**

Serum reactivity to NF was seen in only a few MS patients (3%) by flow cytometry and ELISA, while a higher frequency (8/8) showed antibodies to NF after affinity purification, with the majority (5/8) showing strong reactivity. In the serum of one MS patient, we found persisting IgG3

against NF186 by flow cytometry. These antibodies were additionally found in the paired CSF sample at a comparable level as in the serum, showing no evidence for an intrathecal synthesis.

As MS is a long-term smoldering disease, some patients may harbour low levels of pathogenic antibodies that contribute to the myelin disruption observed. We suspected that anti-NF antibodies may exist at low levels (undetected by our assays) in some patients, and substantiated this suspicion by affinity-purifying these antibodies over NF-conjugated columns from plasma exchange material. We found the majority of functional antibodies to be against NF155 rather than NF186. The purified antibodies to NF were predominantly IgM, and in addition a high IgG reactivity was seen in one sample and high IgA response was seen in three.

Some IgM are natural antibodies, antibodies produced without antigenic stimulation by B1 cells without any somatic mutation; they typically exhibit low affinity reactivity with polyspecificity (Groenwall et al., 2012) and can activate the complement system (Janeway et al., 2007). There are also IgM that are produced after an immune response after somatic hypermutation in IgM memory cells (Janeway et al., 2007; Seifert and Kppers, 2009). Some IgM have been shown to promote remyelination by possibly cross-linking antigens on the oligodendrocyte surface due to its pentameric structure to bring together molecules (Warrington and Rodriguez, 2010). Also, they can prevent the stimulation of autoreactive B2 cells to regulate the production of IgG by, for example, masking antigenic epitopes (Gupta, 2010). However, IgM may have a pathogenic role, as in IgM monoclonal gammopathy-associated neuropathies (Mata et al., 2011). Serum IgA (IgA1) exist as predominantly monomers, and has been shown to regulate autoimmunity and inflammation through its Fc receptor (Jacob et al., 2008). However, in an aggregated form, as immune complexes or macromolecular form, IgA can promote an active immune response through activation of IgA receptors (Monteiro, 2010). Class-switched IgG antibodies are produced by activated B2 cells upon antigen stimulation and have undergone affinity maturation; they can promote complement activation, activate immune cells, or have blocking functions (Janeway et al., 2007). Besides IgM, there are also IgG and IgA natural antibodies, and they can react to a wide range of self-antigens in a polyreactive manner (Spalter et al., 1999). It would be interesting to perform sequence analysis of purified anti-NF antibodies to look for evidence of somatic hypermutation in future experiments to elucidate the origins of these antibodies. At present the collective function of the low levels of anti-NF IgM, IgA, and IgG has yet to be clearly determined. The demonstration of a low concentration of autoantibodies in MS

patients raises the possibility that these antibodies may contribute to the pathogenesis of this chronic smoldering disease.

## 5.5 Potential pathogenic relevance of anti-NF autoantibodies

The pathogenicity of NF-antibody targeting in CNS demyelinating disease was previously shown in an EAE model by Mathey et al. (2007). We investigated the pathogenic potential of NF-reactive antibodies in peripheral inflammatory neuropathies using an EAN model, yielding two main findings. First, antibodies to NF can enhance and prolong an ongoing neuritis. Second, antibodies to NF alone are not pathogenic. Previous studies of this P2-EAN model have demonstrated nerve infiltration by autoreactive T cells and macrophages, yet autoantibodies were not implicated (Lonigro and Devaux, 2009). We added anti-pan-NF mAbs into this disease setting and found that NF targeting exacerbated disease. A similar observation was made in studies using a T cell transfer EAN model in which addition of anti-myelin antibodies greatly exacerbated disease (Spies et al., 1995). These observations support the 'two-hit' model proposed from EAE studies: it postulates that immune-mediated inflammation can open up the blood-brain barrier or somehow alter endothelial cells so that antibodies can gain access into the CNS tissue (Derfuss et al., 2009; Rudick and Trapp, 2009). In our animal studies, it may be that P2-immunization-induced inflammatory mediators made the blood-nerve barrier leaky so that anti-NF antibodies can access the peripheral nerve to mediate nodal disruption. Inflammatory neuropathies are characterized by pronounced immune cell infiltration (Schneider-Hohendorf et al., 2012; Prineas, 1981) that will open blood-nerve barrier and provide access to autoantibodies.

Unexpectedly, almost all the serum reactivities observed were directed against only one isoform of NF. This is surprising because NF155 and NF186 are splice variants such that the 8 extracellular domains from the N-terminus are virtually identical, differing only in the two domains closest to the transmembrane region (Basak et al., 2007). We expressed truncated variants of NF155 and NF186, and identified the Fn3-Fn4 domains as the target for NF155-specific reactivity and Mucin-Fn5 domains for NF186-specificity. Previous studies of NF-autoantibodies in MS patients using rodent isoforms of NF (Mathey et al., 2007) and in myelin-homogenate-induced EAN rat models (Lonigro and Devaux, 2009) have suggested the involvement of antibodies that bound both isoforms of NF. This observation of isoform specificity is unrefutable from our



experiments, and this point is shown for the first time since NF-reactive autoantibodies have been under investigation.

Would the isoform-specific recognition of NF by human autoantibodies be compatible with pathogenicity? NF186 is displayed on the nodes of Ranvier and is directly accessible to antibodies. It has been shown that antibody targeting of NF186 in the presence of complement disrupts nerve conduction (Mathey et al., 2007). The anti-NF186 antibodies that we found in two patients with AIDP and one with MS were of the complement activating isotypes IgG1 and IgG3. In addition, antibodies to NF186 might hinder its binding to gliomedin (the ligand for NF186) in the PNS and the interaction with astrocytic processes in the CNS, thereby resulting in loss of axonal clustering of voltage-gated sodium channels that are needed for saltatory conduction (Eshed et al., 2005). Antibodies to NF155 found in some AIDP, CIDP, and MS patients would be expected to be pathogenic only if their target at the paranodes becomes accessible. Since a disruption of paranodal architecture is a feature of different nerve pathologies such as ischemia and inflammation (Reimer et al., 2011; Maier et al., 2007), these antibodies could contribute to the pathology. It has been reported that anti-NF155 antibodies can inhibit myelination by blocking the formation of the Caspr/contactin - NF155 complex, which is a core structure at paranodal loops for adhesion between axon and glial cell (Charles et al., 2002). Such a disruption of the paranodal junctions can result in severe reduction of conduction velocity even in the absence of obvious demyelination (Sherman et al., 2005). In addition, NF155 antibodies may also interfere with early events of remyelination; it has been shown that during early myelination NF155 localize mainly in oligodendrocyte cell bodies and major branches, and migrate to the distal end of the processes with Caspr (Schafer et al., 2004), antibody binding may disrupt NF155 localization for proper node of Ranvier formation. Since the majority of NF-reactive patients have antibodies directed against NF155, it is tempting to speculate that such antibodies interfere with remyelination in patients.

## 5.6 Outlook

Autoantibodies to neurofascins may have a role in inflammatory diseases in both the CNS and PNS. With the assays developed in this thesis, anti-NF antibodies were found in 4% of patients with AIDP or CIDP, some of which showed high titres. The prognostic value of the presence of anti-NF antibodies for response to plasma exchange remains to be clarified. In

MS patients, anti-NF antibodies are typically detected only with very sensitive assay systems involving prior antibody isolation. These antibodies may have a pathogenic role in this chronic disease in axonal injury or remyelination failure. Interestingly, a recent proteomic study demonstrated perturbed axoglial physiology to be a hallmark of the early events of MS pathogenesis (Dhaunchak et al., 2012). Kamm and Zettl (2012) had hypothesized the existence of a common autoimmune reactivity against myelin antigens that are present in both systems. It would be reasonable to test patients with disorders that affect both the central and peripheral nerve for antibodies against NF.



# Bibliography

- Basak, S., Raju, K., Babiarz, J., Kane-Goldsmith, N., Koticha, D., Grumet, M., 2007. Differential expression and functions of neuronal and glial neurofascin isoforms and splice variants during PNS development. *Developmental Biology* 311, 408–22.
- Black, J.A., Waxman, S.G., 1988. The perinodal astrocyte. *Glia* 1, 169–83.
- Charles, P., Tait, S., Faivre-Sarrailh, C., Barbin, G., Gunn-Moore, F., Denisenko-Nehrbass, N., Guennoc, A.M., Girault, J.A., Brophy, P.J., Lubetzki, C., 2002. Neurofascin is a glial receptor for the paranodin/Caspr-contactin axonal complex at the axoglia junction. *Current Biology* 12, 217–20.
- Dalakas, M.C., Engel, W.K., 1980. Immunoglobulin and complement deposits in nerves of patients with chronic relapsing polyneuropathy. *Archives of neurology* 37, 637–40.
- Davis, J.Q., Lambert, S., Bennett, V., 1996. Molecular composition of the node of Ranvier: identification of ankyrin-binding cell adhesion molecules neurofascin (Mucin+/third FNIII domain) and NrCAM at nodal axon segments. *The Journal of Cell Biology* 135, 1355–67.
- Derfuss, T., Parikh, K., Velhin, S., Braun, M., Mathey, E., Krumbholz, M., Kumpfel, T., Moldenhauer, A., Rader, C., Sonderegger, P., Pullmann, W., Tiefenthaler, C., Bauer, J., Lassmann, H., Wekerle, H., Karagogeos, D., Hohlfeld, R., Linington, C., Meinl, E., 2009. Contactin-2/TAG-1-directed autoimmunity is identified in multiple sclerosis patients and mediates gray matter pathology in animals. *Proceedings of the National Academy of Sciences* 106, 8302–7.
- Devaux, J.J., Odaka, M., Yuki, N., 2012. Nodal proteins are target antigens in Guillain-Barré syndrome. *Journal of the Peripheral Nervous System* 17, 62–71.
- Dhaunchak, A.S., Becker, C., Schulman, H., De Faria, O., Rajasekharan, S., Banwell, B., Coleman, D.R., Bar-Or, A., on behalf of the Canadian Pediatric Demyelinating Disease Group,

2012. Implication of perturbed axoglial apparatus in early pediatric multiple sclerosis. *Annals of Neurology* 71, 601–13.
- Disanto, G., Morahan, J.M., Barnett, M.H., Giovannoni, G., Ramagopalan, S.V., 2012. The evidence for a role of B cells in multiple sclerosis. *Neurology* 78, 823–32.
- Durocher, Y., Perret, S., Kamen, A., 2002. High-level and high-throughput recombinant protein production by transient transfection of suspension-growing human 293-EBNA1 cells. *Nucleic Acids Research* 30, 2–9.
- Eshed, Y., Feinberg, K., Poliak, S., Sabanay, H., Sarig-Nadir, O., Spiegel, I., Jr., J.R.B., Peles, E., 2005. Gliomedin mediates Schwann cell-axon interaction and the molecular assembly of the nodes of Ranvier. *Neuron* 47, 215–29.
- Feinberg, K., Eshed-Eisenbach, Y., Frechter, S., Amor, V., Salomon, D., Sabanay, H., Dupree, J.L., Grumet, M., Brophy, P.J., Shrager, P., Peles, E., 2010. A glial signal consisting of gliomedin and NrCAM clusters axonal Na<sup>+</sup> channels during the formation of nodes of Ranvier. *Neuron* 65, 490–502.
- Groenwall, C., Vas, J., Silverman, G., 2012. Protective roles of natural IgM antibodies. *Frontiers in immunology* 3, 66–.
- Gupta, S., 2010. Antibodies: basic mechanisms and emerging concepts. *Journal of Clinical Immunology* 30, 1–3.
- Hafer-Macko, C.E., Sheikh, K.A., Li, C.Y., Ho, T.W., Cornblath, D.R., McKhann, G.M., Asbury, A.K., Griffin, J.W., 1996. Immune attack on the Schwann cell surface in acute inflammatory demyelinating polyneuropathy. *Annals of Neurology* 39, 625–35.
- Harrison, B.M., Hansen, L.A., Pollard, J.D., McLeod, J.G., 1984. Demyelination induced by serum from patients with Guillain-Barré syndrome. *Annals of Neurology* 15, 163–70.
- Heckman, K.L., Pease, L.R., 2007. Gene splicing and mutagenesis by PCR-driven overlap extension. *Nature Protocols* 2, 924–32.
- Honmou, O., Felts, P.A., Waxman, S.G., Kocsis, J.D., 1996. Restoration of normal conduction properties in demyelinated spinal cord axons in the adult rat by transplantation of exogenous Schwann cells. *The Journal of Neuroscience* 16, 3199–208.
- Howard, P.L., 1981. Principles of antibody elution. *Transfusion* 21, 477–82.

- Hughes, R.A., Cornblath, D.R., 2005. Guillain-Barré syndrome. *The Lancet* 366, 1653–66.
- Jacob, C., Pastorino, A., Fahl, K., Carneiro-Sampaio, M., Monteiro, R., 2008. Autoimmunity in IgA deficiency: revisiting the role of IgA as a silent housekeeper. *Journal of Clinical Immunology* 28, 56–61.
- Janeway, C.A., Travers, P., Walport, M., 2007. *Immunobiology*, 7th Edition. Garland Science.
- Kaida, K., Kusunoki, S., 2010. Antibodies to gangliosides and ganglioside complexes in Guillain-Barré syndrome and Fisher syndrome: mini-review. *Journal of Neuroimmunology* 223, 5–12.
- Kamm, C., Zettl, U.K., 2012. Autoimmune disorders affecting both the central and peripheral nervous system. *Autoimmunity Reviews* 11, 196–202.
- Keegan, M., Koenig, F., McClelland, R., Brueck, W., Morales, Y., Bitsch, A., Panitch, H., Lassmann, H., Weinshenker, B., Rodriguez, M., Parisi, J., Lucchinetti, C.F., 2005. Relation between humoral pathological changes in multiple sclerosis and response to therapeutic plasma exchange. *The Lancet* 366, 579–82.
- Kieseier, B.C., Lehmann, H.C., zu Hoerste, G.M., 2012. Autoimmune diseases of the peripheral nervous system. *Autoimmunity Reviews* 11, 191–5.
- Kirk, J., Plumb, J., Mirakhur, M., McQuaid, S., 2003. Tight junctional abnormality in multiple sclerosis white matter affects all calibres of vessel and is associated with blood-brain barrier leakage and active demyelination. *The Journal of Pathology* 201, 319–27.
- Koeller, H., Kieseier, B.C., Jander, S., Hartung, H.P., 2005. Chronic inflammatory demyelinating polyneuropathy. *New England Journal of Medicine* 352, 1343–56.
- Lassmann, H., Brck, W., Lucchinetti, C., 2001. Heterogeneity of multiple sclerosis pathogenesis: implications for diagnosis and therapy. *Trends in molecular medicine* 7, 115–21.
- Lassmann, H., Brueck, W., Lucchinetti, C.F., 2007. The immunopathology of multiple sclerosis: an overview. *Brain Pathology* 17, 210–8.
- Lehmann, H.C., Hartung, H.P., 2011. Plasma exchange and intravenous immunoglobulins: mechanism of action in immune-mediated neuropathies. *Journal of Neuroimmunology* 231, 61–9.

- Lehmann, H.C., Meyer zu Horste, G., Kieseier, B.C., Hartung, H.P., 2009. Pathogenesis and treatment of immune-mediated neuropathies. *Therapeutic Advances in Neurological Disorders* 2, 261–81.
- Liu, L.Y., Zheng, H., Xiao, H.L., She, Z.J., Zhao, S.M., Chen, Z.L., Zhou, G.M., 2008. Comparison of blood-nerve barrier disruption and matrix metalloproteinase-9 expression in injured central and peripheral nerves in mice. *Neuroscience Letters* 434, 155–9.
- Long, E.O., Rosen-Bronson, S., Karp, D.R., Malnati, M., Sekaly, R.P., Jaraquemada, D., 1991. Efficient cDNA expression vectors for stable and transient expression of HLA-DR in transfected fibroblast and lymphoid cells. *Human Immunology* 31, 229–35.
- Lonigro, A., Devaux, J., 2009. Disruption of neurofascin and gliomedin at nodes of Ranvier precedes demyelination in experimental allergic neuritis. *Brain* 132, 260–73.
- Maier, O., Baron, W., Hoekstra, D., 2007. Reduced raft-association of NF155 in active MS-lesions is accompanied by the disruption of the paranodal junction. *Glia* 55, 885–95.
- Martini, R., 2001. The effect of myelinating Schwann cells on axons. *Muscle & Nerve* 24, 456–66.
- Mata, S., Borsini, W., Ambrosini, S., Toscani, L., Barilaro, A., Piacentini, S., Sorbi, S., Lolli, F., 2011. IgM monoclonal gammopathy-associated neuropathies with different IgM specificity. *European Journal of Neurology* 18, 1067–73.
- Mathey, E.K., Derfuss, T., Storch, M.K., Williams, K.R., Hales, K., Woolley, D.R., Al-Hayani, A., Davies, S.N., Rasband, M.N., Olsson, T., Moldenhauer, A., Velhin, S., Hohlfeld, R., Meinl, E., Linington, C., 2007. Neurofascin as a novel target for autoantibody-mediated axonal injury. *The Journal of Experimental Medicine* 204, 2363–72.
- Mayer, M., Meinl, E., 2012. Glycoproteins as targets of autoantibodies in CNS inflammation: MOG and more. *Therapeutic advances in neurological disorders* 5, 147–59.
- Meinl, E., Derfuss, T., Linington, C., 2010. Identifying targets for autoantibodies in CNS inflammation: strategies and achievements. *Clinical and Experimental Neuroimmunology* 1, 47–60.
- Monteiro, R., 2010. The role of IgA and IgA Fc receptors as anti-inflammatory agents. *Journal of clinical immunology* 30 Suppl 1, S61–4.

- Nave, K.A., 2010. Myelination and the trophic support of long axons. *Nature reviews. Neuroscience* 11, 275–83.
- Nave, K.A., Trapp, B.D., 2008. Axon-glial signaling and the glial support of axon function. *Annual Review of Neuroscience* 31, 535–61.
- Nirula, A., Glaser, S.M., Kalled, S.L., Taylor, F.R., 2011. What Is IgG4? A review of the biology of a unique immunoglobulin subtype. *Current Opinion in Rheumatology* 23.
- Omersel, J., Zager, U., Kveder, T., Bozic, B., 2010. Alteration of antibody specificity during isolation and storage. *Journal of Immunoassay & Immunochemistry* 31, 45–59.
- Owens, T., Bechmann, I., Engelhardt, B., 2008. Perivascular spaces and the two steps to neuroinflammation. *Journal of Neuropathology and Experimental Neurology* 67, 1113–21.
- Peles, E., Nativ, M., Lustig, M., Grumet, M., Schilling, J., Martinez, R., Plowman, G.D., Schlessinger, J., 1997. Identification of a novel contactin-associated transmembrane receptor with multiple domains implicated in protein-protein interactions. *EMBO Journal* 16, 978–88.
- Peters, A., Palay, S.L., Webster, H.d., 1991. *The fine structure of the nervous system*. Oxford University Press.
- Poliak, S., Peles, E., 2003. The local differentiation of myelinated axons at nodes of Ranvier. *Nature Reviews Neuroscience* 4, 968–80.
- Prineas, J.W., 1981. Pathology of the Guillain-Barré syndrome. *Annals of Neurology* 9, 6–19.
- Pruess, H., Schwab, J.M., Derst, C., Goertzen, A., Vermeulen, E., 2011. Neurofascin as target of autoantibodies in Guillain-Barré syndrome. *Brain* 134, 173–.
- van Regenmortel, M.H., 2000. The recognition of proteins and peptides by antibodies. *Journal of immunoassay* 21, 85–108.
- Reimer, M.M., McQueen, J., Searcy, L., Scullion, G., Zonta, B., Desmazieres, A., Holland, P.R., Smith, J., Gliddon, C., Wood, E.R., Herzyk, P., Brophy, P.J., McCulloch, J., Horsburgh, K., 2011. Rapid disruption of axon-glial integrity in response to mild cerebral hypoperfusion. *The Journal of Neuroscience* 31, 18185–94.
- Rios, J.C., Rubin, M., Martin, M.S., Downey, R.T., Einheber, S., Rosenbluth, J., Levinson, S.R., Bhat, M., Salzer, J.L., 2003. Paranodal interactions regulate expression of sodium channel



- subtypes and provide a diffusion barrier for the node of Ranvier. *The Journal of Neuroscience* 23, 7001–11.
- Rock, B., Martins, C.R., Theofilopoulos, A.N., Balderas, R.S., Anhalt, G.J., Labib, R.S., Futamura, S., Rivitti, E.A., Diaz, L.A., 1989. The pathogenic effect of IgG4 autoantibodies in endemic Pemphigus Foliaceus (Fogo Selvagem). *New England Journal of Medicine* 320, 1463–9.
- Rosenbluth, J., 1995. Neuroglia. volume Glial membranes and axoglial junctions. Oxford University Press.
- Rudick, R.A., Trapp, B.D., 2009. Gray-matter injury in multiple sclerosis. *New England Journal of Medicine* 361, 1505–6.
- Salzer, J.L., Brophy, P.J., Peles, E., 2008. Molecular domains of myelinated axons in the peripheral nervous system. *Glia* 56, 1532–40.
- Schafer, D.P., Bansal, R., Hedstrom, K.L., Pfeiffer, S.E., Rasband, M.N., 2004. Does paranode formation and maintenance require partitioning of neurofascin 155 into lipid rafts? *The Journal of Neuroscience* 24, 3176–85.
- Schneider-Hohendorf, T., Schwab, N., Uceyler, N., Goebel, K., Sommer, C., Wiendl, H., 2012. CD8+ T-cell immunity in chronic inflammatory demyelinating polyradiculoneuropathy. *Neurology* 78, 402–8.
- Seifert, M., Kppers, R., 2009. Molecular footprints of a germinal center derivation of human IgM+(IgD+)CD27+ B cells and the dynamics of memory B cell generation. *The Journal of Experimental Medicine* 206, 2659–69.
- Sherman, D.L., Tait, S., Melrose, S., Johnson, R., Zonta, B., Court, F.A., Macklin, W.B., Meek, S., Smith, A.J., Cottrell, D.F., Brophy, P.J., 2005. Neurofascins are required to establish axonal domains for saltatory conduction. *Neuron* 48, 737–42.
- Smith, K.J., Kapoor, R., Felts, P.A., 1999. Demyelination: the role of reactive oxygen and nitrogen species. *Brain Pathology* 9, 69–92.
- Spalter, S.H., Kaveri, S.V., Bonnin, E., Mani, J.C., Cartron, J.P., Kazatchkine, M.D., 1999. Normal human serum contains natural antibodies reactive with autologous ABO blood group antigens. *Blood* 93, 4418–24.

- Spies, J.M., Pollard, J.D., Bonner, J.G., Westland, K.W., James G. McLeod, 1995. Synergy between antibody and P2-reactive T cells in experimental allergic neuritis. *Journal of Neuroimmunology* 57, 77–84.
- Tait, S., Gunn-Moore, F., Collinson, J.M., Huang, J., Lubetzki, C., Pedraza, L., Sherman, D.L., Colman, D.R., Brophy, P.J., 2000. An oligodendrocyte cell adhesion molecule at the site of assembly of the paranodal axo-glia junction. *The Journal of Cell Biology* 150, 657–66.
- Thaxton, C., Pillai, A.M., Pribisko, A.L., Labasque, M., Dupree, J.L., Faivre-Sarrailh, C., Bhat, M.A., 2010. In vivo deletion of immunoglobulin domains 5 and 6 in neurofascin (nfasc) reveals domain-specific requirements in myelinated axons. *The Journal of Neuroscience* 30, 4868–76.
- Traka, M., Goutebroze, L., Denisenko, N., Bessa, M., Nifli, A., Havaki, S., Iwakura, Y., Fukamauchi, F., Watanabe, K., Soliven, B., Girault, J.A., Karagogeos, D., 2003. Association of TAG-1 with Caspr2 is essential for the molecular organization of juxtapanodal regions of myelinated fibers. *The Journal of Cell Biology* 162, 1161–72.
- Uyemura, K., Suzuki, M., Kitamura, K., Horie, K., Ogawa, Y., Matsuyama, H., Nozaki, S., Muramatsu, I., 1982. Neuritogenic determinant of bovine P2 protein in peripheral nerve myelin. *Journal of Neurochemistry* 39, 895–8.
- Vargas, M.E., Watanabe, J., Singh, S.J., Robinson, W.H., Barres, B.A., 2010. Endogenous antibodies promote rapid myelin clearance and effective axon regeneration after nerve injury. *Proceedings of the National Academy of Sciences* 107, 11993–8.
- Walsh, G., Jefferis, R., 2006. Post-translational modifications in the context of therapeutic proteins. *Nature Biotechnology* 24, 1241–52.
- Warrington, A., Rodriguez, M., 2010. Method of identifying natural antibodies for remyelination. *Journal of Clinical Immunology* 30, 50–5.
- Waxman, S.G., 2006. Ions, energy and axonal injury: towards a molecular neurology of multiple sclerosis. *Trends in Molecular Medicine* 12, 192–5.
- Willison, H., 2011. Reply: Neurofascin as target of autoantibodies in Guillain-Barré syndrome. *Brain* 134, 174–.

- Wootla, B., Denic, A., Keegan, B.M., Winters, J.L., Astapenko, D., Warrington, A.E., Bieber, A.J., Rodriguez, M., 2011. Evidence for the role of B cells and immunoglobulins in the pathogenesis of multiple sclerosis. *Neurology Research International* 2011, 780712–.
- Yan, W.X., Taylor, J., Andrias-Kauba, S., Pollard, J.D., 2000. Passive transfer of demyelination by serum or IgG from chronic inflammatory demyelinating polyneuropathy patients. *Annals of Neurology* 47, 765–75.
- Yu, R., Bunge, R., 1975. Damage and repair of the peripheral myelin sheath and node of Ranvier after treatment with trypsin. *The Journal of Cell Biology* 64, 1–14.
- Yuki, N., Hartung, H.P., 2012. Guillain-Barré Syndrome. *New England Journal of Medicine* 366, 2294–304.
- Zonta, B., Tait, S., Melrose, S., Anderson, H., Harroch, S., Higginson, J., Sherman, D.L., Brophy, P.J., 2008. Glial and neuronal isoforms of neurofascin have distinct roles in the assembly of nodes of Ranvier in the central nervous system. *The Journal of Cell Biology* 181, 1169–77.



# Acknowledgments

I would like to express my appreciation to PD Dr. Klaus Dornmair, Prof Dr. Edgar Meinl, Prof. Dr. Reinhard Hohlfeld, and Prof. Dr. Hartmut Wekerle for making this thesis possible. I am fortunate to have benefited from the guidance of my two supervisors, Klaus and Edgar, who endured my endless questioning and generously provided support and advice throughout this period. Thank you for fostering my development to become an independent scientist. I am grateful to Prof. Hohlfeld and Prof. Wekerle for the opportunity to work in their departments at the Max Planck Institute of Neurobiology, and now at the Institute of Clinical Neuroimmunology of the LMU, and for their continual interest and support in my project.

I would like to acknowledge my examination committee Edgar, Prof. Dr. Nikolaus Plesnila, Prof. Dr. Hans-Walter Pfister, and PD Dr. Cornelia Deeg for taking the time to participate in my evaluation. I would also like to thank the members of my thesis committee Klaus and Edgar, Prof. Dr. Mark Huebener, and Dr. Valentin Stein for their guidance, discussions, ideas and criticism.

To my co-operation partners, thank you for all the serum samples for this project. And a special thank you to Prof. Dr. Nobuhiro Yuki, I really appreciated the helpful comments and criticism throughout the preparation of the Neurology paper.

I would also like to thank the IMPRS office in Martinsried (Hans-Joerg, Maxi, and Ingrid) and the GSN office (Alex and Lena) for their support with the mountains of administrative paperwork, as well as for taking care of this lost Canadian while she integrated into a life in Munich.

During my boisterous stay here, I have thoroughly enjoyed the support and company of my colleagues now friends. A special thanks to Joachim, Martina, Ingrid and Heike for all their support in the lab. To Katherina, Marsilius, Vijay and Eddie, thanks for getting my experiments working in the beginning. Thank you to all the members of my lab groups for putting up with my ever erratic ideas and supporting my athletic endeavors. I am happy to have met Jana and Latika during my PhD. We've been through quite a bit together, and now it's going to get even more interesting. I also want to thank my dear friends Hazel, Ingrid, Andrew, and Harald.

Even though my family is a continent away, I always feel their endless support. Thank you for your support in every way, in my education, my well-being, and my growth to become a good person. Finally, thank you Thomas for your loving care, advice and support through the challenges that I faced during the final phases of this endeavour. And thank you, *sir*, for your wild ideas for our next adventure.



# Judy K.M. Ng

Judy.KingMan.Ng@gmail.com

---

## PERSONAL PROFILE

Born 6<sup>th</sup> of June 1985 in Hong Kong  
Canadian



---

2007-2012  
Munich, Germany

### **Ph.D.**

Max Planck Institute of Neurobiology  
Dept. of Neuroimmunology

Ph.D. thesis: *Serological study to detect neurofascin-specific antibodies in patients with autoimmune diseases of the central and peripheral nervous system*; Supervisors: PD Dr. K. Dornmair, Prof Dr. E. Meinl; Dept. Heads: Prof Dr. H. Wekerle, Prof Dr. R. Hohlfeld

2003-2007  
Toronto, Canada

### **Hon. B.Sc.**

University of Toronto (Trinity College)  
Immunology specialist program (GPA 3.81/4.0, 1<sup>st</sup> in class)

Bachelor thesis: *The role of TRADD in B cell development using conditional TRADD knockout mice*; Supervisor /Dept. Head: Prof Dr. Nien-Jung Chen/ Prof Dr. Tak Mak

Internship (2006): *Immune surveillance of tumours by T cell*; Supervisor /Dept. Head: Dr. Thomas Calzascia/ Prof Dr. Pamela Ohashi

(Both projects were carried out at the Campbell Family Cancer Research Institute)

2005  
Ulm, Germany

University of Ulm (student exchange)  
Intensive German training and EU studies

2004  
Hong Kong, China

Chinese University of Hong Kong (student exchange)  
International Asian studies program

1999-2003  
Toronto, Canada

Pope John Paul II catholic secondary school

---

---

## AWARDS & SCHOLARSHIPS

2007-2012	International Max Planck Research School (IMPRS) fellowship
2009	Travel grant for European School of Neuroimmunology
2007	Trinity prize in Immunology (1 <sup>st</sup> in class)
2006	Life Science Scholarship (internship in cancer research lab)
2005	International Exchange Scholarship (University of Ulm)
2005	Chancellor's Award (outstanding academic performance)
2004	Drew Thompson Scholarship (outstanding academic performance)

---

## COMMUNITY INTERESTS

Volunteer	2012 Sahara Race, RacingThePlanet, Egypt
Photographer	2012 TrailMagazin at Ultra Trail du Mont Blanc, France
Student president	2011 Max Planck of Neurobiology, Martinsried, Germany
Organizer	2009 Logistics for <interact> symposium; Munich, Germany
Lab Technician	2007 Biochemistry department, University of Toronto, Canada
Social Volunteer	2007 Soup kitchen, Toronto, Canada
Volunteer	2004-2007 with University of Toronto Volunteer Association, Canada
Instructor	2001-2003 Taekwondo at Hasnem Taekwondo, Toronto, Canada

---

## LANGUAGE PROFICIENCY

English	native
Chinese/Cantonese	native
German	working knowledge

---



---

PUBLICATIONS

**Ng J.K.M.**, Malotka J., Kawakami N., Derfuss T., Khademi M., Olsson T., Linington C., Odaka M., Tackenberg B., Prüss H., Schwab J., Harms L., Harms H., Sommer C., Rasband M., Eshed-Eisenbach Y., Peles E., Hohlfeld R., Yuki N., Dornmair K., Meinl E. *Neurofascin as a target for autoantibodies in peripheral neuropathies*. *Neurology*: 2012 Oct 24. [Epub ahead of print]

CONFERENCE PRESENTATIONS

**Ng J.K.M.**, Malotka J., Kawakami N., Derfuss T., Khademi M., Olsson T., Sämann P., Weber F., Odaka M., Yuki N., Tackenberg B., Brettschneider J., Rasband M., Linington C., Prüss H., Schwab J., Hohlfeld R., Wekerle H., Dornmair K., Meinl E. (2011) *Anti-Neurofascin autoantibodies: Assay development and analysis of inflammatory diseases of the CNS and PNS*. 10<sup>th</sup> Dresden Autoantibodies Symposium; Dresden, Germany. (Oral and Poster)

**Ng J.K.M.**, Malotka J., Derfuss T., Khademi M., Olsson T., Sämann P., Weber F., Odaka M., Yuki N., Tackenberg B., Brettschneider J., Rasband M., Linington C., Hohlfeld R., Wekerle H., Dornmair K., Meinl E. (2010) *Neurofascin-specific autoantibody detection in inflammatory autoimmune diseases*. International Congress of Immunology; Kobe, Japan. Congress on B Cells and Autoimmunity; Nara, Japan. (Poster)

---



## **Eidesstattliche Erklärung/Affidavit**

Hiermit erkläre ich an Eides statt, dass ich die vorliegende Dissertation

Anti-Neurofascin Autoantibodies: Assay Development and Analysis of Inflammatory Diseases of the Peripheral and Central Nervous System

selbst verfasst und keine anderen als die von mir angegebenen Quellen und Hilfsmittel benutzt habe.

I hereby confirm that the dissertation

Anti-Neurofascin Autoantibodies: Assay Development and Analysis of Inflammatory Diseases of the Peripheral and Central Nervous System

is the result of my own work and that I have only used sources or materials listed and specified in the dissertation.

München, den Juli 12, 2012

Munich, date

Judy KM Ng

Unterschrift signature